Investigating the Role of Somatostatin Receptor 4 (Sstr4) in Head and Neck Squamous Cell Carcinoma (HNSCC)

By

Ali Raza Taqvi

Division of Experimental Medicine

Faculty of Medicine and Health Sciences

McGill University, Montreal, Canada

November 2024

A thesis submitted to McGill University in partial fulfillment of the requirements of the degree of Master of Science

TABLE OF CONTENTS

ABSTRACT

Head and Neck Squamous Cell Carcinoma (HNSCC) is the 6th most common cause of cancer-related death worldwide. Next Generation Sequencing (NGS) has proven to be powerful in identifying the molecular landscape of gene mutations in all cancer patients. In HNSCC, genes that are rarely mutated but recurrent in cancer are referred to as 'longtail mutations.' Previous CRISPR-knockout screen consisting of sgRNA library of longtail mutated genes in HNSCC had identified somatostatin receptor 4 (Sstr4) as a potential tumor suppressor and a driver of tumorigenesis in syngeneic immunocompetent mouse models of HNSCC. Somatostatin Receptors (SSTRs) belong to a family of G-protein coupled receptors (GPCR). These receptors are integral to multiple intracellular signaling pathways, with crosstalk between pathways such as cyclic AMP (cAMP), MAPK, and PI3K/Akt, that collectively exert anti-cancer effects (anti-proliferative, anti-angiogenic, anti-inflammatory). However, no established link exists between any SSTRs in HNSCC tumorigenesis. The function and downstream signaling of Sstr4, particularly in HNSCC where the cell of origin is the stratum basale keratinocyte, remains unexplored.

To validate Sstr4 as a tumor suppressor and driver of HNSCC tumorigenesis, we performed a localized and clonal Sstr4 knockout in basal keratinocyte cells of the HNSCC Pik3ca^{H1047R} oncogenic mouse model by utilizing ultrasound-guided in-utero lentivirus injection technology from our lab's previous research. Tumor formation following Sstr4 knockout (Sstr4-KO) occurred rapidly, within 4 to 12 weeks. To further study Sstr4 function, we applied CRISPR/Cas9 technology and generated stable Sstr4-KO, Sstr4-Overexpression (Sstr4-ORF), and Sstr4-DRY (mutant) cells lines of mouse keratinocytes, KT-CHEN. Transcriptomic (RNA-Seq) and proteomic (Co-IP MS) experiments performed revealed enriched pathways and protein-protein interactions (PPIs), elucidating the involvement of MAPK signaling and 14-3-3 proteins in cell proliferation

and actin rearrangement. Cell proliferation assays indicated that functional Sstr4 limits proliferation, consistent with RNA-Seq and Co-IP MS data. Flow cytometry data indicates that activation of Sstr4 limits G1 to S phase progression. The present study demonstrates the tumor suppressor role of Sstr4 and identifies novel druggable targets in its signaling pathways for HNSCC treatment.

RÉSUMÉ

Le carcinome épidermoïde de la tête et du cou (HNSCC) est la 6e cause la plus fréquente de décès liés au cancer dans le monde. Le séquençage de nouvelle génération (NGS) s'est révélé puissant pour identifier le paysage moléculaire des mutations géniques chez tous les patients atteints de cancer. Dans le HNSCC, les gènes rarement mutés mais récurrents dans le cancer sont appelés "mutations de longue traîne". Un criblage CRISPR-knockout précédent, comprenant une bibliothèque de sgRNA ciblant des gènes mutés de longue traîne dans le HNSCC, avait identifié le récepteur de la somatostatine 4 (Sstr4) comme un suppresseur potentiel de tumeur et un moteur de la tumorigenèse dans des modèles murins syngéniques immunocompétents de HNSCC. Les récepteurs de la somatostatine (SSTRs) appartiennent à une famille de récepteurs couplés aux protéines G (GPCR). Ces récepteurs sont essentiels à plusieurs voies de signalisation intracellulaire, avec des interactions entre des voies telles que l'AMP cyclique (cAMP), MAPK et PI3K/Akt, qui exercent collectivement des effets anticancéreux (anti-prolifératifs, anti-angiogéniques, anti-inflammatoires). Cependant, aucun lien établi n'existe entre les SSTRs et la tumorigenèse du HNSCC. La fonction et la signalisation en aval de Sstr4, en particulier dans le HNSCC, où la cellule d'origine est le kératinocyte du stratum basale, restent inexplorées.

Pour valider Sstr4 en tant que suppresseur de tumeur et moteur de la tumorigenèse du HNSCC, nous avons réalisé un knockout localisé et clonal de Sstr4 dans les kératinocytes basaux du modèle murin oncogénique HNSCC Pik3ca^{H1047R} en utilisant la technologie d'injection in utero guidée par ultrasons de lentivirus, issue de nos recherches précédentes en laboratoire. La formation de tumeurs suite au knockout de Sstr4 (Sstr4-KO) est survenue rapidement, en 4 à 12 semaines. Pour étudier plus en profondeur la fonction de Sstr4, nous avons appliqué la technologie CRISPR/Cas9 et généré des lignées cellulaires stables de kératinocytes murins KT-CHEN avec un knockout de Sstr4 (Sstr4-KO), une surexpression de Sstr4 (Sstr4-ORF) et une mutation Sstr4-DRY. Les expériences transcriptomiques (RNA-Seq) et protéomiques (Co-IP MS) réalisées ont révélé des voies enrichies et des interactions protéine-protéine (IPP), mettant en lumière l'implication de la signalisation MAPK et des protéines 14-3-3 dans la prolifération cellulaire et le réarrangement de l'actine. Les essais de prolifération cellulaire ont montré qu'un Sstr4 fonctionnel limite la prolifération, en accord avec les données de RNA-Seq et de Co-IP MS. Les données de cytométrie en flux indiquent que l'activation de Sstr4 limite la progression de la phase G1 à la phase S. La présente étude démontre le rôle de suppresseur de tumeur de Sstr4 et identifie de nouvelles cibles thérapeutiques dans ses voies de signalisation pour le traitement du HNSCC.

ACKNOWLEDGMENTS

I would first like to thank my supervisor Dr. Sampath K. Loganathan who accepted me into his lab and allowed me the scientific freedom to propose experiments, conduct them, and enhance my research skillsets. His humbleness, politeness, graciousness, patience, humor, wisdom, and intellect have allowed me to have the highest respect and appreciation for him. Having him as my supervisor was a miracle. I thank my co-supervisor, Dr. Anie Philip, and my committee members- Dr. Jean-Jacques Lebrun, Dr. Livia Garzia, and Dr. Nicole Ezer for their research suggestions and advice pertaining to careers. Their challenging questions were most welcome and invigorated me to think like a scientist.

My graduate school journey could not have been possible without my outstanding referees- Dr. Naomi Levy-Strumpf, Dr. Andras Kapus, and Dr. Alistair Dias who took their valuable time in making my application complete and believing in my potential to become a great scientist. I am forever grateful for their support and instilling the scientific curiosity in me through coursework. I am also grateful to Dr. Lili-Naz Hazrati who supervised me in my undergraduate research project at University of Toronto at The Hospital for Sick Children.

The Research Institute of McGill University (RI-MUHC) is an outstanding place filled with phenomenal people. I am grateful to all the Core facilities particularly the Immunophenotyping Core personnel. The past and present lab personnel of Loganathan Lab were exceptional people that I had the utmost pleasure of working and interacting with. Adway Kadam, Yue Yan, Nahid Golabi, Xavier Ng, and Marc Andre-Gauthier made me feel welcome upon joining the lab. I am thankful for Adway and Yue for their massive effort in the animal facility and assisting me with my in-vivo experiments when encountering obstacles. I am grateful for the endless advice pertaining to research and career that Adway provided. Yue and Adway made the lab space feel

safe, enjoyable, and organized. The time they invested in training me to conduct experiments related to molecular biology, bacteriology, virology and in-vivo was crucial to the success of my project in graduate school and will hopefully benefit me in the long run. I thank Nahid for the exceptional cell culture skills that she imparted in me and also the timely ordering of any supplies/reagents I requested on Quartzy. Tuan Khang Huynh, who I have known since my undergraduate education has always been my strong supporter and has been pivotal in developing me into the person I am today. Importantly, his exceptional skills in molecular cloning were instrumental to my research. I thank Zahra Kardan for the extensive bioinformatic analysis conducted by her and the prompt assistance she provided pertaining to Deseq2 data. I am grateful for Zahra, Adway, Tuan, and Adele Lopes for lending a hand when I was overwhelmed with experiments and also for sharing their stories that uplifted my state of mind. Dr. Amina Laham was instrumental in the success of my flow cytometry experiments and suggested valuable project advice. Drishti Soni, Adway, and Yue who encouraged me to experiment with new parameters made me the researcher I am today. I am lucky and eternally grateful to be part of an ambitious lab and surrounded by intellectual people that were always willing to help.

The scientific research of this document could not have been completed without the unwavering support of my family. Their unconditional love, motivational speeches, and humorous stories always energized me to seize the day and be the best version of myself to succeed. My dad who I admire, my mother who takes my worries away, and my sister who has always been with me (figuratively), were influential to my success in graduate school.

The words of Nobel laureate Richard Feynman, "Never confuse education with intelligence," reminds us to approach knowledge with humility and curiosity. This principle has guided me throughout this journey and will continue to do so in the future.

CONTRIBUTIONS OF AUTHORS

I hereby declare that I have carried out most of the work described in this thesis unless otherwise stated. All figures and illustrations were properly cited and referenced where applicable. Figures obtained from external sources were used with permission.

Molecular cloning to obtain plasmid constructs for Sstr4-ORF, Sstr4-KO, Sstr4-DRY was done by Tuan Khang Huynh (section 3.1.3). The modification of the lenti CRISPR v2 plasmid to replace Blasticidin-S deaminase with puromycin N-acetyl-transferase (PAC) gene was done by Adway. The cloning of pLKO-NLS-iCre plasmid used for in-vivo lentiviral injections for Sstr4 knockout (Sstr4-KO) was done by past lab member Logine Ghadban (section 3.1.3). Adway also contributed to producing the high-titer lentivirus used for in-vivo lentiviral injection (Section 3.2)

Most of the in-vivo work such as crossing mice strains, ultrasound scans, lentiviral injections, weaning, and tumor extraction was done collectively by Adway, Yue, and Dr. Loganathan (section 3.10.1 & section 3.10.2). The sectioning and staining of the OCT embedded tumor with Hematoxylin and Eosin staining (H&E) was done by the Histopathology Core at McGill University Health Centre-Research Institute (RI-MUHC) (Section 3.10.4)

Transcriptomic work involving library preparation to sequencing of the gene expression changes of Sstr4 cell lines was done by Novogene (section 3.6.2). The sequencing reads were analyzed by Deseq2 package to identify differentially expressed genes (DEGs) which was done by Zahra (section 3.6.3).

The Co-Immunoprecipitation (Co-IP) pulldown assay was performed by Tuan followed by mass spectrometry (MS) that was performed by the proteomics core at the RI-MUHC to identify protein-protein interactions (PPIs) of Sstr4 (section 3.7).

LIST OF FIGURES

LIST OF TABLES

ABBREVIATIONS

AC	Adenylate Cyclase
Adam10	A Disintegrin and Metalloprotease 10
Ajuba	Ajuba LIM Protein
Akt	Protein Kinase B
cAMP	Cyclic Adenosine Monophosphate
CDKN2A	Cyclin-Dependent Kinase Inhibitor 2A
CHO-K1	Chinese Hamster Ovary Cells
CREB	cAMP Response Element-Binding Protein
DEGs	Differentially Expressed Genes
EBV	Epstein-Barr Virus
E2F	E2F Transcription Factor
ECM	Extracellular Matrix
EGFR	Epidermal Growth Factor Receptor
ERK	Extracellular Signal-Regulated Kinase
FAK	Focal Adhesion Kinase
GH	Growth Hormone
GO	Gene Ontology
GPCRs	G-Protein Coupled Receptors
HNSCC	Head and Neck Squamous Cell Carcinoma
HPV	Human Papillomavirus
ILK	Integrin-linked Kinase
JNK	c-Jun N-terminal Kinases

KO	Knockout
KT	Keratinocyte Cell Line
MAPK	Mitogen-Activated Protein Kinase
MEK	Mitogen-Activated Protein Kinase Kinase
MS	Mass Spectrometry
NET	Neuroendocrine Tumor
NGS	Next Generation Sequencing
Notch1	Notch Homolog 1
Pik3ca	Phosphatidylinositol-4,5-bisphosphate 3-kinase catalytic subunit 110-α
PI3K	Phosphoinositide 3-Kinase
PKC	Protein Kinase C
PLC	Phospholipase C
PPI	Protein-Protein Interactions
PTP	Protein Tyrosine Phosphatase
RB1	Retinoblastoma Protein 1
Ras	Rat Sarcoma Virus Gene
Ripk4	Receptor Interacting Serine/Threonine Kinase 4
SHP	Src Homology Phosphatase
Src	Proto-Oncogene Tyrosine-Protein Kinase Src
SSTRs	Somatostatin Receptors
TIDE	Tracking of Indels by Decomposition
TSH	Thyroid-Stimulating Hormone
WT	Wild Type

1 INTRODUCTION

1.1 Head and Neck Cancer Overview

According to the World Health Organization (WHO), Global Durden of Disease (GBD), and Global Cancer Observatory (GCO) databases, cancer is among the leading cause of death worldwide (WHO, 2022; GBD, 2021; GCO, 2024). Cancer is a debilitating disease that affects any organ or tissue of the human body due to uncontrollable cell growth or spread of cells from one region to another (Hanahan & Weinberg, 2011).

Head and neck cancers are a group of cancers originating from various anatomical regions in the head and neck, both internal and external, including the skin, aerodigestive tract, salivary glands, tonsils, and tongue (Johnson et al., 2020). A key distinction between melanoma and head and neck skin cancers lies in the cell of origin responsible for cancer initiation (tumorigenesis) (Gruber & Zito, 2024). Melanoma arises from melanin synthesizing cells, called melanocytes present in the stratum basale layer of the epidermis, whereas non-melanoma skin cancer (NMSC) of the head and neck region arise from the keratinocyte cells of the stratum basale (Yousef et al., 2024; Josiah et al., 2021). While both cancer types may arise from the same anatomical region (skin), they exhibit significant differences in their molecular mutational landscapes, histopathological features, progression patterns, and clinical management approaches (Gruber & Zito, 2024).

1.2 Head and Neck Squamous Cell Carcinoma (HNSCC)

Head and Neck Squamous Cell Carcinoma (HNSCC) has a worldwide incidence rate of approximately 900,000 people per year resulting in approximately 450,000 deaths (Johnson et al., 2020). Head and Neck cancers are the 6th most common subtype of cancer among males in Canada

(Canadian Cancer Statistics, 2023). HNSCCs are a type of NMSC of the mucosal lining of the upper aerodigestive tract in the head and neck regions including pharynx, larynx, and entire oral cavity (Johnson et al., 2020). To be more precise, the skin is composed of 3 layers- epidermis (outer), dermis (middle), and hypodermis (inner) (Simpson et al., 2011). The outer epidermis is further comprised of 5 layers- Stratum corneum (outer), stratum lucideum, stratum granulosum, stratum spinosum, stratum basale (inner) (Simpson et al., 2011).

The stratum corneum is characterized by expression of specific cytokeratins such as cytokeratin-1 (K1) and cytokeratin-10 (K10). The keratinocyte cells in the stratum corneum are derived from the stratum basale keratinocyte cells as part of the programmed skin cell renewal shedding process (Simpson et al., 2011). As the basale keratinocyte stem cells divide asymmetrically, the daughter cells form the stratum spinosum layer. Further programmed differentiation and migration results in the histological arrangement of the epithelium layer, where there is establishment of cell polarity, and thus the maintenance of tissue architecture (Simpson et al., 2011).

Squamous cell carcinoma (SCC) of head and neck cancer arises from the keratinocyte cells located in the inner epidermis layers such as stratum spinosum and stratum granulosum where cells express cytokeratins K1 and K10. These cells are the primary cells of origin for HNSCC tumorigenesis (Simpson et a., 2011; Amberg et al., 2015; Hasan et al., 2023). Basal cell carcinoma (BCC) arises from the keratinocytes located in the stratum basale layer, where biomarkers such as K5 and K14 are highly expressed (Simpson et al., 2011; Hasan et al., 2023). The distinguishing feature between SCC and BCC is the tumor appearance. SCC tumors appear scaly and reddish, whereas BCC tumor appear as bumps (Hasan et al., 2023; Ryu et a., 2018).

1.3 HNSCC Molecular Landscape and Research Rationale

The emergence of cancer arises as a result of mutations in key genes that play a role in regulating cell proliferation, apoptosis, signalling, angiogenesis, differentiation, epigenetic regulation, and metastasis (Hanahan & Weinberg, 2011). There are two main classifications used to group mutated or altered genes in the field of molecular oncology, which are oncogenes and tumor suppressor genes. When a particular gene is mutated, overexpressed, or biochemically hyperactive resulting in the development of cancer, it is referred to as an oncogene. On the contrary, when a gene is mutated, silenced, or biochemically inactive resulting in cancer development, it is referred to as a tumor suppressor gene. Importantly, a gene functioning as a tumor suppressor in one type of cancer may function quite differently in another type of cancer which emphasizes that cellular context is crucial. (Shen et al., 2018)

A preliminary analysis of a subset of 669 HNSCC samples across 4 independent large-scale cancer genomic studies on cBioPortal found that approximately 16,173 genes were altered across all samples (Stransky et al., 2011; Agrawal et al., 2011; Pickering et al., 2013; TCGA, PanCancer Atlas). Tumor Protein 53 (TP53) which is a bona fide tumor suppressor in all cancers has a mutational frequency of 67.2% in HNSCC (Figure.1). Some of the commonly mutated genes such as NOTCH1, possess a mutational frequency of 15.4%, and are highly implicated in HNSCC tumorigenesis (Hasan et al., 2023). This gives NOTCH1 a functional classification of ‘Driver mutation’ when mutated in HNSCC, and NOTCH1 is itself a tumor suppressor gene when functional in skin cells (Nicolas et al., 2001). In addition to the recent sequencing efforts of HNSCC patient samples, research has uncovered hundreds of individually rare but recurrent gene mutations called ‘long-tail’ mutations (Figure.1). The vast majority of these long-tail mutations lack biological relevance and clinical validation (Agrawal et al., 2011.; Stransky et al., 2011).

Previous research conducted an in-vivo CRISPR screening in mouse models of HNSCC by knocking out 484 'long-tail' genes pertaining to HNSCC (Loganathan et al., 2020). Some genes such as Ripk4, Adam10, and Ajuba were shown to be gene upregulation targets downstream of Notch1 (Loganathan et al., 2020). When these Notch1 targets were mutated from the in-vivo CRISPR screening, tumorigenesis was observed within weeks (Loganathan et al., 2020). Strikingly, besides tumor suppressors associated with the Notch1 signaling pathway, additional tumor suppressor genes were identified that were not Notch1 target genes, thus indicating the role of other signaling pathways that can initiate HNSCC tumorigenesis. One of the novel tumor suppressors identified from the previous study was Somatostatin Receptor 4 (Sstr4), which is mutated in less than 1% of HNSCC patients (Figure.1).

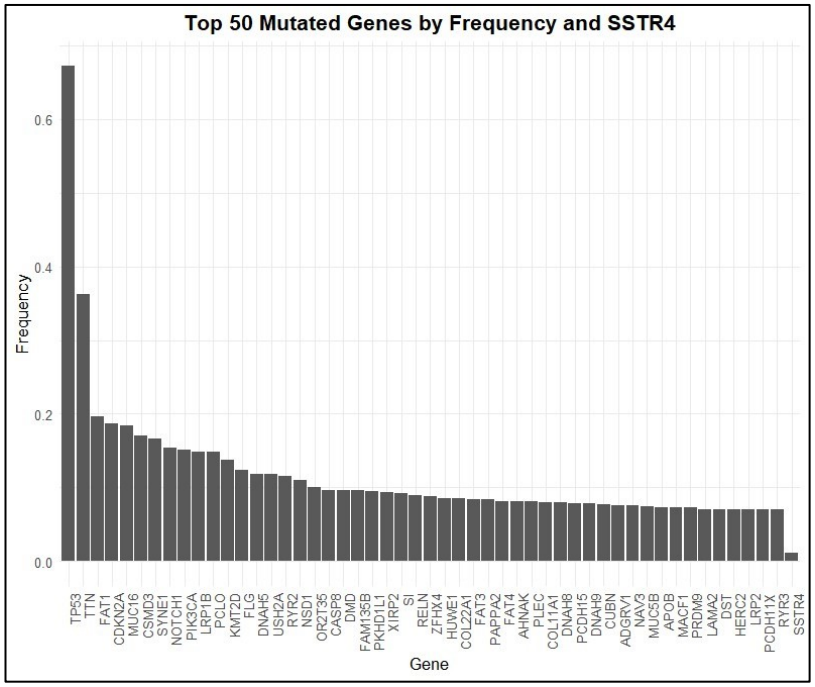

Figure 1: HNSCC Gene Mutation Frequency | Mutation frequency of top 50 genes obtained from 669 HNSCC patient samples from cBioPortal including SSTR4 depicting the 'long-tail' appearance of cancer mutational burden. Data obtained from cBioPortal. Plot made from R Studio.

1.4 Study Aim and Objectives

The overarching goal of this thesis is to investigate the role of Sstr4 in the cellular context of HNSCC, utilizing both in vivo mouse models and in vitro primary mouse keratinocyte cell lines. Although somatostatin receptors (SSTRs) have been extensively studied in other cancers, such as melanoma, pituitary tumors, and breast cancer, they have been significantly understudied in HNSCC (Kumar et al., 2024; Harda et al., 2018; Watt et al., 2009; Theodoropoulou et al., 2006). Notably, Sstr4 remains the least studied of all SSTRs, despite being part of the G-protein coupled receptor (GPCR) family—a class of proteins that represents one of the most druggable targets (Sriram & Insel, 2018). This emphasizes the need to explore the potential of Sstr4 as a drug target for treating HNSCC patients by understanding its function and intracellular signalling. To date, there are no links between Sstr4 and HNSCC and this document is the first of its kind to investigate that link. This document will achieve the following aims-

Aim 1: To validate Sstr4 as a tumor suppressor gene and a driver mutation by evaluating its loss-of-function effects resulting in HNSCC tumorigenesis and solidifying its role in cancer initiation.

Aim 2: To decipher the exact intracellular signaling mechanism through which Sstr4 exerts its tumor suppressor function in HNSCC.

Aim 3: To study the cellular function of Sstr4 examining proliferation behaviors in the cellular context of HNSCC.

2 LITERATURE REVIEW

2.1 Cancer Overview

2.1.1 Prevalence of Cancer in Canada (2023)

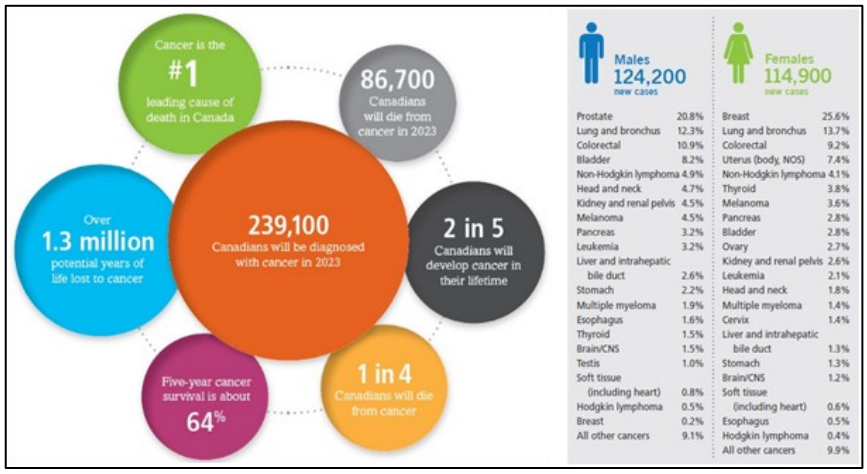

Figure 2: Prevalence of Cancer in Canada | Figures taken from Canadian Cancer Society Statistics report published on 2023.

Cancer is the number one leading cause of death in Canada which affects approximately 240,000 Canadians, of which, one-third will die from it (Figure.2). Prostate and Breast cancers are the most diagnosed in males and females respectively (Figure.2). Across both sexes, head and neck cancer affects approximately 7,500 individuals resulting in 2,100 deaths in Canada (Figure.2). Compared to previous reports, there has been an increase in the number of cases of head and neck, which is expected to rise substantially in the next decades (Canadian Cancer Society; 2021).

Most cases of head and neck cancer are diagnosed at advanced stages. For instance, in the United Kingdom (U.K) 58% of cases are diagnosed in late stages (Stage III/IV), and stage IV is the most common at the time of diagnosis amongst populations above the age of 50 (Conway et al., 2022). This pattern is also observed in Canada where most cases of head and neck cancers are

diagnosed in the advanced stages which consistently leads to poor outcomes due to the lack of effective treatments (MacNeil et al., 2020). Head and neck cancers often go undetected in their early stages due to a combination of factors, including patient-related delays, provider-related delays, and, though less common, instances of misdiagnosis (Kassirian et al., 2020).

2.1.2 Hallmarks of Cancer: Hanahan and Weinberg

A few decades ago, Hanahan and Weinberg (2000) proposed a conceptual framework describing characteristic features that gives cancer cells the advantage to thrive in the human body by sustained proliferation, evading bodily defenses, and spreading to other bodily organs (Hanahan & Weinberg, 2000; Hanahan & Weinberg, 2011). It is due to this cancer biology foundation that has molded cancer research to be carried out more effectively and logically by investigating specific characteristics of cancer cells.

Building on this foundation, the present study involves investigating the proliferative signalling hallmark in HNSCC initiation (Hanahan & Weinberg, 2011). Novel drug targets can be identified, hence targeted, by understanding the intracellular signaling mechanism regulating cell proliferation in keratinocyte cells.

2.1.3 Cancer Initiation: The Knudson Hypothesis

The “Two-Hit Hypothesis” or “The Knudson Hypothesis” proposed by the late Alfred G. Knudson Jr. in 1971 suggests that tumorigenesis begins when both alleles of one tumor suppressor gene are mutated (Knudson, 1971) (Figure.3). According to the hypothesis, the first mutation, also called the first hit, is a mutant allele of a tumor suppressor gene that is often inherited from either parent. The second hit is sporadic, due to environmental factors such as Ultraviolet (UV) radiation

causing DNA damage in genes of chromosomes (Amberg et al., 2015) (Figure.3). This hypothesis was proposed to explain the probability of retinoblastoma occurrence in individuals after obtaining family pedigree (Knudson, 1971). Retinoblastoma is a rare childhood eye cancer initiated by mutations in the retinoblastoma protein 1 gene (RB1) (Wang et al., 1994).

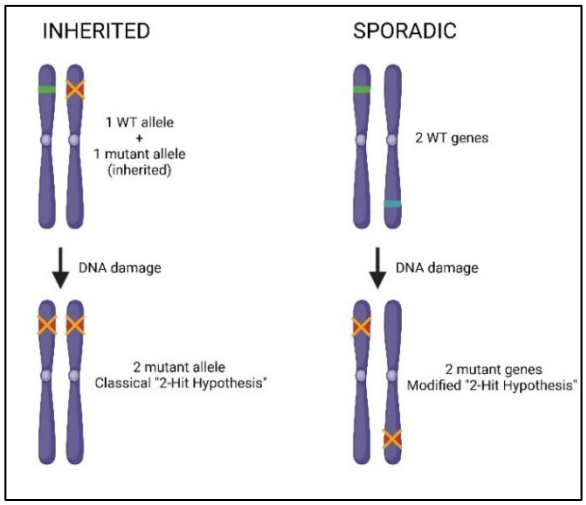

Figure 3: The Knudson Hypothesis Schematic | The Two-Hit Hypothesis can manifest either through the classical inherited mechanism or via a modified sporadic mechanism. (Created with BioRender.com)

For a gene to be classified as a tumor suppressor in any cancer, tumorigenesis should be observed when both alleles of the gene are knocked out by mutation, which meets the Two-Hit Hypothesis (Chernoff, 2021). However, the Two-Hit Hypothesis is more appropriate for cancer initiation and not progression, which is observed by an increase in the number of cells called 'Hyperplasia' (Chernoff, 2021; Johnson et al., 2020). Most literature now support that for tumorigenesis to progress full-scale to malignancy, a third hit is often required resulting in more mutational burden (Chernoff, 2021; Wang et al., 1994; Sellers & Kaelin, 1997). RB1 is hence classified as a tumor suppressor in the initiation of eye cancer and through decades of research its

cellular function is in the regulation of cell cycle through repression of E2F transcription factors (TFs) (Sellers & Kaelin, 1997; Janostiak et al., 2022).

The understanding of tumorigenesis has now evolved beyond the classical Two-Hit Hypothesis (Figure.3). Today, a modified Two-Hit Hypothesis now considers different Haploinsufficient gene mutations involved between closely associated signalling pathways (Fero et al., 1998; Inoue & Fry, 2017). The modified Two-Hit hypothesis is based on the principle of gene dosing as not all genes are haplosufficient nor haploinsufficient. Additionally, our lab conducted CRISPR knockout screen of 484 longtail genes on oncogenic heterozygous $Pik3ca^{H1047R}/+$ gain of function mutation in HNSCC mouse models and revealed novel tumor suppressor and tumorigenesis driver genes such as Adam10, Ripk4, and Ajuba that were target genes for the Notch1/2 signaling pathway (Loganathan et al., 2020). As previously mentioned, Sstr4 was identified as one of the hits of the CRISPR knockout screen, whose functional relevance in HNSCC tumorigenesis remains to be investigated.

2.2 Head and Neck Squamous Cell Carcinoma (HNSCC)

2.2.1 Risk Factors, Diagnosis, Treatments

Almost a decade ago it was found that Head and neck cancer can be characterized as either Human papillomavirus (HPV) negative or HPV positive (Stein et al., 2015). HPV negative (HPV-) head and neck cancer is more common in Canada which is caused mainly due to tobacco consumption and excessive alcohol consumption (Johnson et al., 2020). HPV positive (HPV+) head and neck cancer is due to viral infection mostly by HPV-16 strain (Cramer et al., 2019). Other viral infections such as those caused Epstein-Barr Virus (EBV) strains is also a risk factor for HNSCC tumorigenesis (Johnson et al., 2020). Due to any of the risk factors mentioned, patients

present to the clinic with lesions on the tongue such as leukoplakia, which are the white patches or erythroplakia, which are the red patches (Villa et al., 2011; Rhodus et al., 2014). Leukoplakia is more commonly seen than erythroplakia, however these are uncommon symptoms and are only seen in 0.02% - 2% of cases worldwide (Abati et al., 2020).

The common symptom of HNSCC are lumps of cell mass in relevant anatomical location of Head and neck cancer (Kassirian et al., 2020). The diagnosis of head and neck cancer is made by the pathologist after they receive a biopsy from the surgeon (Kassirian et al., 2020). If tissue staining with hematoxylin and eosin (H&E) shows the disruption of the epithelium layer of the mucosa, then a diagnosis of cancer is made (Johnson et al., 2020). The protein, cyclin-dependent kinase inhibitor 2A (CDKN2A), more commonly known as $p16^{INK4a}$, is overexpressed in HPV+ oral cancers due to the action of E6 and E7 oncoproteins and can therefore be used as an indirect marker of HPV. Furthermore, it also serves as a useful prognostic marker in head and neck cancer. (Johnson et al., 2020; Kassirian et al., 2020)

The treatment for head and neck cancer is very complex and multi-modal. The first-line treatment for head and neck cancer is usually surgery alone or in combination with chemoradiation if the tumor is large (Hasan et al., 2023; Johnson et al., 2020). If the cancer is recurrent or has metastasized to the lymph nodes in the head and neck region, then chemotherapy, radiation, and surgery are all utilized (Rhodus et al., 2014). Immunotherapy is used as a last resort which results in 1-year overall survival (OS) of 30-35%, and 1-year progression free survival (PFS) of 10-17% (Pereira et al., 2022). Even though multi-targeted immunotherapy increases OS and PFS, the 5-year overall survival remains at 65% (Pereira et al., 2022; Du et al., 2019). These statistics not only point out the differential treatment responses between patients but also the need for novel

treatment strategies that are less toxic and effective to improve the OS of all HNSCC patients (Leemans et al., 2018).

2.2.2 Relevant Anatomical Locations

There are three important anatomical sites where head and neck cancer may arise from. The oral cavity, the pharynx (which is the upper respiratory tract) and the larynx (voice box). Squamous cell carcinomas (SCCs) are the most common in the oral cavity as it is the primary point of contact for carcinogens such as tobacco and alcohol (Abati et al., 2020). In the oral cavity the most common locations where squamous cell carcinomas arise from are- the tongue, floor of the mouth, and buccal mucosa which are the inner walls of the cheek (Johnson et al., 2020).

Although head and neck cancers that are negative for HPV or EBV have the highest incidence rates, understanding the role of oncogenic viruses in the pathophysiology of HNSCC remains crucial. This is because cancers caused by these viruses are more easily preventable through vaccines such as GARDASIL®9 that protect against nine serotypes of HPV including HPV-16 and HPV-18 (Cramer et al., 2019). Additionally, HPV+ and EBV+ head and neck cancer have better prognostic outcomes (Gormley et al., 2022; Cramer et al., 2019). Oncogenic Human viruses such as HPV and EBV play a critical role in location-specific HNSCC initiation (Goon et al., 2022). Oropharyngeal cancer (OPC) is a head and neck cancer arising from the oropharynx, and 70% of cases are due to the HPV+ status of patients in the US (Cramer et al., 2019). This stratification and subgrouping of head and neck cancers have increased our understanding of its pathophysiology, which can allow the adoption of personalized and precision treatments for each patient.

2.2.3 HNSCC mechanism of Tumorigenesis and Knowledge Gap

The first trigger for the initiation of head and neck cancer is exposure to carcinogens or infections due to oncogenic viruses (Kassirian et al., 2020; Rivera, 2015). Upon carcinogenic exposure of viral infections in relevant head and neck cancer anatomical locations, there are genetic alterations in the epithelium layers of tissues (Rivera, 2015). The initiation of either SCC or BCC in the oral cavity depends on which epithelial layer undergoes genetic alteration and gains a tumorigenic survival advantage (Simpson et al., 2011). For instance, when genetic alterations occur in $p16^{INK4}$ gene (CDKN2A) in the stratum spinosum layer, this results in cell proliferation affecting tissue architecture and the initiation of tumorigenesis which can be observed as hyperplasia through H&E staining due to increased cell number (Leemans et al., 2018; Goon et al., 2022). Due to further uncontrolled proliferation, there is cancer progression as the cells lose contact with one another, affecting polarity and overall tissue architecture, which subsequently affects signaling, and promotes uncontrolled differentiation resulting in dysplasia appearance through H&E staining. (Rivera, 2015; Goon et al., 2022; Johnson et al., 2020)

As the cells uncontrollably divide and differentiate, they accumulate more genetic alterations possibly in genes involved in DNA damage repair (DDR) pathways which results in genetic instability resulting in more genetic alterations (Rivera, 2015; Stransky et al., 2011). As a result, more genetic alterations are observed, evident by commonly mutated genes such as TP53, NOTCH1, and EGFR (Stransky et al., 2011). The disruption of cell cycle regulation and negative regulation of apoptosis results in rapid tumor growth, which acquires a carcinoma appearance with H&E staining (Johnson et al., 2020). As the tumor grows, the tumor microenvironment promotes E-cadherin loss and increased Matrix Metalloproteinases (MMPs) expression which results in Epithelial to Mesenchymal Transition (EMT) (Rivera, 2015). The primary cancer that began in the

keratinocytes of stratum spinosum layer thus spreads to other areas by blood vessels or lymphatic vessels and becomes invasive carcinoma through metastasis.

The destruction of the epidermis tissue architecture due to impairment of cell adhesion proteins may not be the only primary trigger for tumorigenesis (Simpson et al., 2011). Indeed, the direct contact of carcinogens such as smoking or alcohol with oral epithelium cells may cause genetic alterations in any random gene. However, the synergistic effect of two genes is required to cause tumorigenesis and subsequently tumor progression, as the modified Two-Hit Hypothesis states. Out of the 16,173 genes that are altered in HNSCC patients, relevance of the rarely mutated genes is unknown. It is also unclear if these rarely mutated genes are driver mutations, or passenger mutations as a result of genome instability. Furthermore, the synergistic tumorigenic effect of two genes namely, Sstr4 and mutant $Pik3ca^{H1047}$ genes remains unexplored.

2.3 In-Vivo Model to replicate HNSCC tumorigenesis

2.3.1 Ultrasound Guided In-Utero Embryonic Injection at E9.5 HNSCC mouse model

The first application of ultrasound-guided embryonic injection technique was used to study embryonic development (Liu et al., 1998; Slevin et al., 2006). The application of the technique then evolved to understanding skin epidermal biology (Beronja and Fuchs, 2013). This technique involves genetically manipulating epidermis basal stem cells at embryonic stage 9.5 (E9.5), which is then carried over to adulthood after litter birth of 4-8 pups (Figure.4). The genetic manipulation of the epidermal stem cell layer at E9.5 can be achieved by microinjection of non-viral payloads such as DNA, shRNA, or RNAi. Alternatively, Viral vectors such as Adeno-associated Viruses (AAVs) or Lentiviral vectors (LVs) can also be injected depending on research interests (Figure.4). The genetic modification will persist in the skin epidermis, including the oral cavity, tongues, nose,

and neck region of the mouse. This invasive surgical technique is complex and requires several surgical equipment and devices for increased experimental success (Beronja & Fuchs, 2013).

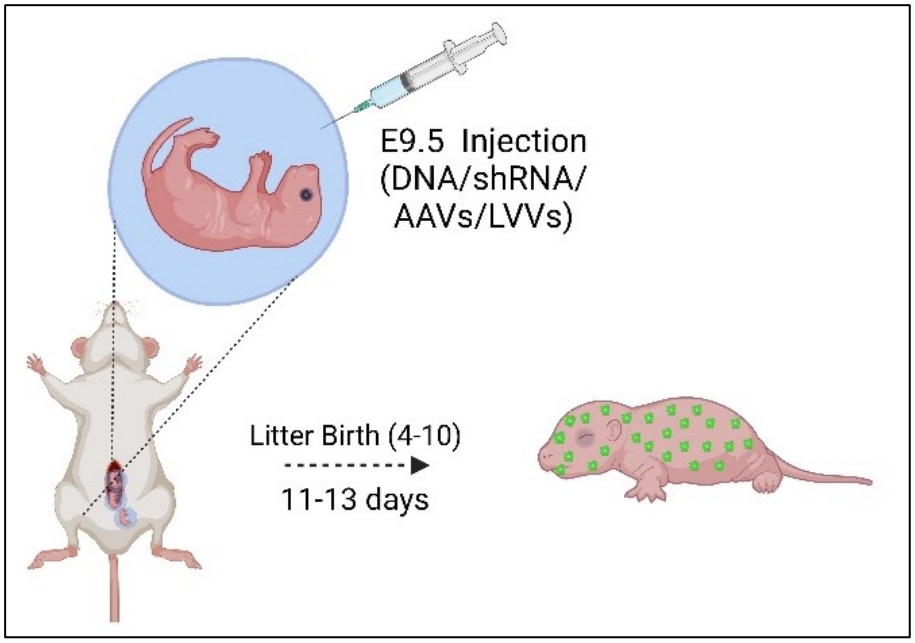

Figure 4: Schematic of Ultrasound-guided in-utero lentivirus injection | A workflow of embryonic stage 9.5 (E9.5) lentiviral injection to manipulate the stratum basale stem cells at the embryonic stage that eventually form the epidermis layers of the mouse skin after birth to study HNSCC. A marker such as Green Fluorescent Protein (GFP) may be incorporated to assure successful lentiviral integration and plasmid construct expression. (Created with BioRender.com)

2.3.2 Advantages of the In-Vivo Model

2.3.2.1 Localized genetic manipulation

Investigating the initiation of HNSCC requires genetic manipulation of the keratinocytes cells of the epidermis which are the cells of origin for HNSCC. Non-surgical methods such as dermabrasion affects tissue architecture and introduces confounding variables during the wound healing process (Ghazizadeh et al., 1999). Recently, topical-based methods have been of interest to deliver non-viral and viral payloads to the epidermis and dermis layers of the skin by utilizing lipid nanoparticles (LNPs) as the delivery formulation (Guri-Lamce et al., 2024; Elsabahy &

Foldvari, 2013). Despite the stratum corneum being the most difficult epidermis layer to penetrate, Niu and colleagues (2017) delivered plasmid DNA (pDNA) using a peptide-conjugated cationic gold nanoparticle formulation as an ointment in mice which successfully penetrated the epidermis layer up to 80μm (Niu et al., 2017).

Though the non-surgical approach may seem lucrative, there are technical challenges associated with it such as- handling of biohazardous substances, optimization of lipid nanoparticle (LNP) formulation for epidermal-specific delivery, maintaining consistent dosing and application to the skin of the mice, and storage of the final formulation. Delivery of Lentiviruses through LNP topical-based methods, poses a risk for multiplicity of infection (MOI) beyond 0.4 resulting in unwanted double viral integration. Using LNPs can also stimulate an immune response after recognition by NLRP3 inflammasome (Lee et al., 2023). Furthermore, topical applications pose experimental reproducibility and scalable challenges when conducting genome-wide screenings.

2.3.2.2 Immune Competent Mouse model

Assessing the oncogenic potential of tumor suppressor genes when knocked-out requires the use of in-vivo mouse models specific for different cancer subtypes mirroring the molecular signatures. To date, genetically engineered mouse models (GEMMs) of HNSCC are limited to transgenic mouse, UV radiation treated mouse, NOD SCID gamma (NSG) mouse, and patient-derived xenograft (PDX) mouse models (Amberg et al., 2015; Chaves et al., 2023; Schuch et al., 2020). PDX mouse models are not relevant in this study as they are generally used for pre-clinical testing of therapeutic compounds (Chaves et al., 2023).

NSG in vivo tumor formation studies involve subcutaneously injecting immortalized cell lines into the hind limbs of NSG mice and monitoring for tumor development (Ren et al., 2006).

Since NSG mice are severely immunodeficient, the injected cells are not rejected by the host and can proliferate. Prior to injection, the cells can be genetically modified to study the function of specific genes. Although this approach is highly effective for assessing gene-specific tumor progression, it is less suitable for investigating the mechanisms of HNSCC initiation in anatomically relevant locations, where the NSG model proves to be inadequate.

Transgenic mice studies work by breeding different mice strains to obtain the target genotype and observe for the expected phenotype. One disadvantage of transgenic mice arises when intended gene alteration becomes embryonically lethal and as a result becomes difficult to propagate mouse colonies. One solution to circumvent this problem is to utilize the Cre-lox system for inducible gene knockout (Amberg et al., 2015; Kim et al., 2018). The gene of interest is flanked by loxP sites (referred to as 'floxed'), and in the presence of Cre-recombinase, the floxed gene is excised, resulting in a gene knockout (Amberg et al., 2015; Beronja et al., 2010). Though this approach may seem appropriate for achieving research objectives in an immunocompetent mouse model, the lack of a localized knockout remains a concern. Most inducible agents for Cre-recombinase expression, such as doxycycline or tamoxifen also require several days of subcutaneous administration which increases the labor involved.

Thus, the ultrasound guided in-utero embryonic injection at E9.5 HNSCC mouse model offers the dual advantage of localized knockout which mirrors HNSCC anatomy as seen in patients, while also maintaining a functioning immune system to observe if the gene of interest confers immune evasion advantage to proliferate uncontrollably.

Importantly, this unique HNSCC mouse model is validated from previous research (Loganathan et al., 2020). Briefly, when mutations in $Pik3ca^{H1047R}$ and TgfβrII-KO were made, tumor formation was observed as early as 45 days after date of birth (Loganathan et al., 2020

Supplementary). Furthermore, no tumor formation was observed when single guide RNA coding for non-targeting control (sgNTC) was injected in just the $Pik3ca^{H1047R}$ heterozygous background. Lastly, an additional CRISPR screening done in the HNSCC mouse model, targeting long-tail genes of breast cancer, resulted in no tumor formation (Loganathan et al., 2020 Supplementary). This highlights the synergistic effect of gene mutations, and the location-specific requirement needed for HNSCC tumorigenesis. In conclusion, the HNSCC mouse model is excellent at investigating gene function with regards to cell proliferation, metastasis, and immune cell-mediated signalling for tumorigenesis.

2.4 Somatostatin Receptor Four (Sstr4)

2.4.1 SSTR Family Overview

Somatostatin Receptors (SSTRs) are G-protein Coupled Receptors (GPCRs) that belong to the Class A Rhodopsin family which are the largest class of GPCRs (87%) (Yang et al., 2021). GPCRs are characterized by having seven transmembrane domains that are localized to the lipid bilayer of the plasma membrane. The N-terminus of the GPCR lies on the extracellular side of the cell, whereas the C-terminus of the GPCR lies on the intracellular side facing the cytoplasm (Coleman et al., 2017). Out of all the FDA approved drugs, 35% of them target GPCRs which emphasizes their importance in regulating and maintaining cellular function and homeostasis (Sriram & Insel, 2018). Currently, out of the 826 GPCRs that have been identified, 165 of GPCRs have validated drug targets including SSTRs (Yang et al., 2021).

There are five subtypes of somatostatin receptors, SSTR1-5, all of which are expressed ubiquitously throughout the human body (Corleto et al., 2004; Gunther et al., 2018; Eychenne et al., 2020). SSTR1 and SSTR2 are highly expressed not only in the central nervous system (CNS) but also in the parotid glands, gastrointestinal (GI) mucosa, and glucagon/insulin-secreting

pancreatic cells (Gunther et al., 2018). However, SSTR4 demonstrates the greatest anatomical specificity, with its highest expression in the CNS, though not significantly higher than that of SSTR1 and SSTR2 (Gunther et al., 2018; Eychenne et al., 2020). It remains an understudied protein with regard to its anatomical biodistribution and function in skin epithelial cells.

2.4.2 Sstr4 Gene Description

The human SSTR4 gene is located on the short arm of chromosome 20 (20p11.21). Consisting of a single exon and no introns it is 3,926 base pairs (bp) in length (NM_001052.4). Its mouse ortholog, Sstr4, is located on Chromosome 2 and also contains a single exon spanning 1,388bp in length (NM_009219.3). Conducting a simple multiple pairwise alignment between human SSTR4 and mouse Sstr4 using the Basic Local Alignment Search Tool (BLAST), there appears to be a significant homology of approximately 80% (NCBI-BLAST; Camacho et al., 2009). The human SSTR4 gene is longer as it contains non-coding enhancer elements upstream of the 5' coding region of the open reading frame (ORF), which is crucial for epigenetic control (Zhao et al., 2022; Klomp et al., 2021).

2.4.3 Sstr4 Protein Structure and Function

The human SSTR4 and mouse Sstr4 have identical structural motifs and amino acid lengths. The human SSTR4 is comprised of 388 amino acids whereas the mouse Sstr4 is shorter by 3 amino acids (Milewska-Kranc et al., 2024; Gunther et al., 2018). A protein BLAST done for human SSTR4 (NP_001043) and mouse Sstr4 (NP_033245) revealed 88% sequence complementarity, with most variability occurring in the extracellular N-terminal region of the protein that is not involved in intracellular signalling events (NCBI-BLAST; Camacho et al.,

2009). There is also considerable conservation of amino acid residues between SSTR4 (Human) and Sstr4 (mouse) that comprise of the α-helices transmembrane (TM) domains. The atomic mass of Sstr4 protein is approximately 43kDa.

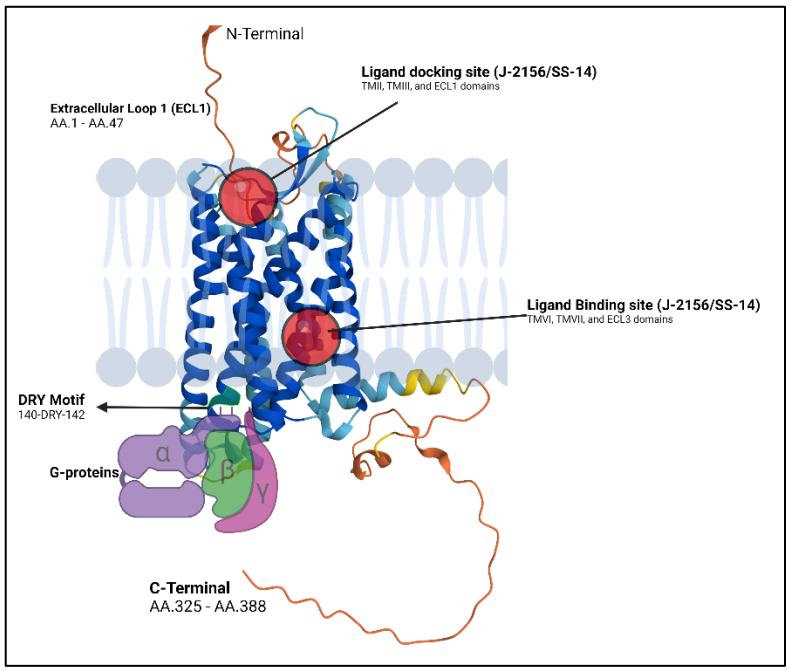

Figure 5: Structure of SSTR4 Protein with Agonist Binding | Crystal structure of mouse Sstr4 localized to the cell plasma membrane (AlphaFoldDB: P49660). The G-proteins (Gα, Gβ, GϒY) are associated with the intracellular side of Sstr4 and are shown as purple, green and magenta colors. Sstr4 ligands such as J-2156 agonist or somatostatin (SS-14) are shown as a red sphere. (Created with BioRender.com)

The structure of SSTR4 has been well studied in addition to validation of conserved GPCR motifs through mutational testing (Zhao et al., 2022). A highly specific ligand for SSTR4, called J-2156 agonist, shows nanomolar affinity (10^{-8}M - 10^{-9}M) to SSTR4 receptor (Weckbecker et al., 2003; Engstrom et al., 2005). Through X-ray crystallography, the ligand docking and binding sites of J-2156 has been elucidated in detail (Zhao et al. 2022) (Figure.5). The helical transmembrane domains (TM) and Extracellular Loops (ECL) play a key role in ligand docking and binding.

Briefly, the TMII, TMIII, and ECL1 form a binding pocket containing amino acids whose functional groups offer hydrogen bonding to the J-2156 ligand (Zhao et al., 2022) (Figure.5). After conformation changes and contractility of the helical transmembrane domains, the ligand then enters a hydrophobic pocket called the ligand binding site created by TM6, TM7, and ECL3 (Zhao et al., 2022) (Figure.5). This results in the activation of SSTR4 and subsequent signal transduction that is initiated by the G-protein trimers (Gα, Gβ, Gϒ) (Gunther et al., 2018).

SSTRs contain a conserved motif called the "DRY motif" (Gunther et al., 2018) (Figure.5). This motif is composed of three key amino acids located in the intracellular side of Sstr4 which are- Aspartic acid (D), Arginine (R), and Tyrosine (Y) (Cakir et al., 2010; Gunther et al., 2018; Bo et al., 2022). The DRY motif in Sstr4 begins from aspartic acid position 140 and ends with tyrosine position 142 (PDB: 7XMS; Gunther et al., 2018) (Figure.5). This motif is required for the physical association of G-protein trimers (Gα, Gβ, Gϒ) in order for signal transduction to be initiated (Cakir et al., 2010; Ben-Schlomo et al., 2013). Mutations in this motif have been shown to impair growth hormone secretion after SSTR2 activation through ligand binding, but in the context of Sstr4 this mutation has not been investigated (Ben-Schlomo et al., 2013). Importantly, in SSTR2 the DRY motif is also crucial for stabilizing the conformation changes of transmembrane domains during ligand binding (Zhao et al., 2002; Ben-Schlomo et al., 2013).

The C-terminal domain of SSTRs plays a critical role in receptor trafficking, internalization, and heterodimerization (Kreienkamp et al., 1998; Somvanshi et al., 2009). Complete deletion of the C-terminal tail or replacing the C-terminal of SSTR4 with that of SSTR1 results in impaired trafficking of the receptor to the plasma membrane (Somvanshi et al., 2009). However, when the C-terminal of SSTR4 was switched with the C-terminal of SSTR5, trafficking was maintained but at a reduced intensity, unlike with the SSTR1 C-terminal, which completely

prevented trafficking (Somvanshi et al., 2009). The C-terminal is also crucial for homodimerization and heterodimerization of SSTRs, which has not been extensively researched despite its importance in gene dosing with regards to cancer tumorigenesis. In HEK293 cells, SSTR4 homodimerizes with itself and heterodimerizes with SSTR5, but not with SSTR1 (Somvanshi et al., 2009). However, no heterodimerization is observed between SSTR4 and SSTR5 in CHO-K1 cells (Rocheville et al., 2000). These findings further emphasize the importance of cellular context, especially with regards to Sstr4. Rodent Sstr4 is incapable of internalization upon ligand binding until the T331A mutation in rat Sstr4 (UniProt: P30937) was introduced and tested in HEK293 cells (Kreienkamp et al., 1998). This mutation corresponds to the T332A mutation in mouse Sstr4 (UniProt: P49660) and has yet to be shown to produce the same effect.

2.4.4 Significance in Other Carcinomas

SSTRs have been investigated extensively in aspects of tumorigenesis and prognostic markers for therapeutic targeting in diverse cancers (Kumar, 2024). The major function of SSTR is to bind to somatostatin hormone (SST) which then downregulates growth hormone (GH) secretion in pituitary, thyroid stimulating hormone (TSH) production in the thyroid, and lastly, glucagon and insulin from pancreas (Patel, 1999; Kumar, 2024). The physiological function of inhibiting GH secretion is particularly important in the context of pituitary adenomas and neuroendocrine tumors (NETs) where excess GH production results in uncontrolled cell proliferation (Kumar, 2024). To counteract this, SSTR agonists such as octreotide and pasireotide that mimic biological somatostatin-14 (SS-14) and somatostatin-28 (SS-28) have been fundamental to the treatment of those cancer patients (Gueorguiev & Grossman et al., 2011; Weckbecker et al., 2003; Milewska-Kranc et al., 2024; Kumar, 2024). There are numerous SSTR

agonists that display varying levels of specificity to each subtype of SSTR which are listed in Table.1 (Milewska-Kranc et al., 2024; Gunther et al., 2018; Engstrom et al., 2005).

In the context of breast cancer, SSTR2 and SSTR5 are highly expressed in primary breast tumors (Pfeiffer et al., 2002; Vikic-Topic et al., 1995). However, a more recent study showed that SSTR4 is expressed in ~71% of patient samples obtained from a cohort of 46 primary breast tumors, and it is second to that of SSTR1 which is expressed in 90% of patient samples (Zou et al., 2019). This makes SSTR an attractive drug target. Overexpression and activation of both SSTR1 and SSTR4 in cell lines of metastatic, ductal adenocarcinoma of the breast, called MDA-MB-435S cell line, resulted in G1 cell cycle arrest which may indicate that SSTR4 exerts its tumor suppressor effects through cell cycle arrest mechanisms (Zou et al., 2019). Previous clinical trials (NCT00002967) have been initiated to investigate the therapeutic effectiveness of octreotide in combination with tamoxifen in breast cancer patients that have no nodal metastasis (N0) and are estrogen receptor positive (ER+) (Chapman et al., 2015). The results of the trial were not promising as octreotide failed to decrease disease free survival (DFS) and the trial was terminated.

Table 1: *Somatostatin and its analogues depicting varying binding affinities between different somatostatin receptors*

SSTR Ligands	Ligand Type	Binding affinities
Somatostatin-14 (SS-14)	Biological ligand	SSTR2 > SSTR5 >> SSTR3 > SSTR4
Somatostatin-28 (SS-28)	Biological ligand	SSTR2 > SSTR5 > SSTR1 > SSTR3
Octreotide	FDA approved drug	SSTR2 > SSTR5 > SSTR3 > SSTR1 > SSTR4
Pasireotide	FDA approved drug	SSTR5 > SSTR2 > SSTR3 > SSTR1 > SSTR4
Lanreotide	FDA approved drug	SSTR2 = SSTR5 > SSTR3 > SSTR1 > SSTR4
Vapreotide	FDA approved drug	SSTR2 > SSTR5 > SSTR3 > SSTR1 > SSTR4
Somatuline	FDA approved drug	SSTR2 > SSTR5 > SSTR3 > SSTR1 > SSTR4
L-803087	Synthetic Agonist	Ki; SSTR4 (0.7nM) >>> SSTR1 (199nM) > SSTR3 (1280nM) > SSTR5 (3880nM) > SSTR2 (4720nM)
J-2156	Synthetic Agonist	Ki; SSTR4 (0.8nM) >>> SSTR1 (350nM) > SSTR5 (460nM) > SSTR3 (1300nM) < SSTR2 (>5000nM)

In small cell lung cancer (SCLC) which comprises of 15% of all lung cancer, SSTR2 expression was found to be the most prominent in terms of expression when compared to other subtypes (Reubi et al., 2001). When SSTR ligands were added to SCLC cell lines such as, NCI-H69 and H-69 cell line xenografts, it reduced tumor growth and tumor associated DNA/RNA possibly through downregulation of epidermal growth factor (EGF) hormone which is a key hormone that activates Epidermal Growth Factor Receptor (EGFR) (Kiaris et al., 2001; Pinski et al., 1994). Clinical trials initiated to investigate SSTR analogues on SCLC showed no benefit, which may possibly be due to differential expression of SSTR2 in a heterogenous poorly differentiated SCLC tumor (Hejna et al., 2002; Cotto et al., 1994; Lehman et al., 2019). To date, SSTR4's involvement in lung cancer has not been investigated.

Malignant Pleural Mesothelioma (MPM) is a cancer originating from the lining of the thoracic cavity that covers the lungs. MPM is the only cancer where SSTR4 activation has shown to exhibit cytostatic effects, but only through the inhibition of CD26 (Yamamoto et al., 2014). Cluster of Differentiation 26 (CD26), also known as dipeptidyl peptidase 4 (DPP4), is an enzyme that cleaves peptides of hormones and cytokines, thereby affecting its biological activity and may function as tumor-promoting or tumor-inhibiting enzyme (Enz et al., 2019). CD26 is highly expressed in SCC of skin compared to normal skin (Kacar et al., 2012). Inhibiting the interaction of SSTR4 and CD26 combined with the activation of SSTR4 with a specific synthetic agonist L-803087 resulted in decreased cell invasion and metastasis in MPM-relevant cell lines and mouse xenograft models (Yamamoto et al., 2014). To date, no studies have thoroughly investigated the function of SSTR4 in the context of cancer initiation of HNSCC. Furthermore, the protein-protein interactions (PPIs) of Sstr4 has been studied only in HEK293 cells but not in any other cancer cell line (Christenn et al., 2007)

2.4.5 Downstream Intracellular Signaling of Sstr4

When somatostatin or its analogues bind to SSTR, the G-protein trimer (α, β, ϒ) becomes activated and dissociates from SSTR4 to carry out several possible signaling cascade events as depicted in Figure.6 (Gunther et al., 2018; Sakamoto & Frank, 2009; Milewska-Kranc et al., 2024).

2.4.5.1 The Cyclic AMP Pathway

The first pathway that SSTR4 may be involved in is the cyclic AMP pathway (Gunther et al., 2018). The activated G-alpha-inhibitory (Gαi) G-protein inhibits Adenylyl Cyclase (AC) which results in more cAMP accumulation, which is needed by Protein Kinase A (PKA) to phosphorylate Serine-133 residue of cAMP response element-binding protein (CREB) (van Keulen et al., 2017).

Phosphorylated CREB either at Ser-133 or Ser-142 is active and performs its function as a transcription factor (TF) regulating genes involved in various cellular processes such as proliferation (Moller et al., 2003; Ampofo et al., 2020; Sakamoto & Frank, 2009; Steven & Seliger, 2016). Thus, in the absence of SSTR signaling, the oncogenic transcription factor CREB is highly active. The active state of CREB is also regulated by Protein Kinase C (PKC), Phospholipase C (PLC), Mitogen-Activated Protein Kinase (MAPK), Protein Kinase B (Akt), and ERK1/2 (Sakamoto & Frank 2009; Farrell et al., 2014; Carper et al., 2022).

CREB is a major oncogenic transcription factor involved in the progression of small cell lung cancer (SCLC), leukemia, and breast cancer (Sakamoto & Frank et al., 2009; Chhabra et al., 2007). In HPV+ HNSCC, CREB is co-activated by CRTC2 resulting in increased cell proliferation (Carper et al., 2022). Whether CREB plays a central oncogenic role in the tumorigenesis of HPV- HNSCC when SSTR4 is mutated remains to be investigated.

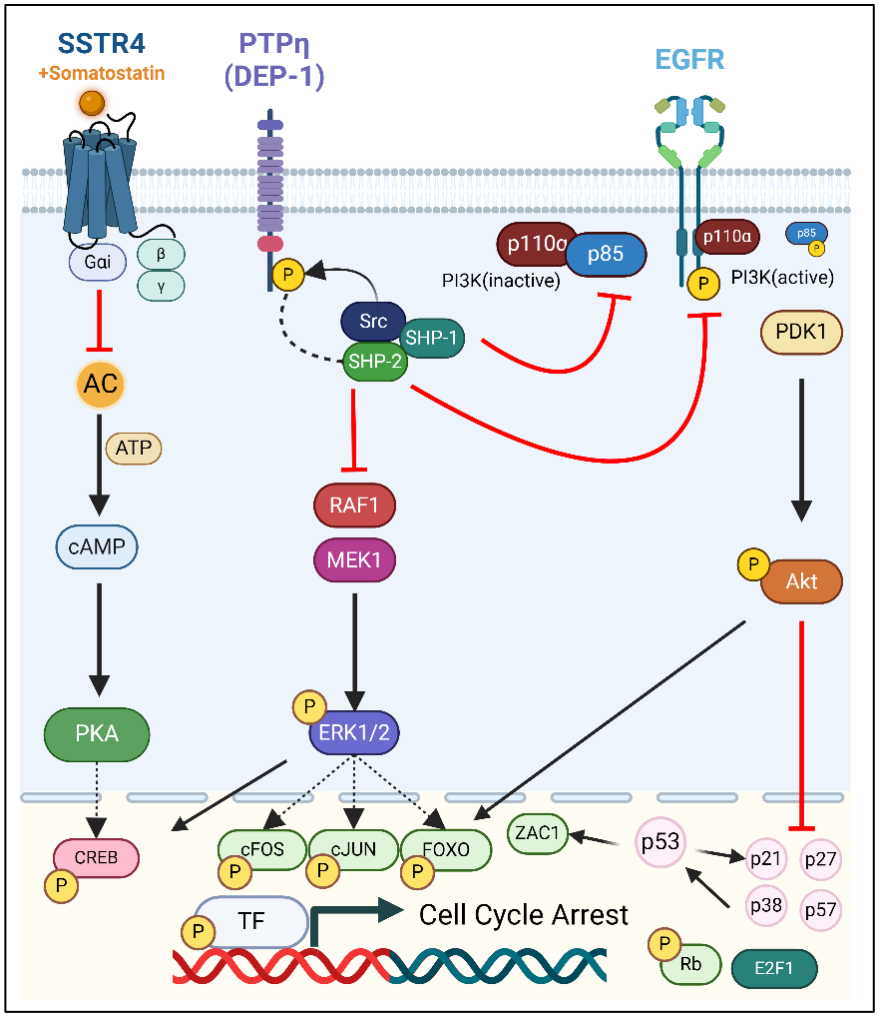

Figure 6: Summarized Intracellular Signalling of Sstr4 | All possible intracellular signaling pathways of Sstr4 made by referencing all available literature published to date irrespective of cellular context. A yellow circle with "P" indicates the action of kinases by phosphorylation of amino acids at specific residues. (Created with BioRender.com)

In leukemic cell line, CREB was shown to overexpress the transcription factor Meis1 (Sakamoto & Frank et al., 2009). Meis1 forms dimers or trimers with HOXA9 which then transcribes genes involved in cell proliferation. Meis1 is a positive regulator of tumorigenesis in esophageal squamous cell carcinoma and leukemia (Yao et al., 2021). But, in solid cancer such as NSCLC and prostate cancer, it is a negative regulator of tumorigenesis (Yao et al., 2021). The

function of Meis1 as a tumor suppressor vs oncogene is cell-type specific which depends on the expression of other TFs that it forms dimers/trimers with to carry out gene regulatory functions. One review paper mentions that Meis1 TF is expressed upon SSTR4 activation, but no primary literature supports this (Milewska-Kranc et al., 2024).

2.4.5.2 The MAPK Signalling

SSTR4 stimulation results in activation of G-proteins which activate numerous phosphotyrosine phosphatases (PTPs) and kinases. The intracellular signaling starts when c-Src is active either by autophosphorylation or by being phosphorylated by C-terminal Src Kinase (Csk) (Alba et al., 2021). For C-Src to be active, it is dephosphorylated at Y527 residue by SHP-2 (Ma et al., 2000; Alba et al., 2021). The active c-Src phosphorylates SHP-2 at specific tyrosine residues, making SHP-2 active (Mitra et al., 2008). c-Src also activates SHP-1 by phosphorylating at p-Y536 & p-Y564, and finally c-Src phosphorylates an unknown tyrosine domain of the PTP receptor, PTP-eta (PTPη) (Abram & Lowell, 2017). Thus, there is a tight regulation of activity between SHP-1, SHP-2, c-Src, and PTPη. Sstr4 activation may also activate NF-KappaB, JNK, and p38 MAPK pathways (Milewska-Kranc et al., 2024; (Kharmate et al., 2011; Florio et al., 1999). Towards the end of the SHP2-Ras-Ref-MEK1/2 MAPK signaling cascade module, ERK1/2 gets inhibited (Roskoski, 2019). (Figure.6)

If SSTR signaling is absent, ERK1/2 is activated that phosphorylates other transcription factors such as- cJUN, cFOS, FOXO (Schummer et al., 2016; Muhammad et al., 2017). cJUN transcribes other genes involved in tumorigenesis such as Cyclin D1 which promotes G1 to S phase cell cycle progression (Schummer et al., 2016; Montalto et al., 2020). More Cyclin D1 results in phosphorylation of Rb, resulting in dissociation of E2F1 TF which positively progresses cell cycle

from G1 to S phase (Abukhdeir & Park, 2008). Phosphorylated cFOS (p-cFOS) is a proto-oncogene involved in epithelial to mesenchymal transition in HNSCC (Muhammad et al., 2017). FOXO is a tumor suppressor transcription factor that initiates apoptosis and cell cycle arrest. The phosphorylation status of FOXO (p-FOXO; inactive) can also be regulated by kinases such as Akt of the PI3K pathway. (Zhang et al., 2011) (Figure.6)

2.4.5.3 The PI3K/Akt Signaling Pathway

Epidermal Growth Factor Receptor (EGFR) which is an oncogene, is amplified in HNSCC and is persistent in 38% to 47% of HNSCC cases (Stransky et al., 2011; Kalyankrishna et al., 2006). Transforming Growth Factor-α (TGF-α) binds to EGFR leading to activation of downstream oncogenic pathways such as PI3K/Akt pathway (Kalyankrishna et al., 2006). EGFR consists of 20 intracellular tyrosine kinase domains involved in a myriad of signaling functions and is thought to be an intermediary to several intracellular signalling pathways (Furcht et al., 2015). In HEK-293 cells co-transfected with SSTR1/5, the total EGFR protein and phosphorylated EGFR (p-EGFR; unknown residue) decreased in a time dependent manner upon agonist addition (Kharmate et al., 2011). In breast cancer, SHP-1/2 dephosphorylates EGFR at a tyrosine residue 1173 (Y1173), thus inhibiting the MAPK/ERK pathway which is a major oncogenic pathway in cancer (Geng et al., 2022). SHP-2 can also regulate EGFR signaling by making the p85 regulatory subunit domain of PI3K, called Pik3ca, inactive by dephosphorylating it at a certain residue (Shi et al., 2021).

Towards the end of the PI3K/Akt Pathway, increased expression levels of $p27^{Kip1}$, $p21^{Cip1}$, Zac1, p38, and p53 genes are observed as well as high amounts Retinoblastoma (Rb) proteins when SSTR4 is stimulated with an agonist (Alderton et al., 2001; Theodoropoulou et al., 2010).

$P27^{kip1}$ (Kinase inhibitory protein) is a Cyclin dependent kinase (Cdk) that is phosphorylated by Akt and functions by preventing the complex of CDK2/cyclin E and CDK2/cyclin A kinase activity thereby initiating cell cycle arrest at G1/S and terminating S Phase progression respectively (Peng et al., 2016; Ding et al., 2020). Tumor protein (TP53) is a potent effector of $p21^{cip1}$ which results in initiating G1 cell cycle arrest (Abukhdeir & Park, 2008). If Cyclin-D-CDK4/6 or Cyclin-E/CDK2 are still complexed, this will result in Rb to be phosphorylated and the subsequent release and activation of E2F1 transcription factor which will drive cell cycle progression into Synthesis (S) Phase (Abukhdeir & Park, 2008). E2F1 transcribes genes such as-Orc1, Mcm proteins, Cdc6 which are involved in DNA replication and cell cycle progression (DeGregori et al., 1995; Ohtani et al., 1999; Yan et al., 1998)

When MDA-MB-435S breast cancer cell line overexpressing SSTR1/4 was stimulated with agonist, flow cytometry data showed decreased cells in S Phase (Zou et al., 2019). Furthermore, SSTR1/4 were co-immunoprecipitated which suggests SSTRs can form heterodimers with one another (Kreienkamp et al. 1998, Somvanshi et al. 2009; Zou et al., 2019). In rat thyroid cells (PCCl3 and PC mos/PTPη) which express all SSTR1-5, the stimulation with somatostatin resulted in increased mRNA and protein expression of PTP-eta (PTPη) (Florio et al., 2001). High PTPη activity resulted in cell cycle arrest due to increased $p27^{kip1}$ (p27) (Florio et al., 2001). When Rat mammosomatotrophinoma GH3 cell line expressing SSTR2 was stimulated with Agonist, high Zac1 expression was found which upregulates Cdks such as $p57^{kip2}$ and $p21^{cip1}$ stopping cell cycle progression (Theodoropoulou et al., 2006). Though there is strong evidence to support that SSTRs function as negative regulators of cell cycle progression, it is unknown whether SSTR4 can exhibit that effect in the context of HNSCC, and if it occurs through dephosphorylation of certain tyrosine residues of EGFR remains unexplored.

In conclusion, SSTR4 stimulation may regulate multiple aspects of cellular and molecular homeostasis, including proliferation, angiogenesis, inflammation, and epigenetic regulation (Gunther et al., 2018; Theodoropoulou et al., 2006; Kharmate et al., 2011; Kumar, 2024). Other SSTRs have been established as tumor suppressors in various types of cancer (Kumar et al., 2024). To date, no study has indicated a signalling mechanism of SSTR4 in HNSCC. In this study, we aim to establish the tumor suppressor function of SSTR4 in HNSCC and to elucidate the intracellular signalling mechanism that governs it.

3 MATERIALS AND METHODS

3.1 Design and Development of Plasmid Constructs

3.1.1 sgRNA selection and design

To construct a plasmid that can efficiently target Sstr4 for knockout requires testing different single-guide RNAs (sgRNAs) against Sstr4 for estimating the knockout efficiency. By utilizing online sgRNA design databases such as CHOP-CHOP and VBC Score, five sgRNAs 23bp long were used exhibiting high predicted K.O efficiency, and non-targeting control sgRNA (sgNTC) with the sequence 5'- ACTGCCATAACACCTAACTT -3' was used. After removing the 3bp PAM recognition site, the 20bp sgRNAs were synthesized as forward (FW) oligonucleotide strand and its reverse (RV) complement oligonucleotide strand by Integrated DNA Technologies (IDT). Additional oligonucleotides were added to the respective ends that will facilitate in ligation to the overhangs created by BsmBI-V2 restriction enzyme after digestion of the lenti CRISPR v2 plasmid (Addgene #52961).

3.1.2 Sstr4-DRY and Sstr4-ORF: Gene block fragment design

The wildtype amino acid sequence of mouse Sstr4 (GenBank: AAI38488.1) was used as the reference open reading frame (ORF), and was modified to achieve the Sstr4-DRY and Sstr4-ORF stable cell lines. To obtain the Sstr4-DRY mutation, three amino acid mutations were made- D140G, R141G, and Y142G. The amino acid sequence was then reverse translated to DNA sequence. Then codon optimization was performed utilizing TWIST BioScience platform in addition with pairwise alignment tool in NCBI website to prevent the unwanted indel formation in Sstr4-DRY and Sstr4-ORF by the endogenous sgRNA that targets Sstr4. Any observable restriction enzyme sites that would hinder transgene expression downstream was removed from

the open reading frames (ORFs) sequences. To obtain the Sstr4-ORF construct, the amino acid sequence of mouse Sstr4 (GenBank: AAI38488.1) was only reverse translated to DNA sequence and codon optimized. For both the DRY and ORF gene blocks, an N-terminal HA-tag (YPYDVPDYA) DNA sequence was added for downstream experiments.

3.1.3 Cloning of sgRNAs and gene blocks to plasmids

The plasmid backbone used to achieve the Sstr4-KO sgRNA1 cell line was the lentiCRISPR v2 (Addgene #52961). Whereas the plasmid backbone used for the in-vivo mouse injection was pLKO-NLS-iCre stuffer v4 (Addgene #158032) which contained Cre-recombinase and absence of Cas9 sequence. Both plasmids had the same cloning strategy for inserting sgRNAs into filler regions of the plasmid. The lentiCRISPR v2 plasmid was digested with Esp3I to remove the 1,885bp sgRNA filler. The digested products was then separated by DNA gel electrophoresis and the expected DNA band was immediately gel purified using the GenepHlow Gel/PCR Kit (Geneaid #DFH300). The FW and RV oligos of each pair of sgRNA were annealed and phosphorylated using polymerase chain reaction (PCR) as done in previous studies (Ran et al., 2013). The digested and purified lentiCRISPR v2 vector was then ligated to each of the five annealed and phosphorylated sgRNA1-5 oligos using Hi-T4 DNA Ligase following manufacturer's protocol (NEB, #M0202L). The ligated mixture was transformed into NEB Stabl competent cells by heat shock where ampicillin was used as a selection marker to acquire bacterial colonies containing the cloned plasmid of interest on LB agar plates. The bacterial colonies were isolated and grown in 5mL LB broth overnight and then underwent plasmid DNA extraction and purification using the Presto™ Mini Plasmid Kit (PDH100). To confirm the presence of the

inserted sgRNA, all ten of the purified plasmids were sent for sanger sequencing using U6 FW primer and checking the presence of sgRNA sequences.

To construct the transgene expression plasmids with Sstr4-DRY and Sstr4-ORF constructs, the gene blocks synthesized by TWIST Bioscience were amplified by PCR using TWIST Adapters. TheLentiCas9 Blast plasmid (Addgene, #52962) was digested with NheI and BamHI and the amplified TWIST fragments of Sstr4 gene blocks were ligated to the plasmid. Following ligation, transformation, inoculation, and miniprep was commended. To validate the plasmid, sanger sequencing using FW primer for EF-1α promoter was used. The final plasmid map is illustrated in Figure.7.

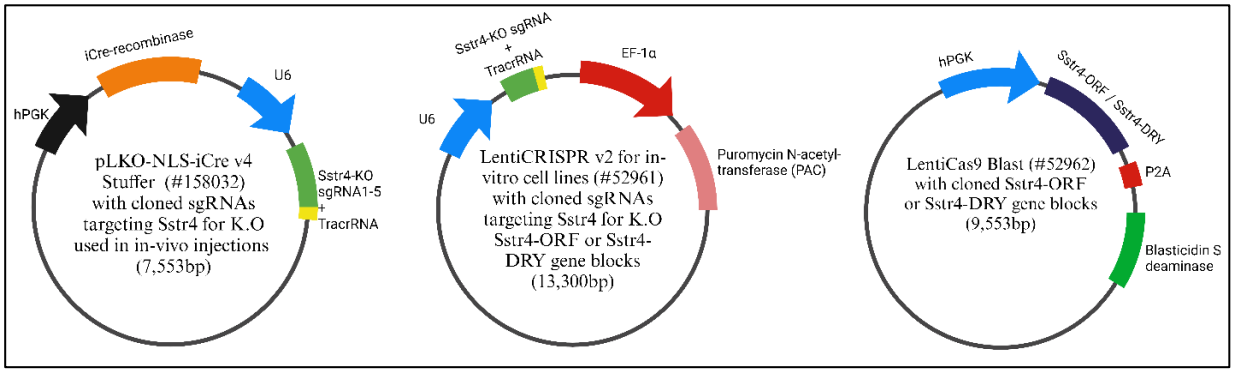

Figure 7: Plasmid Maps of Constructs Cloned | The generation of three plasmids used for downstream in-vitro and in-vivo experiments. hPGK, U6, and EF-1α are promoters that drive expression of the downstream gene fragment. Blasticidin S deaminase (BSD) and Puromycin N-acetyl transferase (PAC) are antibiotic selection markers used for lentiviral transduced cell line selection. (Created with BioRender.com)

3.2 Plasmid packaging by Lentivirus Transfection

The plasmids cloned from Lenti CRISPR v2 and LentiCas9 Blast were packaged into lentiviral vectors of low-titer which could then be used to transduce cell lines resulting in stable gene expression and expected genetic editing. For low titer lentivirus transfection to be used for cell lines, the following lentivirus packaging plasmids- psPAX2(Addgene #12260), pMD2.G

(Addgene #12259), and transfer plasmid (Sstr4-KO sgRNA1) were mixed to a picomolar (pmol) ratio of 0.169:0.0936:0.2132 in serum free media. The plasmid mixture was combined with branched polyethyleneimine (Sigma-Aldrich #408727) to a DNA:PEI ratio of 1:3 based on weight; micrograms (ug). The combined mixture was incubated for 1 hour at room temperature before being added dropwise to HEK293T cells in 6-well plates that were 70% confluent and containing serum free media (SFM), which was regular Dulbecco's Modified Eagle Medium (DMEM) without Fetal Bovine Serum (FBS) and Penicillin/Streptomycin (Pen Strep). The HEK293T cells were incubated overnight (16 hours) in SFM at 37°C and 5% CO_2. The following day the SFM was changed to complete DMEM containing 10% FBS and 1% Pen/Strep. After 48-72 hours, the lentiviral supernatant was collected and filtered through 0.45uM PES filter into 1.5mL centrifuge tubes before being stored in -80C until further use.

High-titer lentiviral vectors was made for the pLKO-Cre stuffer v4 (Addgene #158032) plasmid containing each of the five Sstr4 sgRNAs for in-vivo knockout of Sstr4 in HNSCC mouse model. The following lentivirus packaging plasmids- psPAX2(Addgene #12260), pMD2.G (Addgene #12259), and transfer plasmid (Sstr4-KO sgRNA1) were mixed to a picomolar (pmol) ratio of 1.3:0.72:1.64 in DMEM serum free media (SFM). The plasmid mixture was combined with Branched polyethyleneimine (PEI; Sigma-Aldrich #408727) to a DNA:PEI ratio of 1:3 (w/w). The combined mixture was incubated for 1 hour at room temperature before being added dropwise to HEK293T cells in six 150mm plates that were 70% confluent and contained SFM. The HEK293T cells were incubated overnight (16 hours) in SFM at 37°C and 5% CO2. The following day, SFM was changed to complete DMEM with 1% Pen/Strep and 10% FBS. The supernatant consisting of complete DMEM media with virus particles was collected after 72 hours and underwent lentiviral purification using sucrose cushion and ultracentrifugation method with a final

resuspension volume of 100uL using Cytiva HyClone 1X PBS (Cat. SH30256.FS) (Yan et al., 2023). The concentrated lentiviral packaged plasmid constructs were made into 10uL aliquots and frozen in -80C until future use for mouse embryonic in-utero lentiviral injections.

3.3 Lentivirus Transduction

The low-titer lentivirus that packaged each of the Sstr4 sgRNAs in lentiCRISPR v2 plasmid and the Sstr4 gene constructs in LentiCas9 Blast plasmid was used for lentiviral transduction of KT-CHEN cells. Approximately 300uL of each low-titer lentivirus was added to 30% confluent KT-CHEN cells in 6-well plate along with 10mg/mL polybrene stock to a final concentration of 8ug/mL polybrene (Sigma-Aldrich # H9268). The 6-well plates were then 'spinoculated' by centrifugation at 1100g for 30min. After centrifugation, the wells were washed with PBS followed by addition of E-intermediate media containing low calcium (50uM), following regular culturing conditions of primary mouse keratinocytes (Ge et al., 2017). The cells were allowed to grow for 72 hours. After 72 hours, the cells were split and selected with 2ug/mL puromycin for 72 hours with daily media change and PBS washes until no cells in the non-transduced control well was observed. The cell lines were expanded, and early passages were stored in liquid nitrogen as stocks.

The Sstr4-KO keratinocyte cell line made using sgRNA and displaying high degree of indels, was transduced with the virus packaging the Sstr4 gene block fragments, followed by selection using 4.5ug/mL of Blasticidin for 5-days with daily media change and PBS washes until no cells in the non-transduced control well was observed (Wisent, # 450-190-XL).

3.4 Knock-out efficiency quantification by Tracking of Indels by Decomposition (TIDE)

The unavailability of anti-Sstr4 primary antibody pivoted us to utilize available molecular methods to quantify gene deletion efficiency to confirm protein ablation success. After obtaining transduced and puromycin selected KT-CHEN cell lines with each of the five Sstr4-KO sgRNAs, the whole DNA content was extracted from the cell lines and PCR was done to amplify the region of the indel using 2X Taq Mastermix (FroggaBio, #FBTAQM). Approximately 250bp region upstream and downstream of the expected indel site was amplified by PCR using primers specific for each sgRNA location called 'TIDE primers' which are listed in Table.2. After PCR, the samples were sent for sanger sequencing using only the FW oligo of the TIDE primer depending on the indel location.

Table 2: *List of TIDE primers used to confirm DNA indels in Sstr4-KO sgRNA1-5 cell lines*

Guide-RNA ID	TIDE primer FW	TIDE primer RV	Amplicon (bp)	Annealing Temp. (°C)
sgRNA1	TCATCTTCGTGATCCTACGCTA	GCACGAGCCTAGTGATCTTCTT	582	60.4
sgRNA2	AGCTAATCAACCTGGGAGTGTG	ATAGTAGTCCAGGGGCTCTTCC	551	61.8
sgRNA3	GCGCTCAGAGAAGAAGATCACT	GTCCTAGGAGAGGGAGGGACTA	583	60.4
sgRNA4	GCGCTCAGAGAAGAAGATCACT	GTCCTAGGAGAGGGAGGGACTA	583	60.4
sgRNA5	AAGCTAATCAACCTGGGAGTGT	ATAGTAGTCCAGGGGCTCTTCC	552	61.8

3.5 BCA Assay and Western Blot

3.5.1 Protein Lysate Extraction

After culturing Sstr4 relevant cell lines in 6-well plates to 70-90% confluency, the 6-well plate was processed for protein and immunoassays. This was done by cell scraping following the addition of 100uL 1X RIPA Buffer (Cell Signaling Technologies, #9806) containing 1X protease inhibitor cocktail (Sigma-Aldrich, #P8340). The crude mixture was transferred to a centrifuge tube

and after brief vortexing it was kept on ice for 30min to allow further shearing of cell membrane. Centrifugation at 12,000rpm for 5min at 4°C was done to remove cell debris. The supernatant containing the total protein lysate was used for protein quantification through BCA assay.

3.5.2 BCA Assay

A small volume of the whole cell protein lysate was diluted to 1:10 ratio with a final volume of 50uL. The Pierce™ BCA Protein Assay Kits (Thermofisher Scientific, #23225) was utilized for conducting BCA assay following manufacturer's protocol. Bovine Serum Albumin (BSA) supplied in the kit was used to plot standard curves. The GloMax® Discover Microplate Reader (Promega) machine was used to measure absorbance at 560nm.

3.5.3 Protein lysate denaturation, SDS-PAGE, and Western Blot

All protein lysates were denatured in 2X SDS Sample Buffer (Laemmli buffer) containing bromophenol blue and boiled at 65°C for 5 minutes. 10 microgram (ug) amount of denatured lysates previously calculated from BCA assay were loaded in 10% polyacrylamide gel and gel electrophoresis was done for protein separation at 85V for 25min followed by 130V for 45min.

The polyacrylamide gel was assembled into a sandwich for transfer onto a 0.45uM PVDF membrane which was done at constant current of 400mA for 45min. Ponceau S staining was done for quality control which was washed with 1X TBST (0.5% Tween-20) once before imaging (Thermofisher, # A40000279). Blocking with 5% non-fat skim milk powder in TBST was done for 1 hour followed by overnight 4°C incubation with mouse Anti-HA (BioLegend, #901514) and mouse Anti-β actin (CellSignalling Technologies, # 5125S) primary antibodies at 1:4000 dilution. After three 1X TBST washes, Anti-mouse HRP detection secondary antibody (Cell Signaling

Technologies, #7076) was added at 1:6000 dilution and incubated for 1 hour. After incubation, the blot was washed three times with 1X TBST and then underwent detection. The blot was incubated in Clarity Western ECL Substrate (BioRad, #1705061) for 5 minutes in the dark room before imaging in the Invitrogen iBright 750 gel documentation machine.

3.6 RNA-Sequencing and Analysis

3.6.1 Sample processing

The Sstr4 relevant cell lines KT-CHEN, Sstr4-KO, and SStr4-ORF were cultured in 10cm plates. Only Sstr4-KO and Sstr4-ORF cell lines were incubated with 1uM of J-2156 agonist for 24 hours at 37°C and 5% CO_2. After incubation, the cell culture plates were scraped, RNA was extracted and purified using Qiagen RNeasy Plus Mini Kit (Cat. No. 74134). The purified RNA samples were sent to Novogene for library preparation and subsequent Illumina Sequencing. RNA-sequencing of each cell line was performed in duplicates

3.6.2 RNA-Sequencing

The schematic workflow of RNA-sequencing is shown in (Figure.8). Briefly, the RNA samples first went quality control (QC) through sample quantitation, integrity, and purity using the Agilent 5400 Fragment analyzer system. The RNA Integrity Number (RIN) for all samples measured from Fragment analyzer were above 9.7. After QC analysis, library preparation was done by first purifying only messenger RNAs (mRNAs) through oligo poly-T magnetic bead-based separation. Fragmentation is done to shear RNA into appropriate sizes before reverse transcription and cDNA synthesis. Non-template deoxy Adenosine monophosphate (dAMP) 3' end-tailing is done to prevent concatemer formation and efficient ligation of adapter sequences before whole

genome sequencing on the Illumina NovaSeq X Plus platform. Between 30-52 million raw reads were obtained from Sstr4 cell lines and above 80 million reads from KT-CHEN cell line.

3.6.3 Bioinformatics Analysis

The reads obtained underwent quality control using FastQC. Mapping and aligning of the reads to the reference mm10 mouse genome was done using STAR. Differential gene analysis was done using the DESeq2 R package by comparing read counts between KT-CHEN and each Sstr4 sample. After identification of DEGs for each Sstr4 cell line, the DEGs underwent functional analysis on EnrichR by inputting the upregulated and downregulated DEG sets.

3.7 Co-Immunoprecipitation Mass Spectrometry (Co-IP MS) for PPIs

The Sstr4-ORF cell line was treated with 1uM of J-2156 agonist for 6 hours before harvesting total protein lysate. The cells were scraped after addition of 500uL of Pierce IP Lysis Buffer and kept in ice for 3 hours to obtain efficient lysing and reduced degradation (Thermofisher Cat. No. 87787). The lysate was centrifuged at 12,000rpm for 5min for removal of cell debris such as lipids. The supernatant consisting of total protein lysate underwent protein pulldown assay using the Pierce Anti-HA magnetic beads pulldown assay kit (Thermofisher, Cat. No. 88836). The Sstr4-ORF containing the HA-tag was the ‘bait’ and any proteins interacting with it was considered ‘prey’. All proteins considered to be interacting with Sstr4 that were obtained towards the end of the pulldown assay were sent for mass spectrometry (MS) analysis performed by the Proteomics Core located in RI-MUHC. For controls, the PPIs obtained were contrasted with pulldown results of other HA-tag protein such as Nudt11, which is under investigation in The Loganathan Lab. A pulldown assay for the Wildtype (WT) KT-CHEN cell line was also performed to exclude random proteins obtained at the end of the pulldown assay.

(A)

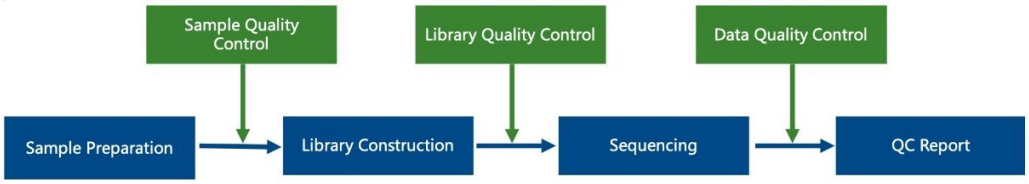

(B)

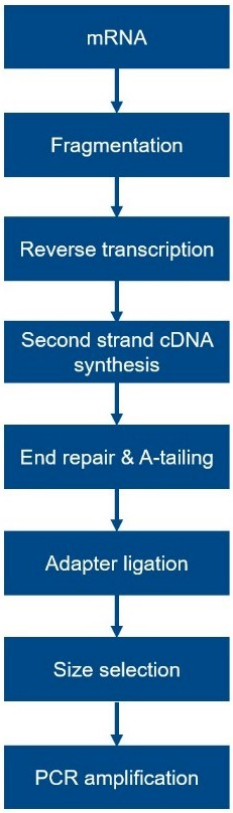

Figure 8: Pipeline of RNA-sequencing as performed by Novogene | (A) RNA quality control (QC) pipeline to test for RNA integrity and purity before library preparation. (B) Library preparation pipeline of whole RNA following QC validation of samples. Figure taken from Novogene website with permission.

3.8 Cell Proliferation Assay: Incucyte SX5

Approximately 5,000 cells were seeded in each well of a 96-well plate and were allowed to adhere to the plate surface overnight. For each specific Sstr4 cell line, a total of six replicates was done with and without J-2156 agonist to account for potential edge effect caused by media evaporation. The 96-well plate with the seeded Sstr4 cell lines was inserted into the SX5 Incucyte machine (Sartorius) where images of each well was captured every 6-hour interval till 66-hour timepoint where confluency was saturated. The image analysis was done on the Incucyte software by first quantifying cell confluency by creating cell masks. After label-free cell identification, raw values of each well for each timepoint was exported and a plot was created on R Studio for data visualization and statistical analysis. For statistical analysis, linear regression and Wilcoxon Rank Sum test was done on R Studio.

3.9 Flow Cytometry Confirming Sstr4 plays a role in G1 Cell Cycle Arrest

All sstr4 relevant cell lines were grown to 90% confluency in T25 flasks and the complete E-intermediate media was changed to DMEM/F12 while still maintaining low calcium (50uM) to prevent differentiation (Beronja et al., 2013; Li, 2012). After 24-hour incubation in SFM DMEM/F12 media for cell synchronization to G1 cell cycle phase, approximately 1.5 x 10^6 were passaged to 10cm plates containing complete E-intermediate media with or without 1uM J-2156 agonist. The remaining cells uplifted from the T25 flasks at zero timepoint were fixed with ice cold 70% ethanol for 30min, then stored in -20°C before proceeding with staining for flow cytometry acquisition. After 30-hour release into E-intermediate media, all eight plates of Sstr4 relevant cell lines were detached by adding 0.05% Trypsin/0.53mM EDTA for 20min. After

centrifugation, the cell pellets were resuspended in 2mL D-PBS. 1mL of cell suspension for each sample was fixed in 9mL of 70% ethanol with continuous vortexing.

For DNA staining, the fixed cells were centrifuged for 2000rpm for 10min and washed with DPBS twice to remove excess ethanol. The cell pellet was resuspended in 1mL DPBS and cell counting was performed on LUNA-FX7 automated cell counter (Logos Biosystems). For every 200,000 cells, 100uL of D-PBS was used for resuspension. 10mg/mL of RNAse A was added to each cell suspension for a final concentration 200ug/mL and allowed to incubate in room temperature for 1 hour. After centrifugation, the cells were resuspended in appropriate volumes of D-PBS. Propidium iodide (PI) which stains for nucleic acid was added to a final concentration of 100ug/mL and allowed to incubate in the dark for at least 5min or up to 2-hour before acquisition on BDFACS Fortessa.

Sample acquisition was performed on BDFACS Fortessa at a low flow rate and the rate of events for all samples was maintained between 50-100 events/sec. In FlowJo application, cell populations were identified with FSC vs SSC gating, doublet discrimination gating FSC-A vs FSC-H. Cell cycle analysis was done on propidium iodide positive cells (PI+) using the univariate Watson-Pragmatic modelling algorithm and adjusting the G1/G2 interval to maintain all Root Mean Square Division (RMSD) values below 2 which enforces precise modelling by FlowJo software. The values of each cell cycle phase for each Sstr4 cell line were exported to Microsoft Excel to visualize the G1 change, S change, and G2 change.

3.10 In-Vivo mouse work

3.10.1 Mouse Breeding

All in-vivo experiments work was done in the animal facility maintained at Research Institute of McGill University Health Center (RI-MUHC). All experiments were conducted following approved standard operating protocol (SOP) in accordance to animal welfare and Canadian Council on Animal Care (CCAC) guidelines (CCAC, 2009)

The entire schematic for in-vivo lentiviral injection is illustrated in Figure.9. For breeding, a male C57BL/6 mice containing a loxP-STOP-loxP (LSL) cassette in the Rosa26 (R26) locus which conditionally expresses Cas9 protein and the green fluorescent protein (GFP) in presence of Cre-recombinase was crossed with a female C57BL/6 mice containing a LSL cassette in the Rosa26 locus which conditionally expresses the oncogenic hyperactive Pik3ca^{H1047R} mutant. The Cas9 protein, GFP, and Pik3ca^{H1047R} oncogene will only be expressed when Cre-recombinase protein a fragment of the pLKO-NLS-iCre plasmid is introduced by lentiviral injection. This results in the cleavage of LSL cassettes which initiates the central dogma processing of DNA to protein resulting in induced expression of Cas9 protein, GFP, and Pik3ca^{H1047R}.

3.10.2 Ultrasound-guided in-utero lentiviral injection

After breeding of the specific mice strains, an ultrasound machine is used to identify the embryonic stage of the pregnant female mouse under general anesthesia with HEPA-filtered oxygen (O2) and isoflurane (3%). At embryonic stage 9.5 (E9.5), a visible circular structure with a white curved C-shaped body located just above the bladder signifies the E9.5 embryonic stage where the in-utero ultrasound-guided lentiviral injection is initiated. At E9.5 embryo stage, invasive open abdomen surgery is performed as done in previous studies (Beronja and Fuchs,

2013; Loganathan et al., 2020; Yan et al., 2023). The lentivirus packaging the plasmid containing Cre-recombinase and sgRNAs against Sstr4 is injected into the amniotic cavity of each of 6-8 embryos with variable volumes ranging from 100 nanoliters (nL) to 1000nL. Following injection, the incisions are sutured, and the female mouse is observed for parturition after 19-21 days. (Figure.9)

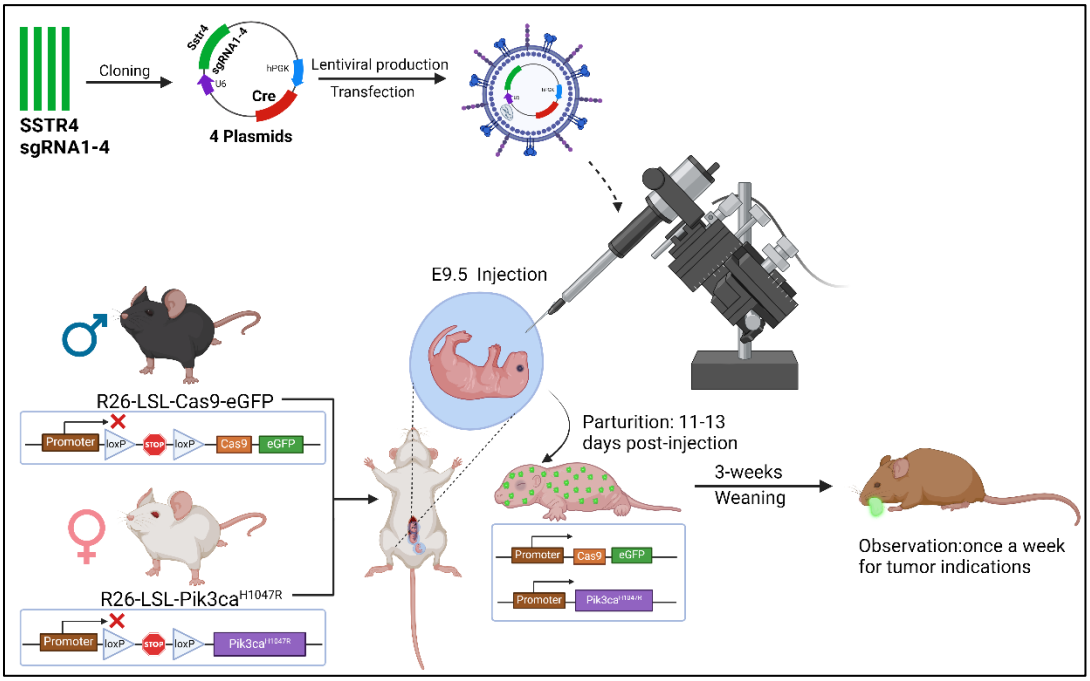

Figure 9: Schematic of in-utero ultrasound-guided lentiviral injection in HNSCC mouse model | The in-vivo model begins by breeding of the male and female mouse with the required genotype. Plasmid contains the sgRNA targeting Sstr4 for knockout. It also contains Cre-recombinase for activating oncogenic Pik3ca mutant of the embryo, GFP, and Cas9 protein to assess Sstr4 potential in tumorigenesis. Lentivirus packaging the plasmid is injected using Nanoject with volumes ranging from 100nL to 1000nL. 11-13 days post-injection, mouse pups are expected in the litter and are imaged for GFP presence on the skin. After weaning, the mice are observed for tumor formation. (Created with BioRender.com)

3.10.3 Tumor monitoring

After parturition, the outer skin of the mouse pups are imaged for GFP by epifluorescence microscope indicating the activation of Cas9-GFP by Cre-recombinase. After 10-weeks, the mice are weaned into separate cages based on their sex and are observed once a week for up to 6-months for tumorigenesis.

3.10.4 Tumor processing, embedding, sectioning, and staining

The mice showing tumors were euthanized when the tumor volume reached $1cm^3$ or the animal exhibited health conditions causing extreme discomfort that breaks guidelines established by CCAC. After euthanasia, the epidermis skin layer containing the tumor was placed on a filter paper and into a cryomold maintain orientation. Embedding was performed with OCT tissue fixative (Fisher Scientific Cat No. 23-730-571). The embedded tumors were sent to the RI-MUHC Histopathology Core for sectioning. Hematoxylin and Eosin (H&E) staining and Ki-67 proliferation marker staining was performed by the Histopathology Core at RI-MUHC.

4 RESULTS

4.1 Knockout of Sstr4 and heterozygous Pik3ca^{H1047R} mutation is sufficient to initiate HNSCC tumorigenesis in in-vivo model within 8-weeks

The functional role and significance of SSTR4 in HNSCC remains largely unexplored. Previous studies have indicated that Sstr4 may function as a tumor suppressor in HNSCC tumorigenesis (Loganathan et al., 2020). Building on previous findings, we sought to validate Sstr4 as a tumor suppressor gene and a driver mutation by evaluating its loss-of-function effects in HNSCC tumorigenesis, thereby solidifying its role in cancer initiation.

To validate Sstr4 function in HNSCC tumorigenesis, we performed in-utero lentiviral injection to induce Sstr4 gene knockout (Sstr4-KO) in the stratum basale layer of the epidermis. The stratum basale with the intended Sstr4-KO gene edit will then divide and form the remaining outer four layers of the epidermis. During in-utero lentiviral injection, eight embryos at the E9.5 stage were injected with the Sstr4-KO high titer high-titer lentivirus that was produced by lentiviral transfection.

Following successful surgery and at the end of parturition, seven mouse pups were born, each exhibiting varying levels of green fluorescent protein (GFP) expression in the epidermal layer of the skin when observed using a stereo fluorescence microscope (Figure.10A). The variability of GFP is due to the varying volumes of lentivirus injected into the amniotic cavity of the embryo. Of a total of five mice that survived and reached young adulthood, all of them were male and three formed tumors. Two of the mice that exhibited high amounts of GFP at the pup stage developed eyesight problems at approximately 38-day (~5-week) timepoint after date of birth (DOB). After 12-days, the tumor progressed rapidly into a tumor mass of greater than 1cm^3 volume near the muzzle region at 50-day (~7-week) timepoint, ultimately affecting vision and causing distress

requiring euthanasia (Figure.10B). Respective brightfield and fluorescence images taken of the tumors that formed on the muzzle region, indicated that the cause of tumor is due to proliferation of cells that contain Sstr4-KO and not due to neighboring cells in proximity of Sstr4-KO epidermal keratinocytes (Figure.10B). Furthermore, the cell boundaries could be distinguished by imaging for GFP indicating that there is a tumor ingrowth (Figure.10B) The tumors exhibited basal cell carcinoma (BCC) like appearance with Hematoxylin and Eosin (H&E) staining due to the presence of the stratum corneum layer (Figure.10C). The third and final mice developed tumors at 89-day (~13-weeks) timepoint and showed a tumor appearance near the muzzle that resembles squamous cell carcinoma (SCC) due to the scaly and reddish appearance (Figure.10D). Respective fluorescence images taken of the SCC showed an outgrowth appearance where cell boundaries could not be identified (Figure.10D). H&E staining done on the SCC mouse tumor exhibited differences in histopathology with BCC mouse tumor and more closely resembled SCC pathology with the absence of the stratum corneum layer (Figure.10E). The two of the five remaining mice that did not show tumors exhibited unexplained mortality. The HNSCC mouse model injected with a non-targeting (NTC) control sgRNA did not result in pups exhibiting tumor phenotype (Figure.10F). Sstr4-KO results in the median overall survival to ~9-weeks, and average tumor-free survival to ~8-weeks (Figure.10F). Thus, the combination of Sstr4-KO and Pik3ca^{H1047R} mutation results in rapid tumorigenesis in our HNSCC mouse model.

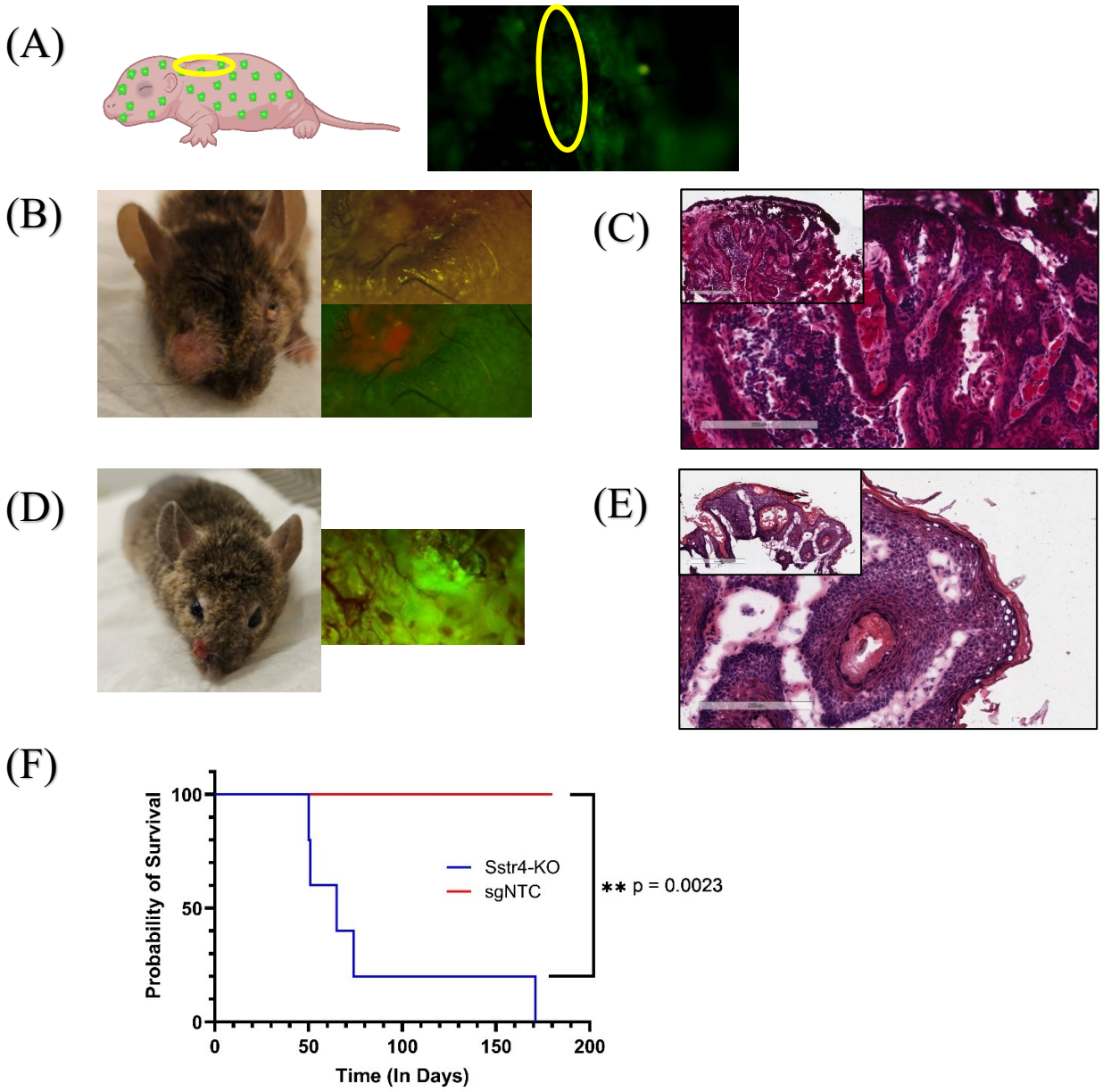

Figure 10: Sstr4-KO and heterozygous Pik3ca^{H1047R} mutation is sufficient to initiate HNSCC tumorigenesis in-vivo within 8-weeks | (A) Presence of Green Fluorescence of the skin cells of the mouse pups that were injected at E9.5 with Sstr4-KO high titer lentivirus. (B) & (C) Mouse with a tumor volume >1cm3 observed at 50-day timepoint along with representative 5X and 20X H&E staining images of the extracted tumor indicating Basal Cell Carcinoma (BCC) appearance. (D) & (E) Mouse with tumor observed at 89-day timepoint along with representative 5X and 20X H&E staining of the extracted tumor indicating Squamous Cell Carcinoma (SCC) appearance. (F) Kaplan-Meier survival curve of Sstr4-KO mice (n=5) and sgNTC (n=5). Log-Rank (Mantel-Cox) statistical test done on GraphPad Prism. $p < 0.05$. (Created with BioRender.com)

4.2 Tracking of Indels by Decomposition (TIDE) shows considerable indels in Sstr4 due to sgRNA1

After validating Sstr4 as a tumor suppressor in HNSCC mouse model, we sought to understand the functional effects of Sstr4 in the context of HNSCC and how it interacts with $Pik3ca^{H1047R}$ mutant. In order to achieve our research objective, we first aimed to establish stable Sstr4 relevant cell lines in primary mouse keratinocyte cell lines (KT-CHEN) background. To establish Sstr4 knockout (Sstr4-KO) cells, the targeting efficiency of five different single guide RNAs (sgRNAs) was tested in-vitro.

After molecular cloning, low titer lentiviral transfection, lentiviral transduction, and TIDE analysis, Sstr4-KO KT-CHEN obtained by sgRNA1 was used for subsequent experiments as significant chromatogram aberrations was observed between wildtype KT-CHEN cells (WT KT-CHEN) and KT-CHEN Sstr4-KO cells that was targeted by sgRNA1 (Figure.11A). Using the TIDE program (tide.nki.nl), the KO efficiency was quantified from the sanger sequencing chromatograms files and found to be 31.4% (Figure.11B).

We also estimated the knockout (KO) efficiency of the remaining four sgRNAs in our cell lines of interest (Table.3). Though the TIDE program displays a KO efficiency of 31.4% for sgRNA1 which is the third highest among all five, the predicted efficiency for all five sgRNAs was indicated to be between 50%-62% in sgRNA design databases such as CHOP-CHOP. Furthermore, the TIDE score is also dependent on factors such as sanger sequencing chromatogram quality and base calling rate.

Table 3: *Sequence and Sstr4 KO efficiency of sgRNAs used*

Guide-RNA ID	Sequence	Cut Site (1-1,388bp)	Predicted K.O%	Actual K.O% (TIDE)	R^2
sgRNA1	GGTGTCAGCGAAGACTGCGA	656bp	56.68%	31.40%	0.77
sgRNA2	GGGCTGGCTGGCAACAACGG	848bp	57.66%	9.50%	0.98
sgRNA3	ACTTCCGGCGCTCTTTCCAG	1067bp	61.33%	67.50%	0.82
sgRNA4	AGCGCAGGCACAGAACCCGC	1083bp	51.28%	21.90%	0.97
sgRNA5	CACTAGGCTCGTGCTAATGG	888bp	59.94%	72.40%	0.9

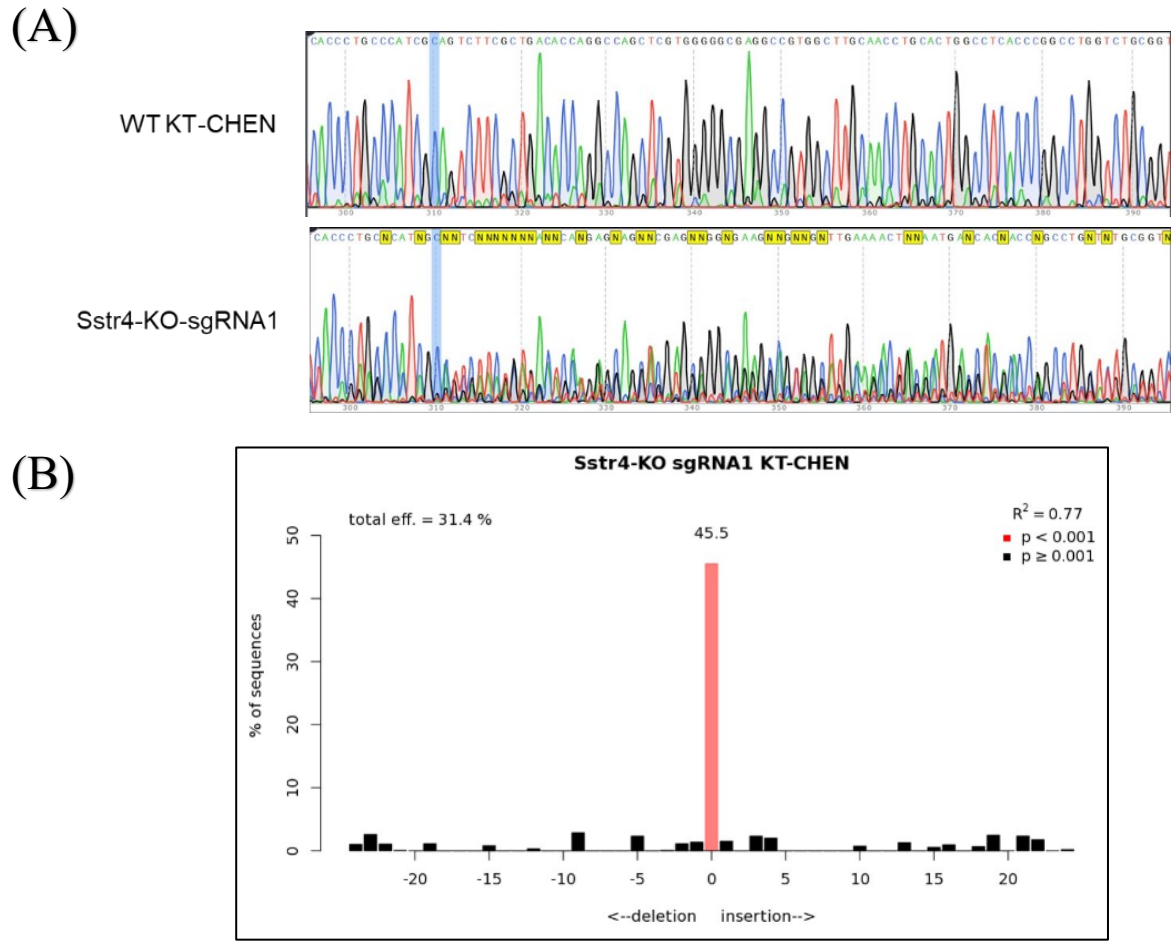

Figure 11: Tracking of Indel by Decomposition (TIDE) Analysis of sgRNA1 Sstr4-KO efficiency | (A) Chromatograms obtained from sanger sequencing after amplification of Sstr4 region around expected indel site shown for both WT KT-CHEN and Sstr4-KO sgRNA1 cells. (B) The distribution of insertions and deletions due to cleavage activity of sgRNA1 and Cas9 protein on Sstr4 region. (Tide.nki.nl).

4.3 Western Blots confirm successful generation of Sstr4 relevant cell lines for downstream research investigations

After the successful generation of Sstr4-KO cell line using sgRNA1, we sought to establish more Sstr4 relevant keratinocyte cell lines that will be utilized to further study Sstr4 in areas of signalling pathways, protein localization, biological processes, and mutational effects. The second cell line that was generated was the rescue of the Sstr4-KO genetic edit. The Sstr4-KO cell line was rescued by expressing N-terminal HA-tag wildtype Sstr4 protein through molecular cloning, lentiviral transfection, lentiviral transduction, and antibiotic selection. The cell line with the rescue of Sstr4-KO is thereafter referred to as Sstr4-ORF. Subsequently, the Sstr4-KO cell line was made to express an N-terminal HA-tagged mutant Sstr4, where the DRY motif is mutated to Glycine. This mutant Sstr4 cell lines is thereafter referred to as Sstr4-DRY.

The four Sstr4 relevant cell lines established (WT, Sstr4-KO, Sstr4-ORF, Sstr4-DRY) to study different aspects of Sstr4 function were validated by SDS-PAGE followed by western blotting with equal amount of total protein lysate loading after protein quantification done though BCA assay. Ponceau S staining done on the blot indicates successful transfer and approximately similar amount of protein lysate loaded (Figure.12A). Expression of functional Sstr4-ORF to rescue Sstr4-KO and the expression of the mutant Sstr4-DRY protein is observed by the presence of HA-tag at approximately 43kDa region (Figure.12B). Equal total protein lysate is confirmed by actin detection (Figure.12B)

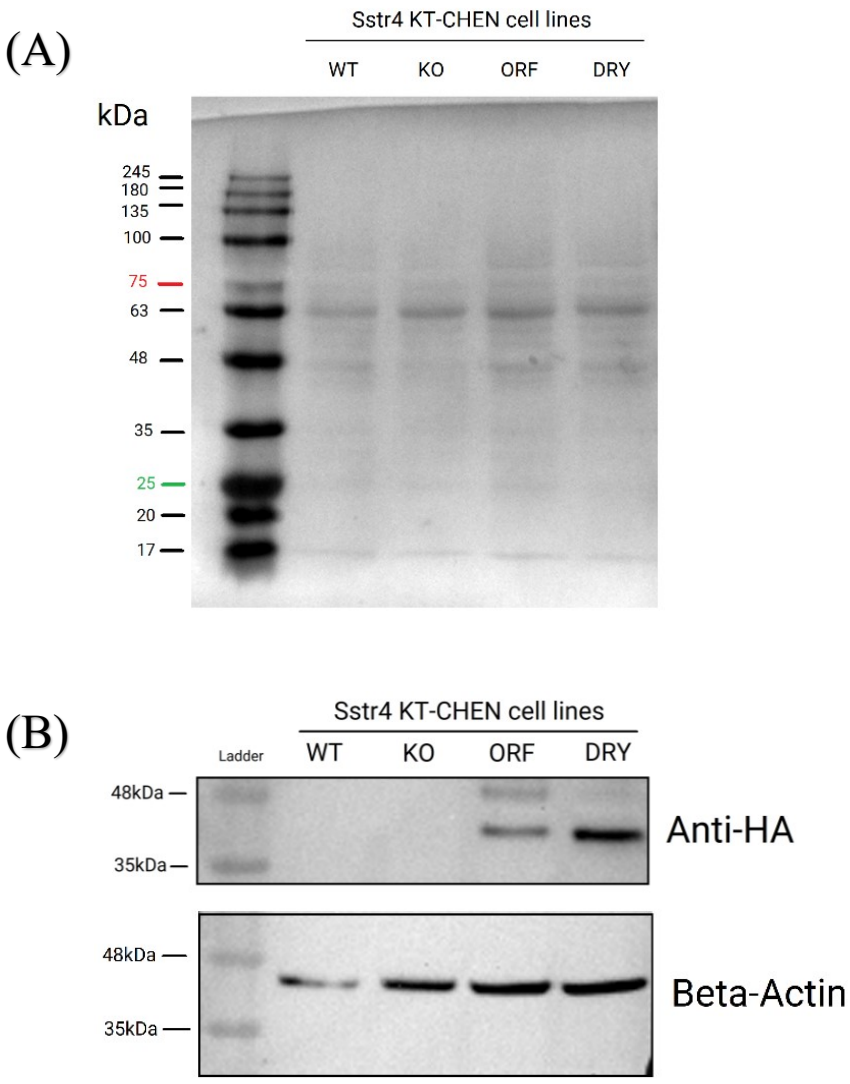

Figure 12: Validation of Sstr4 Relevant Cell Lines for Downstream Transcriptomic and Proteomic Experiments | (A) Ponceau S staining done on 0.45uM PVDF blot containing proteins transferred from SDS-PAGE. (B) Western blot of Sstr4 relevant cell lines

4.4 RNA-Sequencing Reveals Key Biological Processes and Pathways involved in Sstr4 Signaling in mouse Keratinocytes

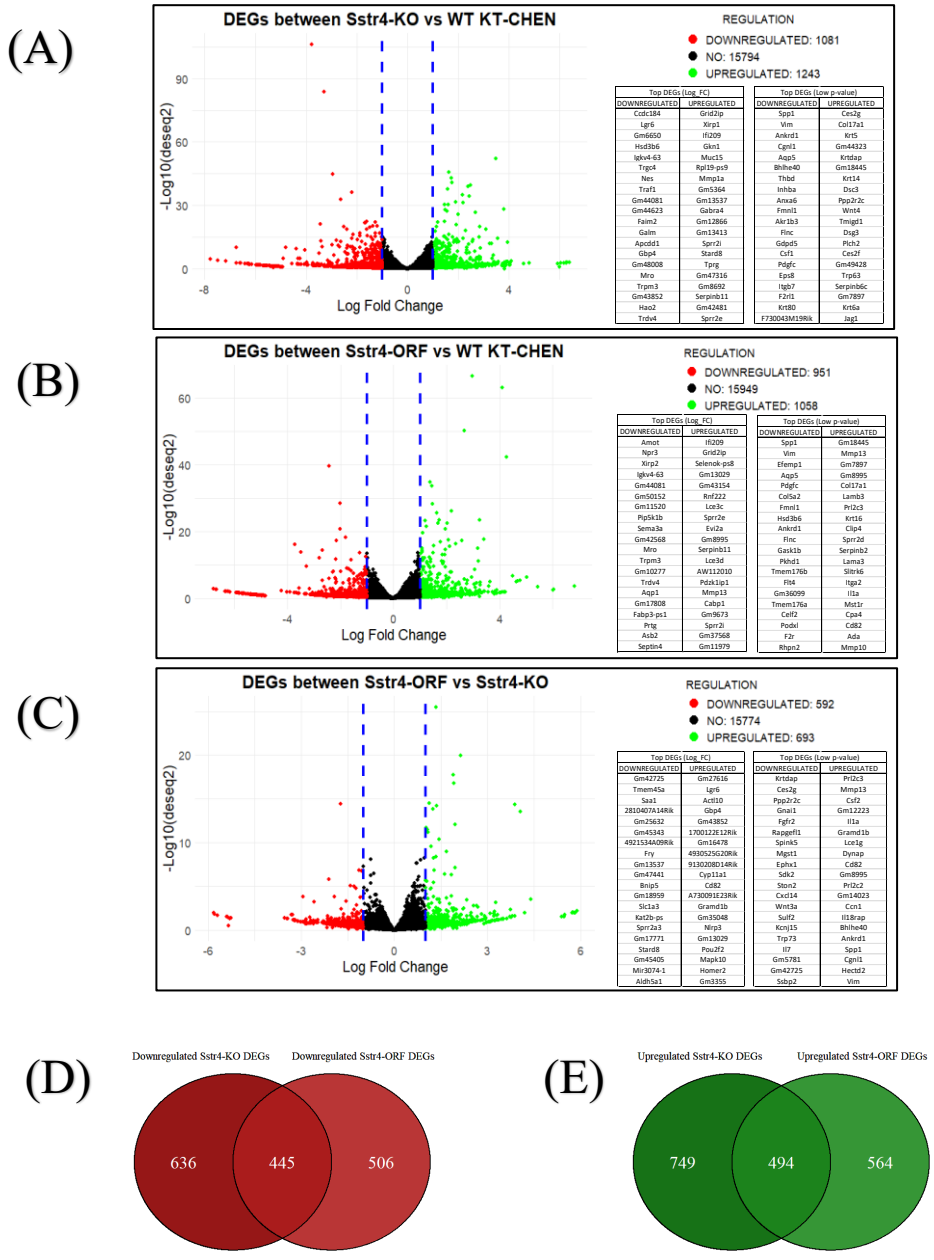

Figure 13: Volcano Plot and Venn Diagram of Differentially Expressed Genes (DEGs) in Sstr4 cell lines | Volcano Plot depicting upregulated and downregulated DEGs between WT KT-CHEN and (A) Sstr4-KO, (B) Sstr4-ORF. (C) Volcano plot depicting DEGs between Sstr4-KO and Sstr4-ORF cell lines. (D) Number of unique and common genes in downregulated DEGs between Sstr4-KO and Sstr4-ORF cell line. (E) Number of unique and common genes in upregulated DEGs between Sstr4-KO and Sstr4-ORF cell line. Plots made with R Studio.

4.4.1 RNA-Sequencing Reveals Differentially Expressed Genes (DEGs) in Sstr4 Cell Lines

To unravel the function and signalling of Sstr4 in mouse keratinocytes KT-CHEN cell line, RNA-sequencing was performed for Sstr4-KO, Sstr4-ORF (rescue), and WT KT-CHEN cell lines. For Sstr4-ORF and Sstr4-KO cell lines, 1uM of J-2156 agonist was added and incubated for 24 hours prior to RNA extraction and subsequent RNA-sequencing.

When comparing gene expression changes between Sstr4-KO and KT-CHEN, RNA-sequencing revealed thousands of differentially expressed genes (DEGs) (Figure.13A). From the volcano plot, 1081 genes were downregulated, and 1243 genes were upregulated because of Sstr4 ablation (Figure.13A). STRING analysis done of the top downregulated genes such as Cgnl1, Flnc, Fmnl1, Eps8, Itgb7, and Spp1 illustrated the role of the genes in cell-cell junctions, Extracellular Matrix (ECM) interaction, and cytoskeleton dynamics (Neri et al., 2011; Chrifi et al., 2017; Szklarczyk et al., 2023; STRING-db.org). Genes such as Jag1 and Wnt4 which are positive regulators of Wnt/beta-catenin signalling were observed to be upregulated (Rodilla et al., 2009). Whereas negative regulator of Wnt signaling genes such as Apcdd1 were downregulated (Shimomura et al., 2010). It is possible that Sstr4 may regulated cell proliferation and apoptosis through Wnt Signaling pathways. Grid2ip, a known biomarker for immune cell infiltration in colorectal cancer, was upregulated by two million-fold following Sstr4 knockout (Sstr4-KO), as revealed by DEGs analysis (Figure.13A). (Zhao et al., 2023)

When comparing gene expression changes between Sstr4-ORF and KT-CHEN, RNA-sequencing revealed equal amounts of DEGs when compared to Sstr4-KO DEGs (Figure.13B). 951 genes were downregulated, and 1058 genes were upregulated because of Sstr4 overexpression and activation (Figure.13B). Notably, genes such as Phosphatidylinositol 4-phosphate 5-kinase type-1 beta (Pip5k1b) was downregulated (Figure.13B). Pip5k1b is involved in the biosynthesis

of phosphatidylinositol 4,5- bisphosphate (PIP2) and along with Rac1 mediates cytoskeleton reorganization in prostate cancer which elucidates that Sstr4 overexpression possibly maintains cellular architecture, regulates metastasis, and regulates Akt signaling (Semanas et al., 2014; Weernink et al., 2004). Genes such as Lama3, Lamb3, and Itga2 responsible for maintaining cell attachment and adhesion to basal membrane were upregulated further highlighting Sstr4 role in cell/tissue architecture maintenance (Figure.13B) (Islam et al., 2023; Kim et al., 2013).

For quality control measure, we compared DEGs between Sstr4-ORF and Sstr4-KO and found 592 downregulated DEGs and 693 upregulated DEGs (Figure.13C). Trp73 involved in apoptosis and Krtdap required for differentiation was downregulated (Figure.13C) (Maeso-Alonso et al., 2021). Wnt3a involved in canonical Frizzled/Wnt signaling was downregulated (Figure.13C) (Shimomura et al., 2010). Other genes such as Fgfr2 involved in cell proliferation were downregulated as well (Lim et al., 2017). These downregulated genes could either be due to Sstr4 activation or ablation. On the contrary, Mapk10, Il18rap, and Nlrp3 genes involved in MAPK signaling were upregulated followed by Csf2 and Il1a involved in NF-KappaB cell signaling and chemotaxis (Yue & Lopez, 2020; Dobre et al., 2022).

To identify unique downregulated and upregulated genes, we found duplicated DEGs in downregulated and upregulated groups, comparing the Sstr4-KO and Sstr4-ORF datasets (Figure.13D). 445 DEGs were common in the downregulated group and 494 DEGs were common in the upregulated group between Sstr4-KO and Sstr4-ORF (Figure.13D and Figure.13E).

4.4.2 Gene Ontology (GO) Analysis of Biological Processes shows enrichment of genes associated with proliferation, cell-cell adhesion, and chemotaxis due to Sstr4

To investigate the functional role of Sstr4, we conducted a Gene Ontology (GO) biological processes analysis of all the 1081 downregulated and 1243 upregulated genes as a result of Sstr4-KO using Enrichr databases. We found that Sstr4-KO results in enrichment of genes related to increased chemotaxis (GO:0050919), increased differentiation (GO:0045445; GO:0048708), decreased adhesion (GO:2000048), and increased hyaluronan ECM secretion (GO:0030213) (Figure.14A & Figure.14B). Sstr4 knockout resulted in increased gene expression of Wnt4, Notch1/4, and Jag1 genes which are indicative of activated Notch1 signalling (Figure.14B) (Rodilla et al., 2009).

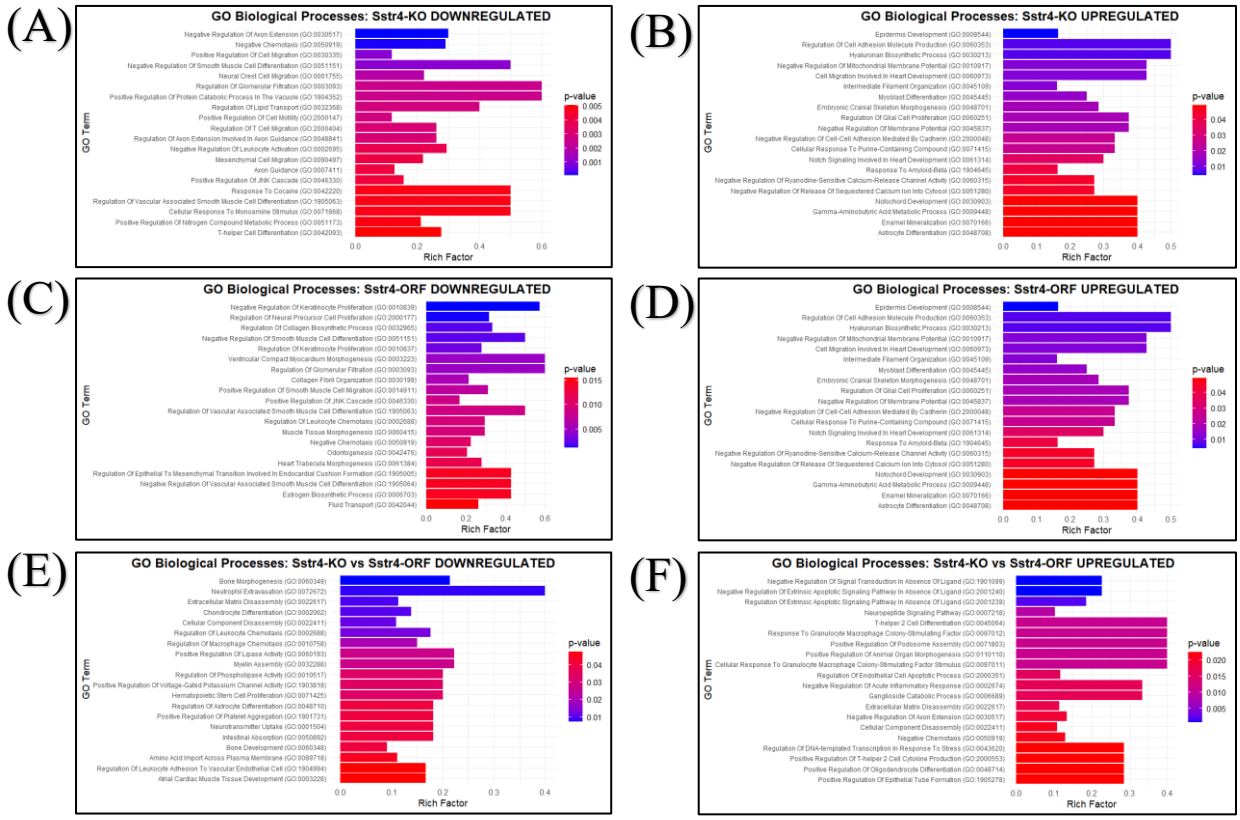

Figure 14: Gene Ontology (GO) Biological Processes Analysis of Sstr4 cell lines | GO analysis performed on Enrichr for: (A-B) Sstr4-KO vs KT-CHEN cell line. (C-D) Sstr4-ORF vs KT-CHEN cell line. (E-F) Sstr4-KO vs Sstr4-ORF cell line. GO analysis indicates possible biological functions of Sstr4 depending on the number of genes enriched for the given pathway. Plots made with R Studio.

The GO analysis data obtained from DEGs identified for the Sstr4-KO condition were cross-examined to the Sstr4-ORF condition. Sstr4-ORF showed enrichment of genes involved in keratinocyte proliferation (GO:0010839; GO:0010837) and cell adhesion regulation (GO:0060353) (Figure.14C & Figure.14D). Importantly, protein tyrosine phosphatase receptor type K (PTPRK) gene in Sstr4-ORF was largely involved for the enrichment of keratinocyte proliferation term. The downregulation of PTPRK was shown to enhance cell proliferation, enhance migration, and increase invasion in non-small cell lung cancer (NSCLC) through STAT3 pathway (Xu et al., 2019). Finally, GO analysis comparing Sstr4-KO and Sstr4-ORF did not reveal any new enrichment of biological processes (Figure.14E & Figure.14F).

4.4.3 Elsevier Pathway analysis of DEGs reveals potential involvement of Wnt/beta-catenin, TNF-alpha, and Notch1 signaling

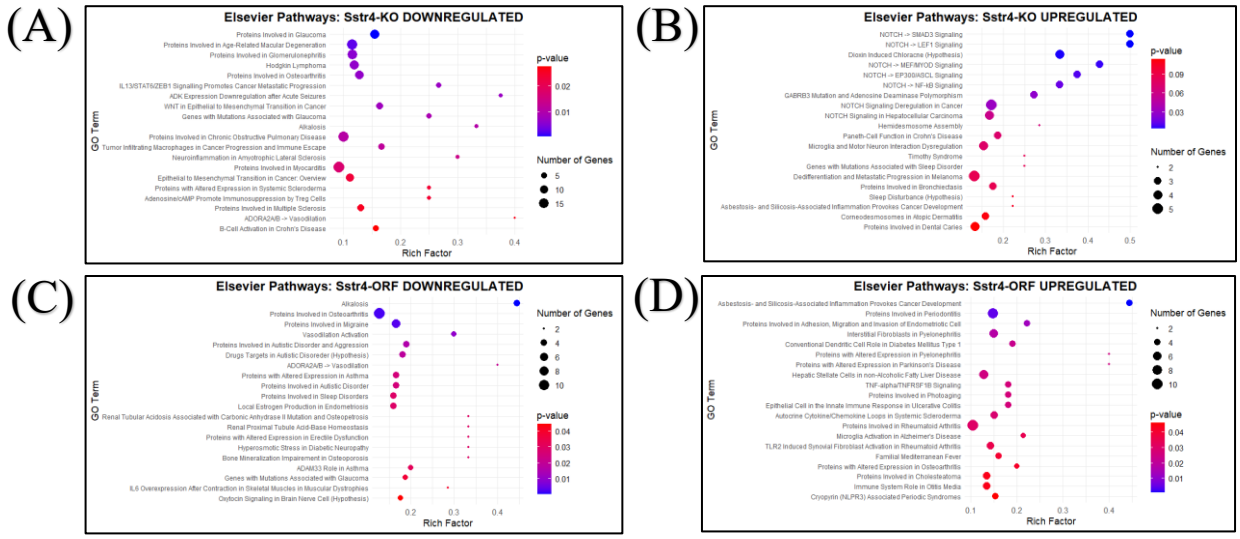

Figure 15: Elsevier Pathway analysis conducted for Sstr4 cell lines utilizing Enrichr database | Thousands of DEGs identified from the volcano plot were inputted in Enrichr database in Elsevier Pathway Analysis for downregulated and upregulated gene subsets for: (A-B) Sstr4-KO cell lines. (C-D) Sstr4-ORF cell line. Elsevier pathway analysis was done to pinpoint all the signalling pathways that are enriched depending on Sstr4 status in the cell lines. Plots made with R Studio.

Conducting Elsevier pathway enrichment analysis of all DEGs identified in the volcano plot for Sstr4 relevant cell lines, various signaling pathways were identified. While Sstr4 may not be important for regulating metastasis through epithelial to mesenchymal transition (Figure.15A), the ablation of Sstr4 showed gene enrichment in Notch signaling and NF-kappaB signaling (Figure.15B). For Notch associated signaling, upregulation of genes such as Jag1, Notch1, and DLL1 were observed repeatedly. The downregulated genes showed enrichment in immune suppression associated genes such as ENTPD1, ADORA2A, and NFATC1. This could indicate that Sstr4 activation not only modulates the cellular functions, but also displays exocrine signaling to modulate chemotaxis of infiltrating immune cells.

Analysis of the downregulated DEGs in the Sstr4-ORF condition did not reveal any significant biologically relevant changes associated with Elsevier pathway enrichment (Figure.15C). However, for Sstr4-ORF upregulated genes, TNFα pathways were enriched due to genes such as IL1B, LTA, FOS, TNF, and BIRC3 (Figure.15D). The upregulation of FOS could indicate phosphorylation of ERK1/2 which is part of the MAPK pathway through p38 activation (Sabio et al., 2014).

To summarize, the functional effects of Sstr4 activation may extend beyond regulation of cell cycle progression as observed from RNA-sequencing data. Enrichment of genes involved in regulation of various pathways were discovered such as- MAPK pathway, TNF-alpha pathway, Notch1/4 pathway, and NF-kappaB. The expression of these stress stimuli could indicate the function of Sstr4 to regulate immune cell chemotaxis and apoptosis.

4.5 Co-Immunoprecipitation Mass Spectrometry (Co-IP MS) reveals protein-protein interactions (PPIs) of Sstr4 and 14-3-3 protein family that regulate MAPK signaling and cell cycle regulation

As previous studies have elucidated the heterodimerization capability of SSTR4 with other SSTRs and EGFR, we sought to investigate if a similar effect is seen in the context of HNSCC in keratinocyte cells (Kharmate et al., 2011; Somvanshi et al., 2009). We performed Co-Immunoprecipitation (Co-IP) along with Mass Spectrometry (MS) to isolate and identify protein-protein interactions (PPIs) of Sstr4-ORF cell line in cellular context of keratinocytes after activation with 1uM of J-2156 agonist incubated for 4 hours.

Unsurprisingly, none of the protein coding genes identified as DEGs in Sstr4 cell lines through RNA-sequencing were direct interactors of Sstr4 (Figure.16A). PPI data suggests substantial involvement of the MAPK signalling and cell cycle regulation (Figure.16B). MAPK6/MAPK4 signalling was indicative through identification of PPIs such as- Taok1, Map2k3, Cdc42, and Epha2 (Figure.16B and Figure.16C).

A remarkable and novel finding was that, in mouse keratinocytes, we identified a cluster of three 14-3-3 proteins namely- 14-3-3 protein theta (θ; Ywhaq), 14-3-3 protein gamma (ɣ, Ywhaqg), and 14-3-3 protein epsilon (ε, Ywhae) (Figure.16.B and Figure.16.C). These 14-3-3 proteins associate with Sstr4 on the cytoplasmic side and do not belong to the G-protein trimer family (Yuan et al., 2019). 14-3-3 proteins have seven isoforms, are highly conserved between eukaryotes, and all eukaryotic cells have at least 1 isoform (Yuan et al., 2019). Several intracellular signalling pathways such as MAPK signaling, PI3K/Akt signaling, and Wnt signaling are also regulated by 14-3-3 proteins (Brandwein & Wang, 2017; Zhu et al., 2015).

(A)

Top hits of Sstr4 PPI					
YWHAE	NOP58	CCT4	RPL32	LSG1	CCDC127
YWHAG	NRG1	BYSL	SQSTM1	MCM5	HSPB1
CKAP4	CDC42	TAOK1	TRMT10C	EPHA2	SRP14
YWHAQ	SYNCRIP	SMNDC1	EHD1	KPNA2	TMEM33
TAF8	DDX49	RPN1	DIAPH3	FMR1	DNAJC25
MTDH	PSMC2	SFPQ	NSUN5	MLF2	MAP2K3

(B)

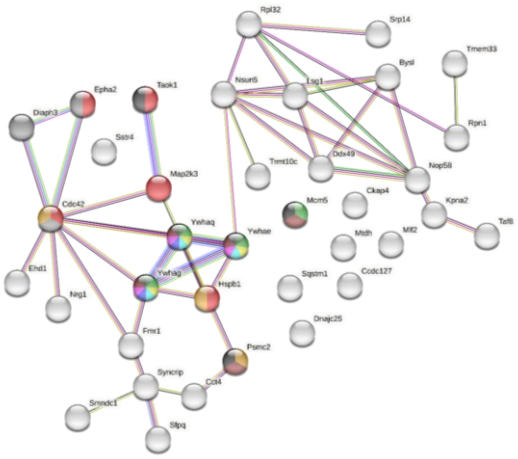

(C)

Local network cluster (STRING)

cluster	description	count in network	strength	false discovery rate
CL:6409	14-3-3 domain, and M-phase inducer phosphatase	3 of 12	2.17	0.0098

KEGG Pathways

pathway	description	count in network	strength	false discovery rate
mmu04110	Cell cycle	4 of 121	1.29	0.0192
mmu05203	Viral carcinogenesis	4 of 194	1.09	0.0377
mmu04010	MAPK signaling pathway	5 of 287	1.01	0.0209

Reactome Pathways

pathway	description	count in network	strength	false discovery rate
MMU-75035	Chk1/Chk2(Cds1) mediated inactivation of Cyclin B:Cdk1 co...	3 of 12	2.17	0.0034
MMU-111447	Activation of BAD and translocation to mitochondria	3 of 12	2.17	0.0034
MMU-9614399	Regulation of localization of FOXO transcription factors	2 of 12	1.99	0.0306
MMU-5625740	RHO GTPases activate PKNs	3 of 22	1.91	0.0034
MMU-9013408	RHOG GTPase cycle	3 of 73	1.38	0.0306
MMU-5687128	MAPK6/MAPK4 signaling	3 of 74	1.38	0.0306
MMU-5628897	TP53 Regulates Metabolic Genes	3 of 74	1.38	0.0306
MMU-69481	G2/M Checkpoints	5 of 144	1.31	0.0034
MMU-9013404	RAC2 GTPase cycle	3 of 86	1.31	0.0349
MMU-9013423	RAC3 GTPase cycle	3 of 91	1.29	0.0392
MMU-195258	RHO GTPase Effectors	6 of 243	1.16	0.0034
MMU-69620	Cell Cycle Checkpoints	6 of 265	1.13	0.0034
MMU-6791226	Major pathway of rRNA processing in the nucleolus and cyt...	4 of 176	1.13	0.0306
MMU-194315	Signaling by Rho GTPases	8 of 603	0.89	0.0034
MMU-8953854	Metabolism of RNA	7 of 599	0.84	0.0084
MMU-162582	Signal Transduction	13 of 2212	0.54	0.0069

Figure 16: Identification of Sstr4-ORF Protein-Protein Interactions (PPIs) by Pulldown Mass Spectrometry Assay | (A) List of all PPI with Sstr4 protein. (B) A Protein network map of all identified pulldown hits created using STRING-db.org. (C) Enriched pathways associated with the PPI hits of Sstr4-ORF pulldown assay. Colors to the right of the table row correlate with the filled colors in the protein network STRING map above.

The 14-3-3 proteins bind to serine/threonine phosphorylated amino acid residues of guanine nucleotide-exchange factors (GEFs) or GTPase activating proteins (GAPs) that regulate GTPases such as Rac1, Rho, and Cdc42 (Brandwein & Wang, 2017; Zhu et al., 2015; Das et al., 2015). Indeed, Cdc42 was also one of the identified hits of pulldown mass spectrometry assay (Figure.16A). Importantly, in squamous cell carcinoma (SCC), it was shown that 14-3-3ε can suppress apoptosis through Cdc25, but in laryngeal SCC it promoted apoptosis and suppressed metastasis (Zhang et al., 2024; Datta et al., 1999). 14-3-3ε protein can also regulate Wnt/β-catenin signalling, PI3K signalling, Hippo/YAP pathway, and MAPK/ERK pathway (Zhang et al., 2024; Datta et al., 1999; Pennington et al., 2018).

Besides regulating signalling, 14-3-3 proteins also regulate cell cycle progression (Figure.16C). For instance, 14-3-3ɣ can regulate G1-S and G2-M cell cycle transition by interacting with specific serine and threonine amino acid residues of p27, FOXO1, p53, and Cdc25C proteins (Hermeking & Benzinger et al., 2006). In HNSCC, it was shown that high expression of 14-3-3eta (η) protein in patient samples is positively correlated with increased apoptosis with activated and translocated intracellular inhibitor of growth gene 4 (ING4) protein (Aseervatham et al., 2022). However, in adenocarcinoma 786-0 cell line with mutated Von-Hippel Lindau (VHL) protein, inhibition of 14-3-3ε and 14-3-3θ decreases cell proliferation through reduced beta-catenin accumulation (Castaneda et al., 2017). Indeed, the regulation of cell proliferation function by different isoforms of 14-3-3 proteins is cell context dependent. Through experimental data obtained from in-vivo, RNA-sequencing, and proteomic experiments, for the Sstr4 relevant cell lines, it would be logical to presume that of the three 14-3-3 proteins identified, they likely perform pro-apoptotic and anti-proliferative functions.

4.6 Incucyte cell proliferation data indicates that functional Sstr4 limits rate of cell growth

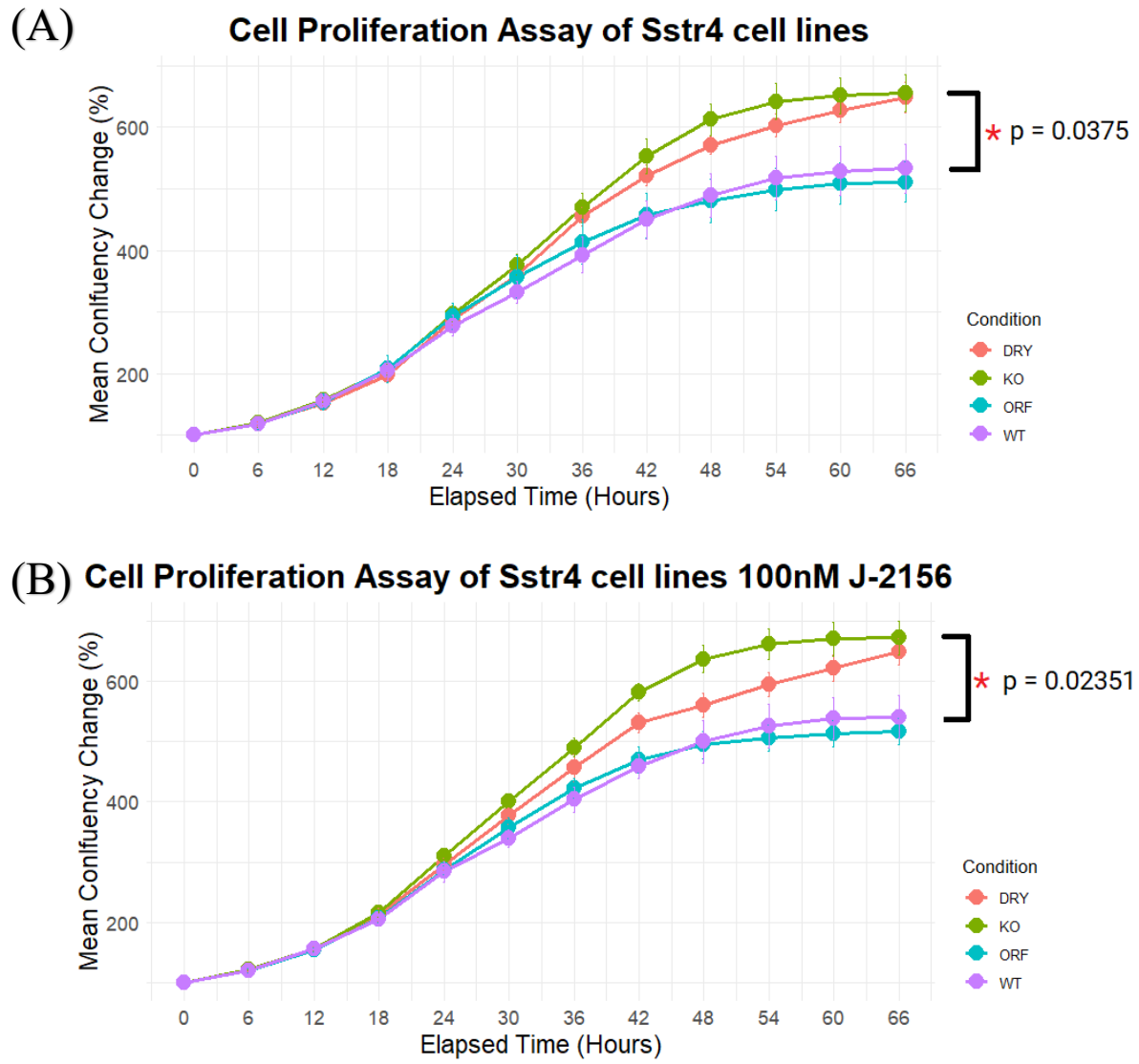

Figure 17: Cell Proliferation Assay of Sstr4 Relevant Cell Lines | (A) Cell proliferation of Sstr4 cell lines without J-2156 agonist. (B) Cell proliferation of Sstr4 cell lines in the presence of 100nM J-2156 agonist present throughout the Incucyte run. Data obtained across two biological replicates. Statistical analysis was done using Wilcoxon Rank Sum test. $p < 0.05$. Linear regression analysis ($R^2 > 0.93$) resulted in p-value <0.0005 for both with and without J-2156 agonist between Sstr4-KO vs WT.

After the identification of Sstr4's potential role in cell cycle regulation through in-vivo, transcriptomic, and proteomic data, we conducted cell proliferation assay utilizing the Incucyte SX5 machine (Sartorius). All Sstr4 relevant keratinocyte cell lines that were established previously through cloning, lentivirus transfection, lentivirus transduction, and antibiotic selection were used for this assay.

KT-CHEN cell lines that express a functional Sstr4 protein (WT, ORF), exhibited reduced cell proliferation rate compared to KT-CHEN cell lines that did not express a wildtype Sstr4 protein (KO, DRY) (Figure.17A). Importantly, Sstr4-ORF, which served as the rescue for Sstr4-KO, exhibited a cell proliferation rate comparable to that of WT KT-CHEN, indicating a successful rescue through genetic modification (Figure.17A & Figure.17B). When Sstr4 relevant cell lines were activated with 100nM J-2156 agonist at timepoint 0-hr onwards, the Sstr4-DRY cell line showed a minor yet insignificant decrease in cell proliferation when compared to Sstr4-KO and WT-KT-CHEN (Figure.17A & Figure.17B). This could indicate that the 14-3-3 proteins don't associate with the DRY motif that was mutated and can potentially exert minor anti-proliferative function. Overall, a functional Sstr4 results in decreased cell proliferation regardless of agonist treatment.

4.7 Flow Cytometry data elucidates the role of Sstr4 in G1 cell cycle arrest which is potentiated in the presence of J-2156 agonist

After validating the anti-proliferative effects of a functional Sstr4 protein in mouse keratinocytes, we next investigated if PI3K/Akt and MAPK signalling is indeed modulated by Sstr4, which regulates the activity of proteins that control cell cycle progression such as- Cyclin-D, p16, p27, and p21 (Alderton et al., 2001). We were interested in PI3K/Akt signalling for several reasons. The primary reason being that our mouse models contained a heterozygous mutation

Pik3ca^{H1047R}. The second being that the PI3K/Akt pathway contains EGFR as the key mediator through phosphorylation of amino acid residue Tyrosine-920 (Y-920) intracellular domain of EGFR by SHP-1/2 (Amelia et al., 2022). Pulldown mass spectrometry data suggests that Sstr4 regulates cell cycle at G2/M phase and 14-3-3ɣ protein regulates cell proliferation at the G1/S and G2/M cell cycle phases (Hermeking & Benzinger et al., 2006). Utilizing flow cytometry, we wanted to assess the cell cycle progression and distribution across different phases of cell cycle (G1, S, G2), and compare it between all relevant Sstr4 cell lines.

Flow cytometry data was acquired from all Sstr4 relevant cell lines after G1 cell cycle arrest and release into complete media (Figure.18A). The addition of 1uM J-2156 agonist for 30hr resulted in minor G1 arrest across all Sstr4 cell lines when comparing 30-hr timepoint with and without J-2156 agonist for each Sstr4 cell line (Figure.18A). The effect of G1 arrest was higher by 4-6% in Sstr4-KO and Sstr4-ORF cell lines when comparing release into complete media for 30hr with and without 1uM of J-2156 agonist (Figure.18A). A moderate G1 arrest was seen for Sstr4-KO cell line with the agonist, which could be explained that at high concentration of J-2156 agonist exceeding 350nM and 460nM, it will bind and activate SSTR1 and SSTR5 respectively, resulting in inhibition of cell proliferation through cell cycle arrest (Figure.18A) (Engström et al., 2005; Zou et al., 2019). Strikingly, Sstr4-DRY did not exhibit G1 arrest, but Sstr4-KO did, when activated by J-2156 agonist (Figure.18A). This finding means that the DRY motif of Sstr4 that is required for the association of G-protein trimer is required for potent G1 arrest, and 14-3-3 proteins are not sufficient for potent cell cycle arrest. Furthermore, exceeding the agonist treated concentration for the Sstr4-DRY cell line did not cause minor G1 arrest similar to Sstr4-KO cell line, this could mean that the DRY motif might affect heterodimerization or localization of the Sstr4 protein to the plasma membrane.

The G2 phases of WT, Sstr4-KO, and Sstr4-DRY were consistent when comparing release into complete media with and without the agonist (Figure.18A). However, there was a difference of 5.5% of G2 cell populations for the Sstr4-ORF cell line with and without the agonist in complete media release which indicates the presence of strong G1 arrest in presence of agonist that reduces the population of cells in G2 phase (Figure.18A).

When performing G1 cell cycle synchronization across all Sstr4 cell lines, the degree of G1 populations at 0-hr timepoint varied between 1-7% (Figure.18A). This required data analysis by observing the 'change' or 'turnover' of populations within each Sstr4 cell line (Figure.18B). The cell cycle 'turnover' is calculated by subtracting G1, S, and G2 percentages of timepoint zero with G1, S, and G2 percentages of 30-hour release with or without agonist within each Sstr4 cell line (Figure.18A & Figure.18B). Upon release of G1 arrest with 30-hour complete media, 42.6% of cells progressed out of G1 phase in WT KT-CHEN, 37.1% of cells progressed out of G1 phase in Sstr4-KO, 40.2% of cells progressed out of G1 phase in Sstr4-DRY, and 33.2% progressed out of G1 phase in Sstr4-ORF (Figure.18B). The percentage of cell cycle progression out of G1 in complete media with and without agonist remained approximately the same for WT KT-CHEN and Sstr4-DRY, but it showed an approximate 5% G1 change for Sstr4-KO and Sstr4-ORF (Figure.18B). The action of 1uM J-2156 agonist increased the G1 change by 11% (Figure.18B). No major difference in 'S phase change' with or without the agonist was observed (Figure.18B). There was a difference in 'G2 change' for Sstr4-ORF with and without agonist, however this is because of less acquisition of cells for Sstr4-ORF at timepoint 0-hour that resulted in the G2 phase population percentage to show zero (Figure.18A & Figure.18B).

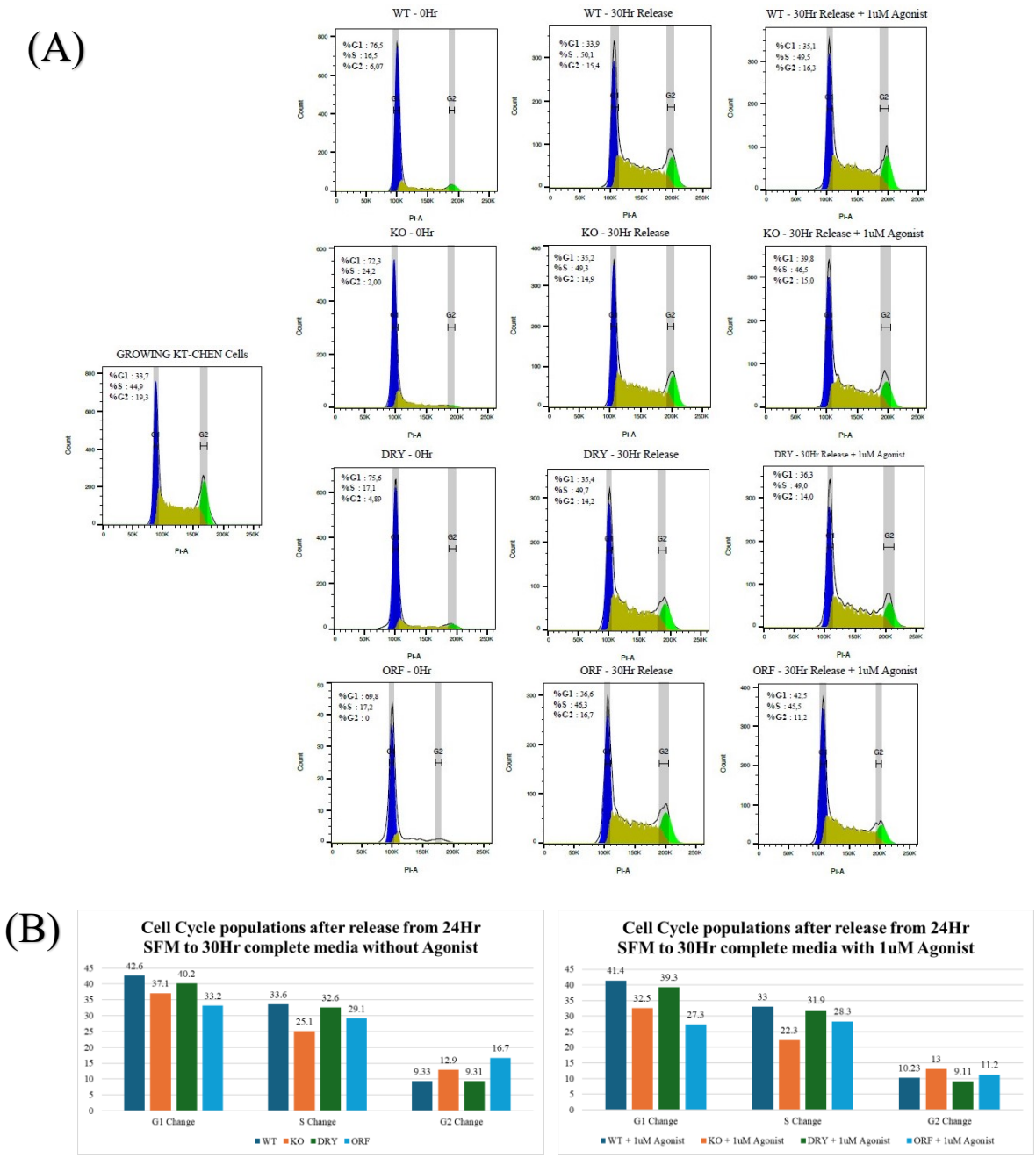

Figure 18: Flow Cytometry Analysis of G1 Arrest in Sstr4 Cell Lines | (A) Cell cycle analysis for each Sstr4 cell line at G1 arrest timepoint 0-hr and complete media release timepoint 30-hr (with/without 1uM J-2156). Identification of phases of cell cycle and modelling of the curve was done using FlowJo software and utilizing the cell cycle analysis program for modelling using Watson Pragmatic algorithm. Modelling was performed after gating for cell population, single cells, and PI+ cells. (B) Visualizing the cell cycle 'turnover' or 'change' by assessing the difference between timepoint 0-hr and 30-hr (with/without) J-2156 agonist. Plots made on FlowJo.

5 DISCUSSION

Cancer is devastating disease that is ever increasing among human populations due to processed foods, lifestyle choices, and environmental carcinogens (Barned et al., 2018; Isaken & Dankel, 2023). Current treatments for HNSCC are outdated and thus research is needed for understanding molecular pathology of HNSCC thereby identifying novel drug targets for therapeutic benefits of patients. The primary aim of this study was to investigate the role of Sstr4 in HNSCC tumorigenesis, particularly in relation to its potential as a tumor suppressor gene.

As indicated with our in-vivo experiments utilizing the ultrasound-guided in-utero lentiviral injection, our results demonstrate that the homozygous loss of Sstr4 coupled to the heterozygous mutation of $Pik3ca^{H1047R}$ is sufficient enough to initiate tumorigenesis in our mouse model. To date, most studies have investigated the tumor suppressor function of Sstr4 in cancers excluding HNSCC. However, no literature has established the tumor suppressor role of Sstr4 in addition to it as a driver of tumorigenesis, which is a novel finding in this study.

An intriguing aspect of our in vivo data is the observed heterogeneity in cancer progression. Specifically, we identified the development of two distinct forms of HNSCC: basal cell carcinoma (BCC) and squamous cell carcinoma (SCC). SCC was observed at a later timepoint than BCC despite identical genetic manipulation of cells in the epidermal layers. One possible explanation for the observation is that development of distinct forms of HNSCC depends on the cell origin. This suggests that the tumor suppressive function of Sstr4 is critical not only in the stratum spinosum/granulosum layers, but also in the stratum basale, all of which contains keratinocytes responsible for the formation of SCC and BCC, respectively. These findings emphasize the highly localized, layer-specific role of Sstr4 in HNSCC tumorigenesis.

While our in-vivo results indicated tumor formation in an immunocompetent mouse model due to Sstr4 knockout, this phenotype was not seen in all cohorts of mice. One likely explanation for this phenomenon could be due to the variable volumes of the lentivirus that was injected, this reasoning corroborates with varying intensities of GFP observed on the epidermis of pups. In the in-vivo experiment, sgNTC injected mice in a heterozygous $Pik3ca^{H1047}$ genetic background only form mild hyperplasia beyond 6-months which could not be detected due to the short span of our experimental timeline (Loganathan et al., 2020). Although our in vivo model is well-suited for studying head and neck cancer, one important consideration is that during lentiviral injection, we also genetically manipulate melanocyte cells in the stratum basale, which are the cells of origin for melanoma. Indeed, mutant $Pik3ca^{H1047R}$ has oncogenic roles in melanoma, but the physical appearance of the tumor in Sstr4-KO mice did not resemble that of melanoma (Candido et al., 2022; Xia et al., 2006). Lastly, though SSTR4 exhibits amplification in 2-4% of HNSCC patients (CBioPortal), we predict that this may be a compensatory mechanism when Sstr4 has missense mutations, as our in-vivo data suggests accelerated tumorigenesis when Sstr4 is lost.

The second aim of this study was to decipher the precise intracellular signaling mechanisms by which Sstr4 exerts its tumor suppressor function in HNSCC. While this aim was not achieved to the full extent, we still obtained crucial preliminary insights about the underlying pathways that are governed by Sstr4 signalling.

The RNA-sequencing data presented in this study provided key insights into the role of Sstr4 in mouse keratinocytes, particularly with respect to enrichment in several biological processes and pathways. The transcriptomic data revealed enrichment in biological processes related to the regulation of cell proliferation, cell adhesion, cytoskeleton organization, and multiple intracellular signaling pathways, including TNF-α, MAPK, Wnt/β-catenin, Notch, and NF-

KappaB signaling, as well as immune chemotaxis. While SSTRs have been previously implicated in cell proliferation and adhesion, particularly through the adhesion of T-cells to the extracellular matrix (ECM) and the modulation of SSTR5 signaling by the cytoskeleton actin-binding protein filamin A (FLNA), their role in immune cell infiltration through chemotaxis has not been extensively studied (Zou et al., 2019; Talme et al., 2011; Peverelli et al., 2022; Yamamoto et al., 2014; Kumar et al., 2024).

Another novel finding for Sstr4 was the enrichment of several pathways previously not reported before for Sstr4 in any cell line such as Wnt/beta-catenin, Notch, NF-KappaB, and TNF-alpha signalling (Kumar et al., 2024). SSTR2 is reported to be involved in Notch, NF-KappaB, and TNF-alpha pathways, whereas, SSTR4 has not (Kumar et al., 2024; Lehman et al., 2019; Guillermet et al., 2003; Guillermet-Guibert et al., 2007). MAPK signalling has been previously reported with regards to Sstr4 (Bito et al., 1994; Alderton et al., 2001). Wnt/beta-catenin pathway activation has not been studied as a result of SSTR activation, however, inhibition of Wnt decreased SSTR expression neuroendocrine tumors (NETs) (Weich et al., 2023).

Although the primary aim of this research was not to explore the inflammation-driven aspects of cancer initiation, it would be valuable to investigate whether the tumors that develop in the mouse models contain infiltrating T-lymphocytes or other immune cells. Future studies could utilize an inflammatory cell antibody panel (ArigoBio #ARG30326) to further explore the potential role of Sstr4 in modulating immune infiltration in tumorigenesis (Johnson et al., 2020; Li et al., 2023). The indication of inflammation was observed for both transcriptomic and proteomic data, largely through MAPK signalling involvement. In Sstr4-KO RNA-sequencing data, MAPK10 (JNK3) was upregulated, which is a kinase known to phosphorylate and activate cJUN resulting in increased cell proliferation (Pritchard & Hayward, 2013). This finding is

comparable to SSTR2 signalling pathway (Kumar et al., 2024). One in five HNSCC patients harbor activating mutations in the MAPK pathway. The novel discovery that Sstr4 knockout downregulates MAPK10 (JNK3) suggests potential for future studies to explore this as a drug target (Ngan et al., 2022).

The downregulation of PTPRK in Sstr4-ORF condition was observed. PTPRK downregulation was shown to enhance cell proliferation, enhance migration, and increase invasion in non-small cell lung cancer (NSCLC) through STAT3 pathway (Xu et al., 2019). In keratinocytes, it was shown that reduced cell-cell contacts decreased PTPRK gene expression through TGF-beta and Notch signalling (Xu et al., 2015). This finding could mean that the rapid cell proliferation due to Sstr4-KO causes hyperplasia, which is followed by sustained oncogenic signalling due to the loss of cell-cell contact and secretion of Matrix metalloproteinases (MMPs) leading to rapid tumorigenesis. It would be of interest to investigate if PTPRK also exhibits tumor suppressor effects due to Sstr4 activation that negatively regulates keratinocyte cell proliferation and invasion (Yu et al., 2009). Furthermore, the exact functional and regulatory role of PTPRK in keratinocytes could lead to further insights in Sstr4 tumor suppressor signaling pathway.

The proteomic data obtained from Co-IP MS found new PPIs for Sstr4. One major class of proteins are the 14-3-3 proteins, specifically the 14-3-3θ, 14-3-3ɣ, and 14-3-3ε. To date, no paper has shown these proteins to associate with SSTRs. While our study lacks the validation to confirm the PPI between 14-3-3 proteins and Sstr4, there is a good logical explanation. These 14-3-3 proteins associate with GPCRs such as SStr4 on the cytoplasmic side, but it is unknown if they associate with the DRY motif (Yuan et al., 2019). The cell proliferation growth assay with the Sstr4-DRY cell line in media containing 100nM J-2156 agonist, showed a slight reduction in cell

growth rate. This observation could indicate that G-protein trimers are not exclusive to Sstr4 signalling, but also the 14-3-3 proteins identified from proteomic data.

MAPK signalling in transcriptomic experiment showed enrichment due to expression of Matrix metalloproteinases (MMPs) that increase the invasiveness of tumors (Jimenez et al., 2015). The involvement of MAPK4 and MAPK6 signaling, as indicated by the proteomic data, was mediated through the effector function of 14-3-3 proteins, which regulate downstream effectors such as JNK and p38, both of which are involved in apoptosis (Kciuk et al., 2022). Future research can investigate if Sstr4 also has functional capabilities in regulating apoptosis by utilizing biomarkers such as cleaved caspase-8 antibody (Cell Signalling Technologies #8592T) (Tummers & Green, 2017).

Importantly, transcription factors (TFs) such as cFOS and FOXO1 appear downstream of MAPK kinase and its regulation is by ERK1/2 in other SSTRs signalling pathways (Sakamoto & Frank 2009; Farrell et al., 2014; Carper et al., 2022: Kumar et al., 2024). It remains unclear whether Sstr4 regulates cell proliferation via cFOS or FOXO1 through the SHP2-MAPK-ERK1/2 signaling pathway, mediated by the G-protein trimer, or through the dissociation of 14-3-3 proteins from the activated Sstr4, which subsequently modulates FOXO1 and cJUN activity (Pennington et al., 2018; Milewska-Kranc et al., 2024). Furthermore, the extent to which EGFR signalling contributes to cell proliferation alongside PI3K/Akt signaling remains unclear, as our in vivo data suggest that a synergistic interaction between mutant PI3K ($Pik3ca^{H1047R}$) and Sstr4-KO is required for HNSCC tumorigenesis.

The transcriptomic and proteomic data revealed the involvement of cytoskeleton organization in Sstr4 keratinocyte cell lines. The cytoskeleton is essential not only for maintaining the structural integrity of the epidermis but also for supporting integrin-linked kinases (ILKs),

which create a sensing network between the cytoskeleton and the extracellular matrix (ECM) to preserve cellular homeostasis (Shrivastava et al., 2015; Jimenez et al., 2015). Pip5k1b, one of the downregulated genes when Sstr4 is overexpressed, synthesizes PIP2 which can bind with Rac1 and initiate cytoskeleton rearrangement and regulate Akt signalling (Semanas et al., 2014; Weernink et al., 2004). Rac1 is a GTPase that was shown to regulate cell proliferation, migration, and NF-KappaB signalling in lung cancer (Moore et al., 1997, Gastonguay et al., 2012). 14-3-3 proteins have also been shown to regulate the active state of Rac1 by binding to serine phosphorylated residue of a Guanine nucleotide Exchange factor (GEFs) such as Tiam1 (Zhu et al., 2015). However, in the cellular context of keratinocyte, the GEF responsible for converting Rac1-GDP (inactive) to Rac1-GTP (active) remains to be discovered. GTPases such as Rac1, Ras, and Cdc42 were top hits from our proteomic analysis. These GTPases function strongly in cytoskeleton dynamics, cell proliferation, and cell migration through MAPK pathway. However, more experimental validation is needed to see how Sstr4 activates these GTPases, since the endocytosis of human SSTR4 upon activation can change cytoskeleton dynamics (Laroche et al., 2005). However, this study did not establish if mouse Sstr4 internalizes upon agonist induction. It is uncertain whether gene enrichment in cytoskeleton related genes occurred due to Sstr4 receptor internalization or Sstr4 receptor signalling.

The final aim of this study was to study the cellular function of Sstr4 examining proliferation behaviors in the cellular context of HNSCC. This was achieved by cell proliferation assay that validated the transcriptomic and proteomic data indicating Sstr4 involvement in cell proliferation. This finding aligns with several studies that indicate the role of SSTRs in cell proliferation (Ben-Shlomo et al., 2013; Theodoropoulou et al., 2006; Milewska-Kranc et al., 2024; Kumar et al, 2024). The finding that Sstr4 is involved in cell proliferation validates previous

studies, but more importantly, it confirms its role in the keratinocyte cellular context (Yamamoto et al., 2014; Somvanshi et al., 2009). Furthermore, to delineate which phase of cell cycle is being regulated by Sstr4 activation, a subsequent flow cytometry experiment was done.

Flow cytometry data indicated that Sstr4 has the ability to restrict cells to G1 phase by delaying entry to the S phase, albeit not strongly. When a potent agonist was given to activate Sstr4, the G1 arrest was more pronounced between agonist treated and non-treated group in some cell lines. In breast cancer cell lines, this was also a similar finding (Zou et al., 2019). Proteomic data indicated that G2/M phase of the cell cycle may also be regulated by Sstr4 function, which future studies can investigate.

6 SUMMARY

In this study, we validated the role of Sstr4 as a tumor suppressor in mouse models and identified key pathways and proteins potentially regulated by Sstr4 signaling. To summarize our findings of proteomic and transcriptomic data of the newly identified proteins and genes, a Sstr4 signaling pathway map is presented in Figure.19. This map describes the mechanism of HNSCC initiation mainly through cell cycle progression and MAPK signalling pathways.

Sstr4 activation results in GTPase activation such as Rac1, Ras, and Cdc42 (Figure.19). 14-3-3 proteins control the active state of these GTPases by inhibiting the PPI to their respective GEFs containing a serine phosphorylated amino acid residue (Das et al., 2015). The 14-3-3 protein family have enormous functions in several pathways including GPCR associated pathways (Kongsamut & Eishingdrelo, 2023). The dissociation of 14-3-3 proteins from the C-terminal tail of Sstr4 requires the activation of Sstr4 and intracellular trafficking by endocytosis (Li et al., 2016; Yuan et al., 2019). 14-3-3 proteins can also inhibit the translocation and hence the function TFs such as FOXO1 and Cdc25 that are involved in anti-apoptosis and G2/M cell cycle progression, which was one of the KEGG pathways identified in the proteomic experiment (Obsilova & Obsil, 2022). The MAPK pathway is regulated by the three GTPases identified, and each has specific intermediary MAP4K, MAP3K, MAP2K, and MAPK proteins associated with it (Pritchard & Hayward, 2013; Kciuk et al., 2022; Cicenas et al., 2018). The Rac1 pathway activates TFs such as cJUN and SP1 through the MAPK/JNK pathway, resulting in increased cell proliferation by G1/S progression and epigenetic changes (O'Connor et al., 2016; Schummer et al., 2016). The Ras pathway activates TFs such as cFOS and cJUN through the canonical MAPK/ERK signaling, where the ERK1/2 active state can also be regulated by the third GTPase Cdc42 (Xiao et al., 2018;

Muhammad et al., 2017; Kciuk et al., 2022). Cdc42 is involved in regulating both JNK and ERK proteins and also regulated downstream effectors such as PAK, IQGAPs, and N-Wasp proteins involved in Proliferation, metastasis, and actin reorganization (Tomasevic et al., 2007; Byrne et al., 2016). Map2k3, identified as a PPI hit, acts downstream of the Cdc42 protein that controls ERK1/2 activation (Pritchard & Hayward, 2013). Cdc42 can also regulate the PI3K pathway and p38 MAPK activity, both of which are involved in various immune signaling and cell proliferation pathways in response to stressors such as hypoxia, DNA damage, and metabolic stress (Pennington et al., 2018).

While our study did not reveal any evidence of EGFR involvement in Sstr4 signalling, we speculate that it may be of importance. The tyrosine residue 845 (Y-845) of EGFR plays a crucial role in regulating actin reorganization, cell proliferation, metastasis, and apoptosis via Src, through the activation of Wnt/β-catenin, MAPK signalling, and PI3K signaling pathways, which are mediated by Focal Adhesion Kinases (FAKs) (Kanteti et al., 2016; Amelia et al., 2022). Actin rearrangement can also be regulated by Rac1 and Wasp (Byrne et al., 2016). EGFR also regulates PI3K/Akt signalling activity through its Y-920 residue (Amelia et a., 2022). The Y-1173 residue can also inhibit the activity of SHP2 thereby activating all three GTPases resulting in sustained cell proliferation and actin rearrangement signalling (Amelia et al., 2022; Ortiz et al., 2024). PTPRK which showed enrichment in keratinocyte proliferation GO term for Sstr4-ORF cell line is involved in regulating EGFR, and PTPRK's downregulation results in NSCLC cancer progression (Xu et al., 2019; Ortiz et al., 2024). The Y-1068 and Y-1086 residue also regulates the MAPK/ERK pathway through Ras GTPase (Figure.19) (Amelia et al., 2022).

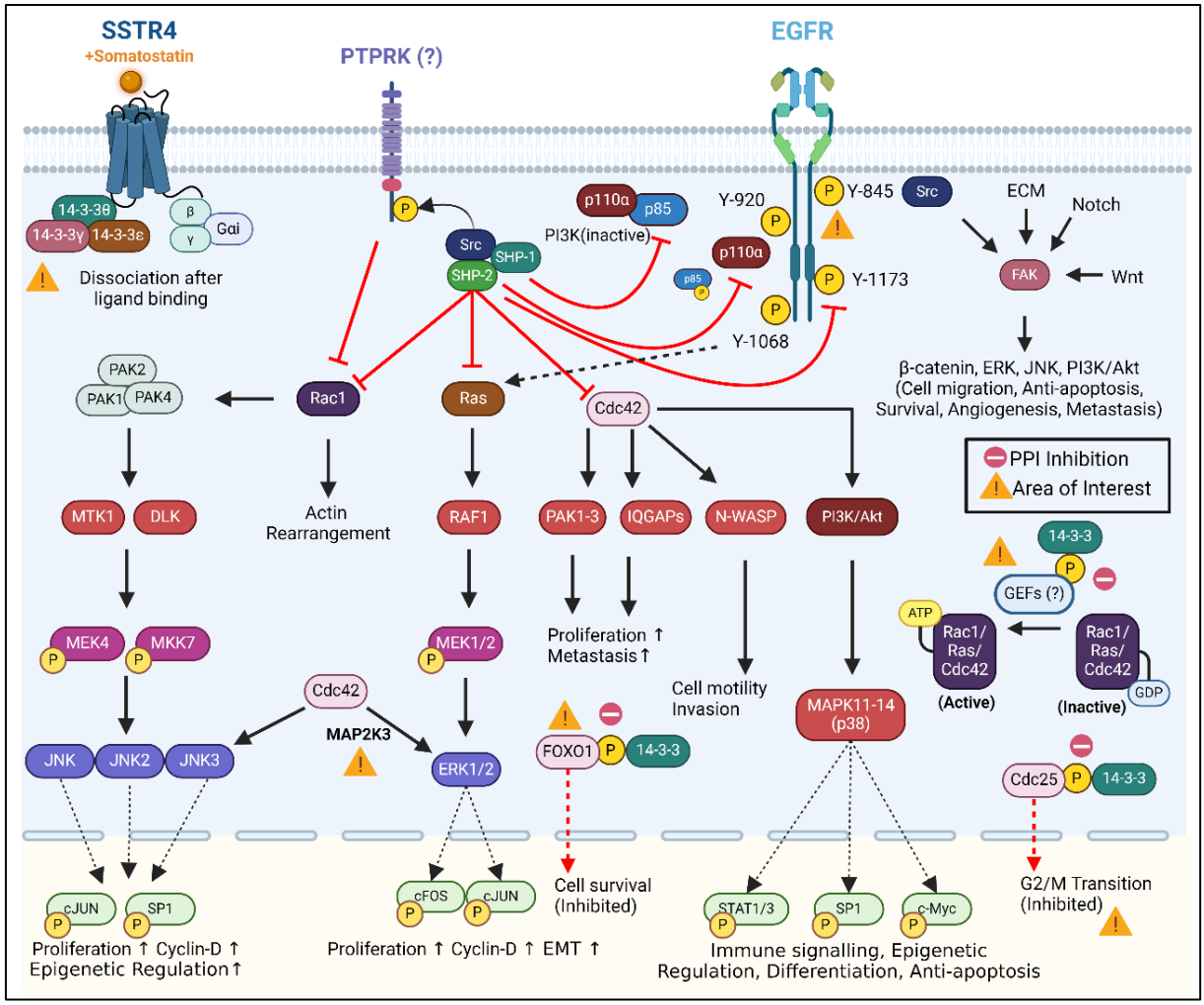

Figure 19: Comprehensive Intracellular signalling map of activated Sstr4 encompassing newly identified signalling pathways and PPI interactors | The figure illustrates Sstr4 signalling with regards to MAPK pathway and cell cycle regulation. The 14-3-3 proteins identified as Sstr4 PPIs are a novel finding that control the active state of GTPases such as Rac1, Rho, and Cdc42 by binding to their GEFs on serine residues (shown right). Rac1 activation leads to MAPK/JNK signalling whereas for Ras it leads to MAPK/ERK signalling. 14-3-3 proteins also inhibit the translocation of FOXO1 and Cdc25 TFs that increase cell cycle progression. The MAPK pathway is also regulated by the inter-communication of EGFR and PI3K pathway. Sstr4 activation may also influence actin cytoskeleton dynamics through the Rac1 pathway or the EGFR-FAK pathway. FAK is regulated by several upstream pathways such as Notch, Wnt, and ECM that can influence downstream effectors such as β-catenin, ERK, JNK, and PI3K/Akt pathway. The minus symbol in red circle indicates inhibition of PPI. The exclamation symbol in orange triangle indicates novel proteins identified in this study and potential areas of interest to investigate. (Created with BioRender.com)

7 FUTURE DIRECTIONS

While our study has pinpointed potential pathways of Sstr4 signalling in tumor suppression, validation of our predicted signalling is needed. Conducting immunoassays for 14-3-3 proteins, EGFR tyrosine phosphorylation sites, transcription factors (cJUN/SP1/cFOS/FOXO1), MAPK signalling proteins (ERK1/2, p38) can elucidate which key signalling pathways are activated in the presence or absence of the Sstr4 agonist.

Proteomic data indicated that G2/M phase of the cell cycle may also be regulated by Sstr4 function. Future experiments can study the G2 arrest in Sstr4 cell lines by a similar flow cytometry experiment as done in this study. G2 synchronization will be done by nocodazole treatment for 16-hours at 100 ng/mL concentration. After G2 arrest, the cells will be released into complete media with/without agonist for 16-hours since G2 phase of cell cycle is much shorter compared to G1 phase (Yiangou et al., 2019).

While GTPases like Rac1, Ras, and Cdc42 are not druggable targets, it would still of interest to investigate which specific GEF binds to the 14-3-3 proteins resulting in the negative regulation of GTPases, thereby discovering novel drug targets against major hubs of oncogenic signalling (Bannoura et al., 2024).

The major finding of two distinct pathology of HNSCC namely SCC and BCC can be further investigated by exploring if cell proliferation or loss of cell polarity due to cytoskeleton rearrangement leads to tumorigenesis. PTPRK promotes cell-cell adhesion between the epithelial cells, and the loss of cell adhesion can enhance Wnt signalling leading to Epithelial to Mesenchymal Transition (EMT) (Young et al., 2024). As explained previously, PTPRK can also regulate EGFR activity, which further downstream is also regulated by FAK activity (Ortiz et al., 2024). Future experiments can utilize EGFR antagonist such as cetuximab, to study the synergistic

interaction between Sstr4 signalling and EGFR tyrosine kinase domains. To conclude, future research should explore whether the loss of cell adhesion or alterations in cell polarity also play a contributory role in HNSCC tumorigenesis besides cell proliferation.

8 CONCLUSION

The purpose of this study was to understand the function of Sstr4 in HNSCC, which was an area previously unexplored. Through the development of in vitro models employing precise cellular context in addition to the in vivo model, we have made significant contributions to the understanding of Sstr4's involvement in HNSCC tumorigenesis.

In conclusion, the insights gained from this study not only deepen our understanding of Sstr4's tumor suppressor role in HNSCC, but also pave the way for future research to uncover novel therapeutic targets that may alter the course of HNSCC progression in patients.

9 BIBLIOGRAPHY

Abati, S., Bramati, C., Bondi, S., Lissoni, A., & Trimarchi, M. (2020). Oral Cancer and Precancer: A Narrative Review on the Relevance of Early Diagnosis. *International Journal of Environmental Research and Public Health*, *17*(24), 9160. https://doi.org/10.3390/ijerph17249160

Abram, C. L., & Lowell, C. A. (2017). Shp1 function in myeloid cells. *Journal of Leukocyte Biology*, *102*(3), 657–675. https://doi.org/10.1189/jlb.2MR0317-105R

Abukhdeir, A. M., & Park, B. H. (2008). P21 and p27. *Expert Reviews in Molecular Medicine*, *10*, e19. https://doi.org/10.1017/S1462399408000744

Agrawal, N., Frederick, M. J., Pickering, C. R., Bettegowda, C., Chang, K., Li, R. J., Fakhry, C., Xie, T.-X., Zhang, J., Wang, J., Zhang, N., El-Naggar, A. K., Jasser, S. A., Weinstein, J. N., Treviño, L., Drummond, J. A., Muzny, D. M., Wu, Y., Wood, L. D., … Myers, J. N. (2011). Exome Sequencing of Head and Neck Squamous Cell Carcinoma Reveals Inactivating Mutations in NOTCH1. *Science*, *333*(6046), 1154–1157. https://doi.org/10.1126/science.1206923

Alba,J., Montagna, M., & D'Abramo, M. (2021). Modelling the Activation Pathways in Full-Length Src Kinase. *Biophysica*, *1*(2), Article 2. https://doi.org/10.3390/biophysica1020018

Alderton, F., Humphrey, P. P. A., & Sellers, L. A. (2001). High-Intensity p38 Kinase Activity Is Critical for p21 cip1 Induction and the Antiproliferative Function of Gi Protein-Coupled Receptors. *Molecular Pharmacology*, *59*(5), 1119–1128. https://doi.org/10.1124/mol.59.5.1119

Amberg, N., Holcmann, M., Glitzner, E., Novoszel, P., Stulnig, G., & Sibilia, M. (2015). Mouse Models of Nonmelanoma Skin Cancer. In R. Eferl & E. Casanova (Eds.), *Mouse Models of Cancer: Methods and Protocols* (pp. 217–250). Springer. https://doi.org/10.1007/978-1-4939-2297-0_10

Amelia, T., Kartasasmita, R. E., Ohwada, T., & Tjahjono, D. H. (2022). Structural Insight and Development of EGFR Tyrosine Kinase Inhibitors. *Molecules*, *27*(3), Article 3. https://doi.org/10.3390/molecules27030819

Ampofo, E., Nalbach, L., Menger, M. D., & Laschke, M. W. (2020). Regulatory Mechanisms of Somatostatin Expression. *International Journal of Molecular Sciences*, *21*(11), 4170. https://doi.org/10.3390/ijms21114170

Aseervatham, J. (2022). Interactions between 14-3-3 Proteins and Actin Cytoskeleton and Its Regulation by microRNAs and Long Non-Coding RNAs in Cancer. *Endocrines*, *3*(4), Article 4. https://doi.org/10.3390/endocrines3040057

Bannoura, S. F., Khan, H. Y., Uddin, M. H., Mohammad, R. M., Pasche, B. C., & Azmi, A. S. (2024). Targeting guanine nucleotide exchange factors for novel cancer drug discovery. *Expert Opinion on Drug Discovery*, *19*(8), 949–959. https://doi.org/10.1080/17460441.2024.2368242

Barnes, J. L., Zubair, M., John, K., Poirier, M. C., & Martin, F. L. (2018). Carcinogens and DNA damage. *Biochemical Society Transactions*, *46*(5), 1213–1224. https://doi.org/10.1042/BST20180519

Ben-Shlomo, A., Pichurin, O., Khalafi, R., Zhou, C., Chesnokova, V., Ren, S.-G., Liu, N.-A., & Melmed, S. (2013). Constitutive Somatostatin Receptor Subtype 2 Activity Attenuates GH Synthesis. *Endocrinology*, *154*(7), 2399–2409. https://doi.org/10.1210/en.2013-1132

Beronja, S., & Fuchs, E. (2013). RNAi-Mediated Gene Function Analysis in Skin. *Methods in Molecular Biology (Clifton, N.J.)*, *961*, 351–361. https://doi.org/10.1007/978-1-62703-227-8_23

Bito, H., Mori, M., Sakanaka, C., Takano, T., Honda, Z., Gotoh, Y., Nishida, E., & Shimizu, T. (1994). Functional coupling of SSTR4, a major hippocampal somatostatin receptor, to adenylate cyclase inhibition, arachidonate release and activation of the mitogen-activated protein kinase cascade. *The Journal of Biological Chemistry*, *269*(17), 12722–12730.

Brandwein, D., & Wang, Z. (2017). Interaction between Rho GTPases and 14-3-3 Proteins. *International Journal of Molecular Sciences*, *18*(10), 2148. https://doi.org/10.3390/ijms18102148

Brenner, D. R., Poirier, A., Woods, R. R., Ellison, L. F., Billette, J.-M., Demers, A. A., Zhang, S. X., Yao, C., Finley, C., Fitzgerald, N., Saint-Jacques, N., Shack, L., Turner, D., & Holmes, E. (2022). Projected estimates of cancer in Canada in 2022. *CMAJ*, *194*(17), E601–E607. https://doi.org/10.1503/cmaj.212097

Brizuela, M., & Winters, R. (2024). Histology, Oral Mucosa. In *StatPearls*. StatPearls Publishing. http://www.ncbi.nlm.nih.gov/books/NBK572115/

Byrne, K. M., Monsefi, N., Dawson, J. C., Degasperi, A., Bukowski-Wills, J.-C., Volinsky, N., Dobrzyński, M., Birtwistle, M. R., Tsyganov, M. A., Kiyatkin, A., Kida, K., Finch, A. J., Carragher, N. O., Kolch, W., Nguyen, L. K., von Kriegsheim, A., & Kholodenko, B. N. (2016). Bistability in the Rac1, PAK, and RhoA Signaling Network Drives Actin Cytoskeleton Dynamics and Cell Motility Switches. *Cell Systems*, *2*(1), 38–48. https://doi.org/10.1016/j.cels.2016.01.003

Canadian Cancer Statistics Advisory Committee in collaboration with the Canadian Cancer Society, Statistics Canada and the Public Health Agency of Canada. Canadian Cancer Statistics 2021. Toronto, ON: Canadian Cancer Society; 2021. From- cancer.ca/Canadian-Cancer-Statistics-2021-EN, accessed [15 September 2024].

Canadian Cancer Statistics Advisory Committee in collaboration with the Canadian Cancer Society, Statistics Canada and the Public Health Agency of Canada. Canadian Cancer Statistics 2023. Toronto, ON: Canadian Cancer Society; 2023. From- cancer.ca/Canadian-Cancer-Statistics-2023-EN, accessed [15 September 2024].

Canadian Council on Animal Care. (2009). Canadian Council on Animal Care. ISBN: 978-0-919087-50-7. Retrieved from http://www.ccac.ca

Candido, S., Salemi, R., Piccinin, S., Falzone, L., & Libra, M. (2022). The PIK3CA H1047R Mutation Confers Resistance to BRAF and MEK Inhibitors in A375 Melanoma Cells through the Cross-Activation of MAPK and PI3K-Akt Pathways. *Pharmaceutics*, *14*(3), 590. https://doi.org/10.3390/pharmaceutics14030590

Cakir, M., Dworakowska, D., & Grossman, A. (2010). Somatostatin receptor biology in neuroendocrine and pituitary tumours: Part 1 – molecular pathways. *Journal of Cellular and Molecular Medicine*, *14*(11), 2570–2584. https://doi.org/10.1111/j.1582-4934.2010.01125.x

Camacho, C., Coulouris, G., Avagyan, V., Ma, N., Papadopoulos, J., Bealer, K., and Madden, T.L. 2009. BLAST+: architecture and applications. BMC Bioinformatics, 10, 421.

Carbone, A. (2020). Cancer Classification at the Crossroads. *Cancers*, *12*(4), 980. https://doi.org/10.3390/cancers12040980

Carper, M. B., Goel, S., Zhang, A. M., Damrauer, J. S., Cohen, S., Zimmerman, M. P., Gentile, G. M., Parag-Sharma, K., Murphy, R. M., Sato, K., Nickel, K. P., Kimple, R. J., Yarbrough,

W. G., & Amelio, A. L. (2022). Activation of the CREB Coactivator CRTC2 by Aberrant Mitogen Signaling promotes oncogenic functions in HPV16 positive head and neck cancer. *Neoplasia (New York, N.Y.)*, *29*, 100799. https://doi.org/10.1016/j.neo.2022.100799

Castañeda, A., Serrano, C., Hernández-Trejo, J. A., Gutiérrez-Martínez, I. Z., Montejo-López, W., Gómez-Suárez, M., Hernández-Ruiz, M., Betanzos, A., Candelario-Martínez, A., Romo-Parra, H., Arias-Montaño, J. A., Schnoor, M., Meraz Ríos, M. A., Gutierrez-Castillo, M. E., Martínez-Dávila, I. A., Villegas-Sepúlveda, N., Martinez-Fong, D., & Nava, P. (2017). pVHL suppresses Akt/β-catenin-mediated cell proliferation by inhibiting 14-3-3ζ expression. *Biochemical Journal*, *474*(16), 2679–2689. https://doi.org/10.1042/BCJ20161097

CCAC GUIDELINES. (2003). *The Canadian Veterinary Journal*, *44*(8), 631.

Chapman, J.-A. W., Costantino, J. P., Dong, B., Margolese, R. G., Pritchard, K. I., Shepherd, L. E., Gelmon, K. A., Wolmark, N., & Pollak, M. N. (2015). Octreotide LAR and tamoxifen versus tamoxifen in phase III randomize early breast cancer trials: NCIC CTG MA.14 and NSABP B-29. *Breast Cancer Research and Treatment*, *153*(2), 353–360. https://doi.org/10.1007/s10549-015-3547-4

Chaves, P., Garrido, M., Oliver, J., Pérez-Ruiz, E., Barragan, I., & Rueda-Domínguez, A. (2023). Preclinical models in head and neck squamous cell carcinoma. *British Journal of Cancer*, *128*(10), 1819–1827. https://doi.org/10.1038/s41416-023-02186-1

Chernoff, J. (2021). The two-hit theory hits 50. *Molecular Biology of the Cell*, *32*(22), rt1. https://doi.org/10.1091/mbc.E21-08-0407

Chhabra, A., Fernando, H., Watkins, G., Mansel, R. E., & Jiang, W. G. (2007). Expression of transcription factor CREB1 in human breast cancer and its correlation with prognosis. *Oncology Reports*, *18*(4), 953–958. https://doi.org/10.3892/or.18.4.953

Chrifi, I., Hermkens, D., Brandt, M. M., van Dijk, C. G. M., Bürgisser, P. E., Haasdijk, R., Pei, J., van de Kamp, E. H. M., Zhu, C., Blonden, L., Kros, J. M., Duncker, D. J., Duckers, H. J., & Cheng, C. (2017). Cgnl1, an endothelial junction complex protein, regulates GTPase mediated angiogenesis. *Cardiovascular Research*, *113*(14), 1776–1788. https://doi.org/10.1093/cvr/cvx175

Christenn, M., Kindler, S., Schulz, S., Buck, F., Richter, D., & Kreienkamp, H.-J. (2007). Interaction of brain somatostatin receptors with the PDZ domains of PSD-95. *FEBS Letters*, *581*(27), 5173–5177. https://doi.org/10.1016/j.febslet.2007.10.003

Cicenas, J., Zalyte, E., Rimkus, A., Dapkus, D., Noreika, R., & Urbonavicius, S. (2018). JNK, p38, ERK, and SGK1 Inhibitors in Cancer. *Cancers*, *10*(1), Article 1. https://doi.org/10.3390/cancers10010001

Coleman, J. L. J., Ngo, T., & Smith, N. J. (2017). The G protein-coupled receptor N-terminus and receptor signalling: N-tering a new era. *Cellular Signalling*, *33*, 1–9. https://doi.org/10.1016/j.cellsig.2017.02.004

Cotto, C., Quoix, E., Thomas, F., Henane, S., & Trillet-Lenoir, V. (1994). Phase I study of the somatostatin analogue somatuline in refractory small-cell lung carcinoma. *Annals of Oncology*, *5*(3), 290–291. https://doi.org/10.1093/oxfordjournals.annonc.a058812

Cramer, J. D., Burtness, B., Le, Q. T., & Ferris, R. L. (2019). The changing therapeutic landscape of head and neck cancer. *Nature Reviews Clinical Oncology*, *16*(11), Article 11. https://doi.org/10.1038/s41571-019-0227-z

Das, M., Nuñez, I., Rodriguez, M., Wiley, D. J., Rodriguez, J., Sarkeshik, A., Yates, J. R., Buchwald, P., & Verde, F. (2015a). Phosphorylation-dependent inhibition of Cdc42 GEF

Gef1 by 14-3-3 protein Rad24 spatially regulates Cdc42 GTPase activity and oscillatory dynamics during cell morphogenesis. *Molecular Biology of the Cell*, *26*(19), 3520–3534. https://doi.org/10.1091/mbc.E15-02-0095

Das, M., Nuñez, I., Rodriguez, M., Wiley, D. J., Rodriguez, J., Sarkeshik, A., Yates, J. R., Buchwald, P., & Verde, F. (2015b). Phosphorylation-dependent inhibition of Cdc42 GEF Gef1 by 14-3-3 protein Rad24 spatially regulates Cdc42 GTPase activity and oscillatory dynamics during cell morphogenesis. *Molecular Biology of the Cell*, *26*(19), 3520–3534. https://doi.org/10.1091/mbc.E15-02-0095

Datta, Sandeep Robert, Brunet, Anna, & Greenberg, Michael E. (1999). *Cellular survival: A play in three Akts—PubMed*. https://pubmed-ncbi-nlm-nih-gov.proxy3.library.mcgill.ca/10579998/

DeGregori, J., Kowalik, T., & Nevins, J. R. (1995). Cellular targets for activation by the E2F1 transcription factor include DNA synthesis- and G1/S-regulatory genes. *Molecular and Cellular Biology*, *15*(8), 4215–4224.

Ding, L., Cao, J., Lin, W., Chen, H., Xiong, X., Ao, H., Yu, M., Lin, J., & Cui, Q. (2020). The Roles of Cyclin-Dependent Kinases in Cell-Cycle Progression and Therapeutic Strategies in Human Breast Cancer. *International Journal of Molecular Sciences*, *21*(6), 1960. https://doi.org/10.3390/ijms21061960

Dobre, M., Trandafir, B., Milanesi, E., Salvi, A., Bucuroiu, I. A., Vasilescu, C., Niculae, A. M., Herlea, V., Hinescu, M. E., & Constantinescu, G. (2022). Molecular profile of the NF-κB signalling pathway in human colorectal cancer. *Journal of Cellular and Molecular Medicine*, *26*(24), 5966–5975. https://doi.org/10.1111/jcmm.17545

Du, E., Mazul, A. L., Farquhar, D., Brennan, P., Anantharaman, D., Abedi-Ardekani, B., Weissler, M. C., Hayes, D. N., Olshan, A. F., & Zevallos, J. P. (2019). Long-term Survival in Head and Neck Cancer: Impact of Site, Stage, Smoking, and Human Papillomavirus Status. *The Laryngoscope*, *129*(11), 2506–2513. https://doi.org/10.1002/lary.27807

Elsabahy, M., & Foldvari, M. (2013). Needle-free Gene Delivery Through the Skin: An Overview of Recent Strategies. *Current Pharmaceutical Design*, *19*(41), 7301–7315. https://doi.org/10.2174/13816128113199990369

Engström, M., Tomperi, J., El-Darwish, K., Åhman, M., Savola, J.-M., & Wurster, S. (2005). Superagonism at the Human Somatostatin Receptor Subtype 4. *Journal of Pharmacology and Experimental Therapeutics*, *312*(1), 332–338. https://doi.org/10.1124/jpet.104.075531

Enz, N., Vliegen, G., De Meester, I., & Jungraithmayr, W. (2019). CD26/DPP4—A potential biomarker and target for cancer therapy. *Pharmacology & Therapeutics*, *198*, 135–159. https://doi.org/10.1016/j.pharmthera.2019.02.015

Farrell, S. R., Rankin, D. R., Brecha, N. C., & Barnes, S. (2014). Somatostatin receptor subtype 4 modulates L-type calcium channels via Gβγ and PKC signaling in rat retinal ganglion cells. *Channels*, *8*(6), 519–527. https://doi.org/10.4161/19336950.2014.967623

Ferlay J, Ervik M, Lam F, Laversanne M, Colombet M, Mery L, Piñeros M, Znaor A, Soerjomataram I, Bray F (2024). Global Cancer Observatory (GCO): Cancer Today. Lyon, France: International Agency for Research on Cancer. Available from: https://gco.iarc.who.int/today, accessed [10 September 2024].

Fero, M. L., Randel, E., Gurley, K. E., Roberts, J. M., & Kemp, C. J. (1998). The murine gene p27 Kip1 is haplo-insufficient for tumour suppression. *Nature*, *396*(6707), 177–180. https://doi.org/10.1038/24179

Furcht, C. M., Buonato, J. M., & Lazzara, M. J. (2015). EGFR-activated Src family kinases maintain GAB1-SHP2 complexes distal from EGFR. *Science Signaling*, *8*(376), ra46–ra46. https://doi.org/10.1126/scisignal.2005697

Gastonguay, A., Berg, T., Hauser, A. D., Schuld, N., Lorimer, E., & Williams, C. L. (2012). The role of Rac1 in the regulation of NF-kB activity, cell proliferation, and cell migration in non-small cell lung carcinoma. *Cancer Biology & Therapy*, *13*(8), 647–656. https://doi.org/10.4161/cbt.20082

Ge, Y., Gomez, N. C., Adam, R. C., Nikolova, M., Yang, H., Verma, A., Lu, C. P.-J., Polak, L., Yuan, S., Elemento, O., & Fuchs, E. (2017). Stem Cell Lineage Infidelity Drives Wound-Repair and Cancer. *Cell*, *169*(4), 636-650.e14. https://doi.org/10.1016/j.cell.2017.03.042

Geng, Q., Xian, R., Yu, Y., Chen, F., & Li, R. (2022). SHP-1 acts as a tumor suppressor by interacting with EGFR and predicts the prognosis of human breast cancer. *Cancer Biology & Medicine*, *19*(4), 468–485. https://doi.org/10.20892/j.issn.2095-3941.2020.0501

Ghazizadeh, S., Harrington, R., & Taichman, L. B. (1999). In vivo transduction of mouse epidermis with recombinant retroviral vectors: Implications for cutaneous gene therapy. *Gene Therapy*, *6*(7), 1267–1275. https://doi.org/10.1038/sj.gt.3300956

Global Burden of Disease (GBD) 2021. From: https://vizhub.healthdata.org/gbd-compare/, accessed [10 September 2024].

Goon, P., Schürmann, M., Oppel, F., Shao, S., Schleyer, S., Pfeiffer, C. J., Todt, I., Brasch, F., Scholtz, L.-U., Göerner, M., & Sudhoff, H. (2022). Viral and Clinical Oncology of Head and Neck Cancers. *Current Oncology Reports*, *24*(7), 929–942. https://doi.org/10.1007/s11912-022-01263-7

Gormley, M., Creaney, G., Schache, A., Ingarfield, K., & Conway, D. I. (2022). Reviewing the epidemiology of head and neck cancer: Definitions, trends and risk factors. *British Dental Journal*, *233*(9), 780–786. https://doi.org/10.1038/s41415-022-5166-x

Gruber, P., & Zito, P. M. (2024). Skin Cancer. In *StatPearls*. StatPearls Publishing. http://www.ncbi.nlm.nih.gov/books/NBK441949/

Gueorguiev, M., & Grossman, A. B. (2011). A new therapeutic era for pituitary tumors. *Nature Reviews Endocrinology*, *7*(2), Article 2. https://doi.org/10.1038/nrendo.2010.233

Guillermet, J., Saint-Laurent, N., Rochaix, P., Cuvillier, O., Levade, T., Schally, A. V., Pradayrol, L., Buscail, L., Susini, C., & Bousquet, C. (2003). Somatostatin receptor subtype 2 sensitizes human pancreatic cancer cells to death ligand-induced apoptosis. Proceedings of the National Academy of Sciences of the United States of America, 100(1), 155–160. https://doi.org/10.1073/pnas.0136771100

Guillermet-Guibert, J., Saint-Laurent, N., Davenne, L., Rochaix, P., Cuvillier, O., Culler, M. D., Pradayrol, L., Buscail, L., Susini, C., & Bousquet, C. (2007). Novel synergistic mechanism for sst2 somatostatin and TNFalpha receptors to induce apoptosis: Crosstalk between NF-kappaB and JNK pathways. Cell Death and Differentiation, 14(2), 197–208. https://doi.org/10.1038/sj.cdd.4401939

Gunther, T., Tulipano, G., Dournaud, P., Bousquet, C., Csaba, Z., Kreienkamp, H.-J., Lupp, A., Korbonits, M., Castaño, J. P., Wester, H.-J., Culler, M., Melmed, S., & Schulz, S. (2018). International Union of Basic and Clinical Pharmacology. CV. Somatostatin Receptors: Structure, Function, Ligands, and New Nomenclature. *Pharmacological Reviews*, *70*(4), 763–835. https://doi.org/10.1124/pr.117.015388

Guri-Lamce, I., AlRokh, Y., Kim, Y., Maeshima, R., Graham, C., Hart, S. L., McGrath, J. A., & Jacków-Malinowska, J. (2024). Topical gene editing therapeutics using lipid nanoparticles:

'Gene creams' for genetic skin diseases? *British Journal of Dermatology*, *190*(5), 617–627. https://doi.org/10.1093/bjd/ljad528

Hanahan, D., & Weinberg, R. A. (2011). Hallmarks of Cancer: The Next Generation. *Cell*, *144*(5), 646–674. https://doi.org/10.1016/j.cell.2011.02.013

Harda, K., Szabo, Z., Szabo, E., Olah, G., Fodor, K., Szasz, C., Mehes, G., Schally, A. V., & Halmos, G. (2018). Somatostatin Receptors as Molecular Targets in Human Uveal Melanoma. *Molecules : A Journal of Synthetic Chemistry and Natural Product Chemistry*, *23*(7), 1535. https://doi.org/10.3390/molecules23071535

Hasan, N., Nadaf, A., Imran, M., Jiba, U., Sheikh, A., Almalki, W. H., Almujri, S. S., Mohammed, Y. H., Kesharwani, P., & Ahmad, F. J. (2023). Skin cancer: Understanding the journey of transformation from conventional to advanced treatment approaches. *Molecular Cancer*, *22*, 168. https://doi.org/10.1186/s12943-023-01854-3

Hejna, M., Schmidinger, M., & Raderer, M. (2002). The clinical role of somatostatin analogues as antineoplastic agents: Much ado about nothing? *Annals of Oncology*, *13*(5), 653–668. https://doi.org/10.1093/annonc/mdf142

Hermeking, H., & Benzinger, A. (2006). 14-3-3 proteins in cell cycle regulation. *Seminars in Cancer Biology*, *16*(3), 183–192. https://doi.org/10.1016/j.semcancer.2006.03.002

Inoue, K., & Fry, E. A. (2017). Haploinsufficient tumor suppressor genes. *Advances in Medicine and Biology*, *118*, 83–122.

Isaksen, I. M., & Dankel, S. N. (2023). Ultra-processed food consumption and cancer risk: A systematic review and meta-analysis. *Clinical Nutrition (Edinburgh, Scotland)*, *42*(6), 919–928. https://doi.org/10.1016/j.clnu.2023.03.018

Islam, K., Balasubramanian, B., Venkatraman, S., Thummarati, P., Tunganuntarat, J., Phueakphud, N., Kanjanasirirat, P., Khumpanied, T., Kongpracha, P., Kittirat, Y., Tohtong, R., Janvilisri, T., Wongtrakoongate, P., Borwornpinyo, S., Namwat, N., & Suthiphongchai, T. (2023). Upregulated LAMA3 modulates proliferation, adhesion, migration and epithelial-to-mesenchymal transition of cholangiocarcinoma cells. *Scientific Reports*, *13*(1), 22598. https://doi.org/10.1038/s41598-023-48798-8

Janostiak, R., Torres-Sanchez, A., Posas, F., & de Nadal, E. (2022). Understanding Retinoblastoma Post-Translational Regulation for the Design of Targeted Cancer Therapies. *Cancers*, *14*(5), 1265. https://doi.org/10.3390/cancers14051265

Jimenez, L., Jayakar, S. K., Ow, T. J., & Segall, J. E. (2015). Mechanisms of Invasion in Head and Neck Cancer. *Archives of Pathology & Laboratory Medicine*, *139*(11), 1334–1348. https://doi.org/10.5858/arpa.2014-0498-RA

Johnson, D. E., Burtness, B., Leemans, C. R., Lui, V. W. Y., Bauman, J. E., & Grandis, J. R. (2020). Head and neck squamous cell carcinoma. *Nature Reviews Disease Primers*, *6*(1), Article 1. https://doi.org/10.1038/s41572-020-00224-3

Josiah, A. J., Twilley, D., Pillai, S. K., Ray, S. S., & Lall, N. (2021). Pathogenesis of Keratinocyte Carcinomas and the Therapeutic Potential of Medicinal Plants and Phytochemicals. *Molecules*, *26*(7), 1979. https://doi.org/10.3390/molecules26071979

Kacar, A., Arikok, A. T., Kokenek Unal, T. D., Onder, E., Hucumenoglu, S., & Alper, M. (2012). Stromal Expression of CD34, α-Smooth Muscle Actin and CD26/DPPIV in Squamous Cell Carcinoma of the Skin: A Comparative Immunohistochemical Study. *Pathology & Oncology Research*, *18*(1), 25–31. https://doi.org/10.1007/s12253-011-9412-9

Kalyankrishna, S., & Grandis, J. R. (2006). Epidermal Growth Factor Receptor Biology in Head and Neck Cancer. *Journal of Clinical Oncology*, *24*(17), 2666–2672. https://doi.org/10.1200/JCO.2005.04.8306

Kanteti, R., Batra, S. K., Lennon, F. E., & Salgia, R. (2016). FAK and paxillin, two potential targets in pancreatic cancer. *Oncotarget*, *7*(21), 31586–31601. https://doi.org/10.18632/oncotarget.8040

Kassirian, S., Dzioba, A., Hamel, S., Patel, K., Sahovaler, A., Palma, D. A., Read, N., Venkatesan, V., Nichols, A. C., Yoo, J., Fung, K., Mendez, A., & MacNeil, S. D. (2020). Delay in diagnosis of patients with head-and-neck cancer in Canada: Impact of patient and provider delay. *Current Oncology*, *27*(5), e467–e477. https://doi.org/10.3747/co.27.6547

Kciuk, M., Gielecińska, A., Budzinska, A., Mojzych, M., & Kontek, R. (2022a). Metastasis and MAPK Pathways. *International Journal of Molecular Sciences*, *23*(7), Article 7. https://doi.org/10.3390/ijms23073847

Kciuk, M., Gielecińska, A., Budzinska, A., Mojzych, M., & Kontek, R. (2022b). Metastasis and MAPK Pathways. *International Journal of Molecular Sciences*, *23*(7), Article 7. https://doi.org/10.3390/ijms23073847

Kharmate, G., Rajput, P. S., Watt, H. L., Somvanshi, R. K., Chaudhari, N., Qiu, X., & Kumar, U. (2011). Role of somatostatin receptor 1 and 5 on epidermal growth factor receptor mediated signaling. *Biochimica et Biophysica Acta (BBA) - Molecular Cell Research*, *1813*(6), 1172–1189. https://doi.org/10.1016/j.bbamcr.2011.03.006

Kiaris, H., Schally, A. V., Nagy, A., Szepeshazi, K., Hebert, F., & Halmos, G. (2001). A targeted cytotoxic somatostatin (SST) analogue, AN-238, inhibits the growth of H-69 small-cell lung carcinoma (SCLC) and H-157 non-SCLC in nude mice. *European Journal of Cancer (Oxford, England: 1990)*, *37*(5), 620–628. https://doi.org/10.1016/s0959-8049(00)00437-8

Kim, H., Kim, M., Im, S.-K., & Fang, S. (2018). Mouse Cre-LoxP system: General principles to determine tissue-specific roles of target genes. *Laboratory Animal Research*, *34*(4), 147–159. https://doi.org/10.5625/lar.2018.34.4.147

Kim, J. W., Seymen, F., Lee, K. E., Ko, J., Yildirim, M., Tuna, E. B., Gencay, K., Shin, T. J., Kyun, H. K., Simmer, J. P., & Hu, J. C.-C. (2013). LAMB3 Mutations Causing Autosomal-dominant Amelogenesis Imperfecta. *Journal of Dental Research*, *92*(10), 899. https://doi.org/10.1177/0022034513502054

Klomp, M. J., Dalm, S. U., de Jong, M., Feelders, R. A., Hofland, J., & Hofland, L. J. (2021). Epigenetic regulation of somatostatin and somatostatin receptors in neuroendocrine tumors and other types of cancer. *Reviews in Endocrine & Metabolic Disorders*, *22*(3), 495–510. https://doi.org/10.1007/s11154-020-09607-z

Knudson, A. G. (1971). Mutation and Cancer: Statistical Study of Retinoblastoma. *Proceedings of the National Academy of Sciences of the United States of America*, *68*(4), 820–823.

Kreienkamp, H.-J., Roth, A., & Richter, D. (1998). Rat Somatostatin Receptor Subtype 4 Can Be Made Sensitive to Agonist-Induced Internalization by Mutation of a Single Threonine (Residue 331). *DNA and Cell Biology*, *17*(10), 869–878. https://doi.org/10.1089/dna.1998.17.869

Kumar, U. (2024). Somatostatin and Somatostatin Receptors in Tumour Biology. *International Journal of Molecular Sciences*, *25*(1), Article 1. https://doi.org/10.3390/ijms25010436

Laroche, G., Rochdi, M. D., Laporte, S. A., & Parent, J.-L. (2005). Involvement of Actin in Agonist-induced Endocytosis of the G Protein-coupled Receptor for Thromboxane A2.

Journal of Biological Chemistry, *280*(24), 23215–23224. https://doi.org/10.1074/jbc.M414071200

Lee, Y., Jeong, M., Park, J., Jung, H., & Lee, H. (2023). Immunogenicity of lipid nanoparticles and its impact on the efficacy of mRNA vaccines and therapeutics. *Experimental & Molecular Medicine*, *55*(10), 2085–2096. https://doi.org/10.1038/s12276-023-01086-x

Leemans, C. R., Snijders, P. J. F., & Brakenhoff, R. H. (2018). The molecular landscape of head and neck cancer. *Nature Reviews Cancer*, *18*(5), Article 5. https://doi.org/10.1038/nrc.2018.11

Lehman, J. M., Hoeksema, M. D., Staub, J., Qian, J., Harris, B., Callison, J. C., Miao, J., Shi, C., Eisenberg, R., Chen, H., Chen, S.-C., & Massion, P. P. (2019). Somatostatin Receptor 2 signaling promotes growth and tumor survival in Small Cell Lung Cancer. *International Journal of Cancer*, *144*(5), 1104–1114. https://doi.org/10.1002/ijc.31771

Li, H., Eishingdrelo, A., Kongsamut, S., & Eishingdrelo, H. (2016). G-protein-coupled receptors mediate 14-3-3 signal transduction. *Signal Transduction and Targeted Therapy*, *1*(1), 1–8. https://doi.org/10.1038/sigtrans.2016.18

Li, L. (2013). Mouse Epidermal Keratinocyte Culture. In S. H. Randell & M. L. Fulcher (Eds.), *Epithelial Cell Culture Protocols: Second Edition* (pp. 177–191). Humana Press. https://doi.org/10.1007/978-1-62703-125-7_12

Lim, W., Bae, H., Bazer, F. W., & Song, G. (2017). Stimulatory effects of fibroblast growth factor 2 on proliferation and migration of uterine luminal epithelial cells during early pregnancy. *Biology of Reproduction*, *96*(1), 185–198. https://doi.org/10.1095/biolreprod.116.142331

Liu, A., Joyner, A. L., & Turnbull, D. H. (1998). Alteration of limb and brain patterning in early mouse embryos by ultrasound-guided injection of *Shh*-expressing cells. *Mechanisms of Development*, *75*(1), 107–115. https://doi.org/10.1016/S0925-4773(98)00090-2

Loganathan, S. K., Schleicher, K., Malik, A., Quevedo, R., Langille, E., Teng, K., Oh, R. H., Rathod, B., Tsai, R., Samavarchi-Tehrani, P., Pugh, T. J., Gingras, A.-C., & Schramek, D. (2020). Rare driver mutations in head and neck squamous cell carcinomas converge on NOTCH signaling. *Science*, *367*(6483), 1264–1269. https://doi.org/10.1126/science.aax0902

Ma, Y.-C., Huang, J., Ali, S., Lowry, W., & Huang, X.-Y. (2000). Src Tyrosine Kinase Is a Novel Direct Effector of G Proteins. *Cell*, *102*(5), 635–646. https://doi.org/10.1016/S0092-8674(00)00086-6

Maeso-Alonso, L., López-Ferreras, L., Marques, M. M., & Marin, M. C. (2021). P73 as a Tissue Architect. *Frontiers in Cell and Developmental Biology*, *9*, 716957. https://doi.org/10.3389/fcell.2021.716957

Milewska-Kranc, A., Ćwikła, J. B., & Kolasinska-Ćwikła, A. (2024). The Role of Receptor–Ligand Interaction in Somatostatin Signaling Pathways: Implications for Neuroendocrine Tumors. *Cancers*, *16*(1), Article 1. https://doi.org/10.3390/cancers16010116

Mitra, S., Beach, C., Feng, G.-S., & Plattner, R. (2008). SHP-2 IS A NOVEL TARGET OF ABL KINASES DURING CELL PROLIFERATION. *Journal of Cell Science*, *121*(Pt 20), 3335–3346. https://doi.org/10.1242/jcs.035691

Moller, L. N., Stidsen, C. E., Hartmann, B., & Holst, J. J. (2003). Somatostatin receptors. *Biochimica et Biophysica Acta (BBA) - Biomembranes*, *1616*(1), 1–84. https://doi.org/10.1016/S0005-2736(03)00235-9

Montalto, F. I., & De Amicis, F. (2020). Cyclin D1 in Cancer: A Molecular Connection for Cell Cycle Control, Adhesion and Invasion in Tumor and Stroma. *Cells*, *9*(12), 2648. https://doi.org/10.3390/cells9122648

Moore, K. A., Sethi, R., Doanes, A. M., Johnson, T. M., Pracyk, J. B., Kirby, M., Irani, K., Goldschmidt-Clermont, P. J., & Finkel, T. (1997). Rac1 is required for cell proliferation and G2/M progression. *Biochemical Journal*, *326*(Pt 1), 17–20.

Muhammad, N., Bhattacharya, S., Steele, R., Phillips, N., & Ray, R. B. (2017). Involvement of c-Fos in the promotion of cancer stem-like cell properties in head and neck squamous cell carcinoma. *Clinical Cancer Research : An Official Journal of the American Association for Cancer Research*, *23*(12), 3120–3128. https://doi.org/10.1158/1078-0432.CCR-16-2811

Neri, P., Ren, L., Azab, A. K., Brentnall, M., Gratton, K., Klimowicz, A. C., Lin, C., Duggan, P., Tassone, P., Mansoor, A., Stewart, D. A., Boise, L. H., Ghobrial, I. M., & Bahlis, N. J. (2011). Integrin β7-mediated regulation of multiple myeloma cell adhesion, migration, and invasion. *Blood*, *117*(23), 6202–6213. https://doi.org/10.1182/blood-2010-06-292243

Ngan, H.-L., Law, C.-H., Choi, Y. C. Y., Chan, J. Y.-S., & Lui, V. W. Y. (2022). Precision drugging of the MAPK pathway in head and neck cancer. Npj Genomic Medicine, 7(1), 1–10. https://doi.org/10.1038/s41525-022-00293-1

Nicolas, M., Wolfer, A., Raj, K., Kummer, J. A., Mill, P., van Noort, M., Hui, C., Clevers, H., Dotto, G. P., & Radtke, F. (2003). Notch1 functions as a tumor suppressor in mouse skin. *Nature Genetics*, *33*(3), 416–421. https://doi.org/10.1038/ng1099

Niu, J., Chu, Y., Huang, Y.-F., Chong, Y.-S., Jiang, Z.-H., Mao, Z.-W., Peng, L.-H., & Gao, J.-Q. (2017). Transdermal Gene Delivery by Functional Peptide-Conjugated Cationic Gold Nanoparticle Reverses the Progression and Metastasis of Cutaneous Melanoma. *ACS Applied Materials & Interfaces*, *9*(11), 9388–9401. https://doi.org/10.1021/acsami.6b16378

Obsilova, V., & Obsil, T. (2022). Structural insights into the functional roles of 14-3-3 proteins. *Frontiers in Molecular Biosciences*, *9*. https://doi.org/10.3389/fmolb.2022.1016071

O'Connor, L., Gilmour, J., & Bonifer, C. (2016). The Role of the Ubiquitously Expressed Transcription Factor Sp1 in Tissue-specific Transcriptional Regulation and in Disease. *The Yale Journal of Biology and Medicine*, *89*(4), 513–525.

Ohtani, K., Iwanaga, R., Nakamura, M., Ikeda, M., Yabuta, N., Tsuruga, H., & Nojima, H. (1999). Cell growth-regulated expression of mammalian MCM5 and MCM6 genes mediated by the transcription factor E2F. *Oncogene*, *18*(14), 2299–2309. https://doi.org/10.1038/sj.onc.1202544

Ortiz, M. M. O., Patel, D. M., Swiatnicki, M., & Andrechek, E. R. (2024). *Unravelling biological processess and EGFR pathway regulation by the receptor-like protein tyrosine phosphatase PTPRH in non-small cell lung cancer* (p. 2024.06.13.598886). bioRxiv. https://doi.org/10.1101/2024.06.13.598886

Patel, Y. C. (1999). Somatostatin and Its Receptor Family. *Frontiers in Neuroendocrinology*, *20*(3), 157–198. https://doi.org/10.1006/frne.1999.0183

Peng, C., Zeng, W., Su, J., Kuang, Y., He, Y., Zhao, S., Zhang, J., Ma, W., Bode, A. M., Dong, Z., & Chen, X. (2016). Cyclin dependent kinase 2 (CDK2) is a key mediator for EGF-induced cell transformation mediated through the ELK4/c-Fos signaling pathway. *Oncogene*, *35*(9), 1170–1179. https://doi.org/10.1038/onc.2015.175

Pennington, K. L., Chan, T. Y., Torres, M. P., & Andersen, J. L. (2018). The dynamic and stress-adaptive signaling hub of 14-3-3: Emerging mechanisms of regulation and context-dependent protein–protein interactions. *Oncogene*, *37*(42), 5587–5604. https://doi.org/10.1038/s41388-018-0348-3

Pereira, D., Martins, D., & Mendes, F. (2022). Immunotherapy in Head and Neck Cancer When, How, and Why? *Biomedicines*, *10*(9), 2151. https://doi.org/10.3390/biomedicines10092151

Peverelli, E., Treppiedi, D., & Mantovani, G. (n.d.). *Molecular mechanisms involved in somatostatin receptor regulation in corticotroph tumors: The role of cytoskeleton and USP8 mutations in: Endocrine Oncology Volume 2 Issue 1 (2022)*. Retrieved September 19, 2024, from https://eo.bioscientifica.com/view/journals/eo/2/1/EO-22-0042.xml

Pfeiffer, M., Koch, T., Schröder, H., Laugsch, M., Höllt, V., & Schulz, S. (2002). Heterodimerization of Somatostatin and Opioid Receptors Cross-modulates Phosphorylation, Internalization, and Desensitization*. *Journal of Biological Chemistry*, *277*(22), 19762–19772. https://doi.org/10.1074/jbc.M110373200

Pickering, C. R., Zhang, J., Yoo, S. Y., Bengtsson, L., Moorthy, S., Neskey, D. M., Zhao, M., Ortega Alves, M. V., Chang, K., Drummond, J., Cortez, E., Xie, T., Zhang, D., Chung, W., Issa, J.-P. J., Zweidler-McKay, P. A., Wu, X., El-Naggar, A. K., Weinstein, J. N., … Frederick, M. J. (2013). Integrative Genomic Characterization of Oral Squamous Cell Carcinoma Identifies Frequent Somatic Drivers. Cancer Discovery, 3(7), 770–781. https://doi.org/10.1158/2159-8290.CD-12-0537

Pinski, J., Schally, A. V., Halmos, G., Szepeshazi, K., Groot, K., O'Byrne, K., & Cai, R. Z. (1994). Effects of somatostatin analogue RC-160 and bombesin/gastrin-releasing peptide antagonists on the growth of human small-cell and non-small-cell lung carcinomas in nude mice. *British Journal of Cancer*, *70*(5), 886–892.

Pritchard, A. L., & Hayward, N. K. (2013). Molecular Pathways: Mitogen-Activated Protein Kinase Pathway Mutations and Drug Resistance. *Clinical Cancer Research*, *19*(9), 2301–2309. https://doi.org/10.1158/1078-0432.CCR-12-0383

Ren, Q., Kari, C., Quadros, M. R. D., Burd, R., McCue, P., Dicker, A. P., & Rodeck, U. (2006). Malignant Transformation of Immortalized HaCaT Keratinocytes through Deregulated Nuclear Factor κB Signaling. *Cancer Research*, *66*(10), 5209–5215. https://doi.org/10.1158/0008-5472.CAN-05-4158

Reubi, J. C., Waser, B., Schaer, J. C., & Laissue, J. A. (2001). Somatostatin receptor sst1-sst5 expression in normal and neoplastic human tissues using receptor autoradiography with subtype-selective ligands. *European Journal of Nuclear Medicine*, *28*(7), 836–846. https://doi.org/10.1007/s002590100541

Rhodus, N. L., Kerr, A. R., & Patel, K. (2014). Oral Cancer: Leukoplakia, Premalignancy, and Squamous Cell Carcinoma. *Dental Clinics of North America*, *58*(2), 315–340. https://doi.org/10.1016/j.cden.2013.12.004

Rivera, C. (2015). Essentials of oral cancer. *International Journal of Clinical and Experimental Pathology*, *8*(9), 11884–11894. https://doi.org/10.5281/zenodo.192487

Rocheville, M., Lange, D. C., Kumar, U., Sasi, R., Patel, R. C., & Patel, Y. C. (2000). Subtypes of the Somatostatin Receptor Assemble as Functional Homo- and Heterodimers*. *Journal of Biological Chemistry*, *275*(11), 7862–7869. https://doi.org/10.1074/jbc.275.11.7862

Rodilla, V., Villanueva, A., Obrador-Hevia, A., Robert-Moreno, A., Fernández-Majada, V., Grilli, A., López-Bigas, N., Bellora, N., Albà, M. M., Torres, F., Duñach, M., Sanjuan, X.,

Gonzalez, S., Gridley, T., Capella, G., Bigas, A., & Espinosa, L. (2009). Jagged1 is the pathological link between Wnt and Notch pathways in colorectal cancer. *Proceedings of the National Academy of Sciences of the United States of America*, *106*(15), 6315–6320. https://doi.org/10.1073/pnas.0813221106

Roskoski, R. (2019). Targeting ERK1/2 protein-serine/threonine kinases in human cancers. *Pharmacological Research*, *142*, 151–168. https://doi.org/10.1016/j.phrs.2019.01.039

Ryu, T. H., Kye, H., Choi, J. E., Ahn, H. H., Kye, Y. C., & Seo, S. H. (2018). Features Causing Confusion between Basal Cell Carcinoma and Squamous Cell Carcinoma in Clinical Diagnosis. *Annals of Dermatology*, *30*(1), 64–70. https://doi.org/10.5021/ad.2018.30.1.64

Sabio, G., & Davis, R. J. (2014). TNF and MAP kinase signaling pathways. Seminars in Immunology, 26(3), 237–245. https://doi.org/10.1016/j.smim.2014.02.009

Sakamoto, K. M., & Frank, D. A. (2009). CREB in the Pathophysiology of Cancer: Implications for Targeting Transcription Factors for Cancer Therapy. *Clinical Cancer Research : An Official Journal of the American Association for Cancer Research*, *15*(8), 2583–2587. https://doi.org/10.1158/1078-0432.CCR-08-1137

Schuch, L. F., Silveira, F. M., Wagner, V. P., Borgato, G. B., Rocha, G. Z., Castilho, R. M., Vargas, P. A., & Martins, M. D. (2020). Head and neck cancer patient-derived xenograft models—A systematic review. *Critical Reviews in Oncology/Hematology*, *155*, 103087. https://doi.org/10.1016/j.critrevonc.2020.103087

Schummer, P., Kuphal, S., Vardimon, L., Bosserhoff, A. K., & Kappelmann, M. (2016). Specific c-Jun target genes in malignant melanoma. *Cancer Biology & Therapy*, *17*(5), 486–497. https://doi.org/10.1080/15384047.2016.1156264

Seller, W.R & Kaelin, W.J. (1997, November 1). *Role of the retinoblastoma protein in the pathogenesis of human cancer. | Journal of Clinical Oncology*. https://ascopubs-org.proxy3.library.mcgill.ca/doi/10.1200/JCO.1997.15.11.3301?url_ver=Z39.88-2003&rfr_id=ori:rid:crossref.org&rfr_dat=cr_pub%20%200pubmed

Sellers, W. R., & Kaelin, W. G. (1997). Role of the retinoblastoma protein in the pathogenesis of human cancer. *Journal of Clinical Oncology: Official Journal of the American Society of Clinical Oncology*, *15*(11), 3301–3312. https://doi.org/10.1200/JCO.1997.15.11.3301

Semenas, J., Hedblom, A., Miftakhova, R. R., Sarwar, M., Larsson, R., Shcherbina, L., Johansson, M. E., Härkönen, P., Sterner, O., & Persson, J. L. (2014). The role of PI3K/AKT-related PIP5K1α and the discovery of its selective inhibitor for treatment of advanced prostate cancer. *Proceedings of the National Academy of Sciences*, *111*(35), E3689–E3698. https://doi.org/10.1073/pnas.1405801111

Shen, L., Shi, Q., & Wang, W. (2018). Double agents: Genes with both oncogenic and tumor-suppressor functions. *Oncogenesis*, *7*(3), 1–14. https://doi.org/10.1038/s41389-018-0034-x

Shi, L., ssBian, Z., Kidder, K., Liang, H., & Liu, Y. (2021). Non-Lyn Src family kinases activate SIRPα-SHP-1 to dampen proinflammatory macrophage polarization. *Journal of Immunology (Baltimore, Md. : 1950)*, *207*(5), 1419–1427. https://doi.org/10.4049/jimmunol.2100266

Shimomura, Y., Agalliu, D., Vonica, A., Luria, V., Wajid, M., Baumer, A., Belli, S., Petukhova, L., Schinzel, A., Brivanlou, A. H., Barres, B. A., & Christiano, A. M. (2010). APCDD1 is a novel Wnt inhibitor mutated in hereditary hypotrichosis simplex. *Nature*, *464*(7291), 1043–1047. https://doi.org/10.1038/nature08875

Shrivastava, S., Steele, R., Sowadski, M., Crawford, S. E., Varvares, M., & Ray, R. B. (2015). Identification of molecular signature of head and neck cancer stem-like cells. *Scientific Reports*, *5*, 7819. https://doi.org/10.1038/srep07819

Simpson, C. L., Patel, D. M., & Green, K. J. (2011). Deconstructing the skin: Cytoarchitectural determinants of epidermal morphogenesis. *Nature Reviews. Molecular Cell Biology*, *12*(9), 565–580. https://doi.org/10.1038/nrm3175

Slevin, J. C., Byers, L., Gertsenstein, M., Qu, D., Mu, J., Sunn, N., Kingdom, J. C., Rossant, J., & Adamson, S. L. (2006). High resolution ultrasound-guided microinjection for interventional studies of early embryonic and placental development in vivo in mice. *BMC Developmental Biology*, *6*, 10. https://doi.org/10.1186/1471-213X-6-10

Somvanshi, R. K., Billova, S., Kharmate, G., Rajput, P. S., & Kumar, U. (2009). C-tail mediated modulation of somatostatin receptor type-4 homo- and heterodimerizations and signaling. *Cellular Signalling*, *21*(9), 1396–1414. https://doi.org/10.1016/j.cellsig.2009.04.007

Sriram, K., & Insel, P. A. (2018). G Protein-Coupled Receptors as Targets for Approved Drugs: How Many Targets and How Many Drugs? *Molecular Pharmacology*, *93*(4), 251–258. https://doi.org/10.1124/mol.117.111062

Stein, A. P., Saha, S., Kraninger, J. L., Swick, A. D., Yu, M., Lambertg, P. F., & Kimple, R. (2015). Prevalence of human papillomavirus in oropharyngeal cancer: A systematic review. *Cancer Journal (Sudbury, Mass.)*, *21*(3), 138–146. https://doi.org/10.1097/PPO.0000000000000115

Steven, A., & Seliger, B. (2016). Control of CREB expression in tumors: From molecular mechanisms and signal transduction pathways to therapeutic target. *Oncotarget*, *7*(23), 35454–35465. https://doi.org/10.18632/oncotarget.7721

Stransky, N., Egloff, A. M., Tward, A. D., Kostic, A. D., Cibulskis, K., Sivachenko, A., Kryukov, G. V., Lawrence, M. S., Sougnez, C., McKenna, A., Shefler, E., Ramos, A. H., Stojanov, P., Carter, S. L., Voet, D., Cortés, M. L., Auclair, D., Berger, M. F., Saksena, G., … Grandis, J. R. (2011). The Mutational Landscape of Head and Neck Squamous Cell Carcinoma. *Science*, *333*(6046), 1157–1160. https://doi.org/10.1126/science.1208130

Szklarczyk, D., Kirsch, R., Koutrouli, M., Nastou, K., Mehryary, F., Hachilif, R., Gable, A. L., Fang, T., Doncheva, N. T., Pyysalo, S., Bork, P., Jensen, L. J., & von Mering, C. (2022). The STRING database in 2023: Protein–protein association networks and functional enrichment analyses for any sequenced genome of interest. Nucleic Acids Research, 51(D1), D638–D646. https://doi.org/10.1093/nar/gkac1000

Talme, T., Ivanoff, J., Hägglund, M., Van Neerven, R. J. J., Ivanoff, A., & Sundqvist, K. G. (2001). Somatostatin receptor (SSTR) expression and function in normal and leukaemic T-cells. Evidence for selective effects on adhesion to extracellular matrix components via SSTR2 and/or 3. *Clinical and Experimental Immunology*, *125*(1), 71–79. https://doi.org/10.1046/j.1365-2249.2001.01577.x

Theodoropoulou, M., Stalla, G. K., & Spengler, D. (2010). ZAC1 target genes and pituitary tumorigenesis. *Molecular and Cellular Endocrinology*, *326*(1), 60–65. https://doi.org/10.1016/j.mce.2010.01.033

Theodoropoulou, M., Zhang, J., Laupheimer, S., Paez-Pereda, M., Erneux, C., Florio, T., Pagotto, U., & Stalla, G. K. (2006). Octreotide, a Somatostatin Analogue, Mediates Its Antiproliferative Action in Pituitary Tumor Cells by Altering Phosphatidylinositol 3-Kinase Signaling and Inducing Zac1 Expression. *Cancer Research*, *66*(3), 1576–1582. https://doi.org/10.1158/0008-5472.CAN-05-1189

The Cancer Genome Atlas Network. Comprehensive genomic characterization of head and neck squamous cell carcinomas. Nature 517, 576–582 (2015). https://doi-org.proxy3.library.mcgill.ca/10.1038/nature14129

Tomasevic, N., Jia, Z., Russell, A., Fujii, T., Hartman, J. J., Clancy, S., Wang, M., Beraud, C., Wood, K. W., & Sakowicz, R. (2007). Differential regulation of WASP and N-WASP by Cdc42, Rac1, Nck, and PI(4,5)P2. *Biochemistry*, *46*(11), 3494–3502. https://doi.org/10.1021/bi062152y

Tummers, B., & Green, D. R. (2017a). Caspase-8; regulating life and death. *Immunological Reviews*, *277*(1), 76–89. https://doi.org/10.1111/imr.12541

Tummers, B., & Green, D. R. (2017b). Caspase-8; regulating life and death. *Immunological Reviews*, *277*(1), 76–89. https://doi.org/10.1111/imr.12541

van Keulen, S. C., & Rothlisberger, U. (2017). Exploring the inhibition mechanism of adenylyl cyclase type 5 by n-terminal myristoylated Gαi1. *PLoS Computational Biology*, *13*(9), e1005673. https://doi.org/10.1371/journal.pcbi.1005673

Vikic-Topic, S., Raisch, K. P., Kvols, L. K., & Vuk-Pavlović, S. (1995). Expression of somatostatin receptor subtypes in breast carcinoma, carcinoid tumor, and renal cell carcinoma. *The Journal of Clinical Endocrinology & Metabolism*, *80*(10), 2974–2979. https://doi.org/10.1210/jcem.80.10.7559883

Villa, A., Villa, C., & Abati, S. (2011). Oral cancer and oral erythroplakia: An update and implication for clinicians. *Australian Dental Journal*, *56*(3), 253–256. https://doi.org/10.1111/j.1834-7819.2011.01337.x

Wang, J. Y. J., Knudson, E. S., & Welch, P. J. (1994). The Petinoblastoma Tumor Suppressor Protein. In G. F. Vande Woude & G. Kleln (Eds.), *Advances in Cancer Research* (Vol. 64, pp. 25–85). Academic Press. https://doi.org/10.1016/S0065-230X(08)60834-9

Watt, H. L., Kharmate, G. D., & Kumar, U. (2009). Somatostatin receptors 1 and 5 heterodimerize with epidermal growth factor receptor: Agonist-dependent modulation of the downstream MAPK signalling pathway in breast cancer cells. *Cellular Signalling*, *21*(3), 428–439. https://doi.org/10.1016/j.cellsig.2008.11.012

Weckbecker, G., Lewis, I., Albert, R., Schmid, H. A., Hoyer, D., & Bruns, C. (2003). Opportunities in somatostatin research: Biological, chemical and therapeutic aspects. *Nature Reviews Drug Discovery*, *2*(12), Article 12. https://doi.org/10.1038/nrd1255

Weernink, P. A. O., Meletiadis, K., Hommeltenberg, S., Hinz, M., Ishihara, H., Schmidt, M., & Jakobs, K. H. (2004). Activation of type I phosphatidylinositol 4-phosphate 5-kinase isoforms by the Rho GTPases, RhoA, Rac1, and Cdc42. *The Journal of Biological Chemistry*, *279*(9), 7840–7849. https://doi.org/10.1074/jbc.M312737200

Weich, A., Rogoll, D., Peschka, M., Weich, W., Pongracz, J., Brand, M., Fröhlich, M., Serfling, S. E., Rowe, S. P., Kosmala, A., Reiter, F. P., Meining, A., Werner, R. A., & Scheurlen, M. (2023). Wnt/β-catenin modulating drugs regulate somatostatin receptor expression and internalization of radiolabelled octreotide in neuroendocrine tumor cells. Nuclear Medicine Communications, 44(4), 259–269. https://doi.org/10.1097/MNM.0000000000001666

World Health Organization (WHO) 2021. From https://www.who.int/news-room/fact-sheets/detail/cancer, accessed [15 September 2024]

Xia, S., Lu, Y., Wang, J., He, C., Hong, S., Serhan, C. N., & Kang, J. X. (2006). Melanoma growth is reduced in fat-1 transgenic mice: Impact of omega-6/omega-3 essential fatty acids. Proceedings of the National Academy of Sciences, 103(33), 12499–12504. https://doi.org/10.1073/pnas.0605394103

Xu, X., Li, D., Liu, J., Ma, Z., Huang, H., Min, L., Dai, L., & Dong, S. (2019). Downregulation of PTPRK Promotes Cell Proliferation and Metastasis of NSCLC by Enhancing STAT3 Activation. *Analytical Cellular Pathology (Amsterdam)*, *2019*, 4265040. https://doi.org/10.1155/2019/4265040

Xu, Y., Xue, S., Zhou, J., Voorhees, J. J., & Fisher, G. J. (2015). Notch and TGF-β pathways cooperatively regulate receptor protein tyrosine phosphatase-κ (PTPRK) gene expression in human primary keratinocytes. *Molecular Biology of the Cell*, *26*(6), 1199–1206. https://doi.org/10.1091/mbc.E14-12-1591

Yamamoto, J., Ohnuma, K., Hatano, R., Okamoto, T., Komiya, E., Yamazaki, H., Iwata, S., Dang, N. H., Aoe, K., Kishimoto, T., Yamada, T., & Morimoto, C. (2014). Regulation of somatostatin receptor 4-mediated cytostatic effects by CD26 in malignant pleural mesothelioma. *British Journal of Cancer*, *110*(9), Article 9. https://doi.org/10.1038/bjc.2014.151

Yan, Y., Gauthier, M.-A., Malik, A., Fotiadou, I., Ostrovski, M., Dervovic, D., Ghadban, L., Tsai, R., Gish, G., Loganathan, S. K., & Schramek, D. (2023). The NOTCH-RIPK4-IRF6-ELOVL4 Axis Suppresses Squamous Cell Carcinoma. *Cancers*, *15*(3), Article 3. https://doi.org/10.3390/cancers15030737

Yan, Z., DeGregori, J., Shohet, R., Leone, G., Stillman, B., Nevins, J. R., & Williams, R. S. (1998). Cdc6 is regulated by E2F and is essential for DNA replication in mammalian cells. *Proceedings of the National Academy of Sciences of the United States of America*, *95*(7), 3603–3608.

Yang, D., Zhou, Q., Labroska, V., Qin, S., Darbalaei, S., Wu, Y., Yuliantie, E., Xie, L., Tao, H., Cheng, J., Liu, Q., Zhao, S., Shui, W., Jiang, Y., & Wang, M.-W. (2021). G protein-coupled receptors: Structure- and function-based drug discovery. *Signal Transduction and Targeted Therapy*, *6*(1), 1–27. https://doi.org/10.1038/s41392-020-00435-w

Yao, M., Gu, Y., Yang, Z., Zhong, K., & Chen, Z. (2021). MEIS1 and its potential as a cancer therapeutic target (Review). *International Journal of Molecular Medicine*, *48*(3), 181. https://doi.org/10.3892/ijmm.2021.5014

Young, K. A., Wojdyla, K., Lai, T., Mulholland, K. E., Aldaz Casanova, S., Antrobus, R., Andrews, S. R., Biggins, L., Mahler-Araujo, B., Barton, P. R., Anderson, K. R., Fearnley, G. W., & Sharpe, H. J. (2024). The receptor protein tyrosine phosphatase PTPRK promotes intestinal repair and catalysis-independent tumour suppression. *Journal of Cell Science*, *137*(14), jcs261914. https://doi.org/10.1242/jcs.261914

Yousef, H., Alhajj, M., Fakoya, A. O., & Sharma, S. (2024). Anatomy, Skin (Integument), Epidermis. In *StatPearls*. StatPearls Publishing. http://www.ncbi.nlm.nih.gov/books/NBK470464/

Yu, H., Pardoll, D., & Jove, R. (2009). STATs in cancer inflammation and immunity: A leading role for STAT3. *Nature Reviews. Cancer*, *9*(11), 798–809. https://doi.org/10.1038/nrc2734

Yuan, L., Barbash, S., Kongsamut, S., Eishingdrelo, A., Sakmar, T. P., & Eishingdrelo, H. (2019a). 14-3-3 signal adaptor and scaffold proteins mediate GPCR trafficking. *Scientific Reports*, *9*(1), 11156. https://doi.org/10.1038/s41598-019-47478-w

Yuan, L., Barbash, S., Kongsamut, S., Eishingdrelo, A., Sakmar, T. P., & Eishingdrelo, H. (2019b). 14-3-3 signal adaptor and scaffold proteins mediate GPCR trafficking. *Scientific Reports*, *9*, 11156. https://doi.org/10.1038/s41598-019-47478-w

Yue, J., & López, J. M. (2020). Understanding MAPK Signaling Pathways in Apoptosis. *International Journal of Molecular Sciences*, *21*(7), 2346. https://doi.org/10.3390/ijms21072346

Zhang, X., Tang, N., Hadden, T. J., & Rishi, A. K. (2011). Akt, FoxO and regulation of apoptosis. *Biochimica et Biophysica Acta (BBA) - Molecular Cell Research*, *1813*(11), 1978–1986. https://doi.org/10.1016/j.bbamcr.2011.03.010

Zhang, Y., Yan, M., Yu, Y., Wang, J., Jiao, Y., Zheng, M., & Zhang, S. (2024). 14–3-3ε: A protein with complex physiology function but promising therapeutic potential in cancer. *Cell Communication and Signaling*, *22*(1), 72. https://doi.org/10.1186/s12964-023-01420-w

Zhao, R., Shi, H., Yin, J., Sun, Z., & Xu, Y. (2022). Promoter Specific Methylation of SSTR4 is Associated With Alcohol Dependence in Han Chinese Males. *Frontiers in Genetics*, *13*, 915513. https://doi.org/10.3389/fgene.2022.915513

Zhao, W., Han, S., Qiu, N., Feng, W., Lu, M., Zhang, W., Wang, M., Zhou, Q., Chen, S., Xu, W., Du, J., Chu, X., Yi, C., Dai, A., Hu, L., Shen, M. Y., Sun, Y., Zhang, Q., Ma, Y., … Zhao, Q. (2022). Structural insights into ligand recognition and selectivity of somatostatin receptors. *Cell Research*, *32*(8), Article 8. https://doi.org/10.1038/s41422-022-00679-x

Zhu, G., Fan, Z., Ding, M., Zhang, H., Mu, L., Ding, Y., Zhang, Y., Jia, B., Chen, L., Chang, Z., & Wu, W. (2015). An EGFR/PI3K/AKT axis promotes accumulation of the Rac1-GEF Tiam1 that is critical in EGFR-driven tumorigenesis. *Oncogene*, *34*(49), 5971–5982. https://doi.org/10.1038/onc.2015.45

Zou, Y., Tan, H., Zhao, Y., Zhou, Y., & Cao, L. (2019). Expression and selective activation of somatostatin receptor subtypes induces cell cycle arrest in cancer cells. *Oncology Letters*, *17*(2), 1723–1731. https://doi.org/10.3892/ol.2018.9773